Multivalent MHC Blockers targeting HLA-DQ2 Antigen-presentation

Raymond T. Yan
(B.S. Biochemistry, University of Oregon)

A THESIS SUBMITTED

FOR THE DEGREE OF MASTER OF CHEMISTRY

DEPARTMENT OF CHEMISTRY

NATIONAL UNIVERSITY OF SINGAPORE

2010

ACKNOWLEDGEMENT

I would like to start off by thanking Ambalika Sagarika Khadria for her timely and practical advice as a sympathetic friend over a phone conversation during my uncertainty regarding the drafting of this thesis. I am grateful to her for helping me reconcile my Singapore experience, my idealisms, and shortcomings at a decisive moment through a realization that pursuit of science is not just all about theories and idealisms. With that note, I am fortunate and happy to now have the opportunity to formally thank so many others who have contributed to my ability in completing the work entailed in this thesis.

I want to, of course, thank Dr. Kim Chu Young, my co-supervisor, for providing me the opportunity to work on the multivalent project. I appreciated his patience with me as well as his persistent reminders of deadlines, weekly reports, and periodic write-ups. His persistence as a supervisor has helped me tremendously in drafting this thesis. I truly thank him for giving me an opportunity to get a better sense for science research and providing a lab environment where I could learn to understand my own weaknesses and strengths, both academically and professionally.

I want to thank Dr. Huaqiang Zeng, my main supervisor, for working with me during my candidature. I appreciate his flexibility and willingness to accommodate my research pursuits during my candidacy.

Thank you to Dr. Kinya Hotta for keeping the lab running as smoothly as possible so that everyone's projects could progress without too much hiatus. I want to thank Michelle in PPC for her mass spectrometry services, especially her willingness to do last minute MALDI-TOF MS on my samples. I want to thank Saytin in PPC for allowing me to access the PPC facility even after facility hours.

I want to thank our collaborator, Dr. Ludvig Sollid, in Norway. In particular, I want to thank Elin Bergseng for performing the biological assays and communicating the data with efficiency and clarity.

I want to thank Dr. Martin Lear and Dr. Xue Feng for being on my thesis committee and their support during my candidature. I would like to extend my thanks to NUS chemistry department for providing me the research scholarship so that I can conduct the research work in this thesis.

I want to thank a very helpful labmate and a very good friend, Sathya Dev Undurthi. He has made my experience in Singapore a memorable one to say the least. I know for sure my life in Singapore would have been much more difficult and intolerable if I didn't have him as a friend. I am grateful to him for putting out the effort to show his friendship.

A big thank you to my friend, Priya Jayaraman, for being a buddy both in and out of the lab. When lab work was tedious, Priya was a great person to banter with to relieve stress. And I appreciate her occasional South Indian home cooking.

I want to thank my friend Ashish Maurya for stopping by the lab and providing comical relief. I am appreciative of his attempts to remind me that having a social life is healthy and beneficial when doing science research. His "emotional support" was greatly appreciated.

I want to thank my friend, Nyugen Ngoc Bao Tram, for her unrelenting commitment to offer her assistance. I am grateful to be on the receiving end of her generosity in various things regarding my lab work. I also appreciate her time and input on all our scientific discussions.

I would like to thank Mingzhu and Xi for contributing to the lab environment. I want to mention a thank you to Anand for his kindness and help, especially during my departure from Singapore up until the departure gates at Changi Airport.

Finally, I need to thank Sandy Chadwick for being my family away from home when I first arrived in Singapore to pursue my candidature at NUS. Without her help, it would not have been a smooth beginning at NUS. I dedicate this thesis to those that I have come to known in Singapore who truly care about helping someone full of naïve idealisms to survive in a real world. I deeply appreciate their acts of kindness and care that was given to me.

TABLE OF CONTENTS

Chapter 2: Materials and Methods

SUMMARY

The aim of this project is to design multivalent MHC blockers as competitive inhibitors of HLA-DQ2 antigen presentation. The implications of such inhibitors serve as a therapeutic agent towards the onset of autoimmunity in celiac disease. Our initial approach is to create a small multivalent library consisting of dimers, trimers, tetramers, and octamers. These multivalent constructs are covalently linked to an α-I gliadin analog (wheat gluten peptide) through a thiol-reactive core molecule (i.e. multivalent linkers). These multivalent constructs will be used to test the multivalent hypothesis, which assumes that a molecule with more copies of binding ligand will favor its binding affinity. To verify such hypothesis, biochemical binding assay with HLA-DQ2 will be performed, followed by T cell proliferation assay to measure blocking efficiencies. This study begins to address the important issue regarding structural optimization (i.e. linker length and valency) in rational design for achieving competitive MHC blocking through a multivalent strategy.

Chapter 1: Introduction

Celiac disease is an autoimmune disorder of the intestinal mucosa. This disorder was first broadly recognized in the second century AD by Aretaeus who described it as a malabsorption syndrome. In 1888, the first modern account of the disease was published in a paper, "On the Coeliac Affection Characteristic". It mentions that "the allowance of farinaceous foods must be small" and the patient can only be cured through means of a diet (Hourigan, 2006). Histological findings of this disease include villous atrophy, crypt hyperplasia, and intraepithelial lymphocytosis. If chronic symptoms persist, the increased risk of more life-threatening complications such as intestinal adenocarcinoma and enteropathy-associated T-cell lymphoma can result. Other associated diseases include Down's syndrome, Turner's syndrome, and Type 1 diabetes. Celiac patients may experience diarrhea, abdominal distention, failure to thrive, neurological symptoms (depression), and anemia from chronic disease progression (Green, 2007).

Celiac pathogenesis has been associated with ingestion of gluten found in wheat. Oral tolerance is lost as a result of a food antigen. Celiac patients have abnormal $CD4^+$ T cell-initiated immune response towards gluten in the gut lumen. Gluten-specific T cells isolated from celiac lesions produce predominantly interferon-γ (IFN-γ). Other cytokines that are involved in celiac disease are IFN-α and IL-18. It is possible that IFN-α plays a role in the activation of T_H1-cell development in celiac disease and drives the immunopathology. Interestingly, tissue transglutaminase (TG2) promoter contains response elements for the pro-inflammatory cytokines IL-6 and tumour-necrosis factor (TNF). An increase in levels of serum antibodies to gluten and autoantigens in celiac patients can suggest an adaptive immune response. Modern serological testing for IgA

anti-tissue transglutaminase (tTG) antibody or indirect immunofluorescence assays for IgA endomysial antibody are considered highly accurate in diagnosis with high sensitivities and specificity. Interactions made between TG2 and gluten peptides create a hapten-carrier-like complex, and with the help of gluten-specific T cells, TG2-specific B cells produce TG2-specific antibody (Hourigan, 2006).

Before the mechanisms of the adaptive immunity initiate in celiac patients, a loss of integrity in the gut epithelium between the lumen and the lamina propria establishes a "pro-inflammatory" environment. Wheat gluten induces production of intestinal peptide zonulin, which acts on tight junctions and increases epithelial permeability. Leakage of "non-self" antigens from the gut lumen activates the innate immune response. The resulting adverse autoimmune response is evoked onto the intestinal lumen where T lymphocytes attack the epithelial lining of the intestinal tract. Celiac pathogenesis appears to illicit an innate immune response as well as a complex adaptive immune response. However, the prospects of understanding how gluten antigen serves as an initial stimulus of the disease would give further insight in preventing the progression of celiac disorder.

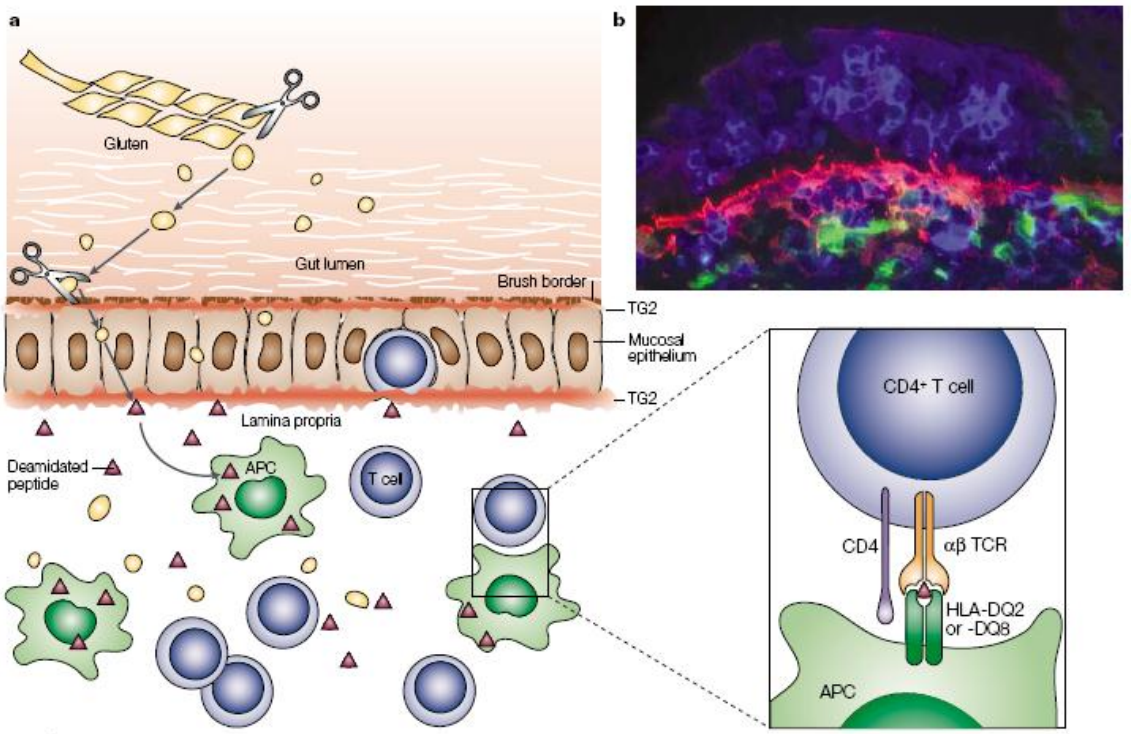

Figure 3 | **The coeliac small-intestine lesion.** Depiction of the intestinal mucosa with emphasis on the factors that take part in the development and control of coeliac disease. **a** | The parts of gluten that are resistant to processing by luminal and brush-border enzymes will survive digestion, and can be transported across the mucosal epithelium as polypeptides. Gluten peptides are deamidated by tissue transglutaminase (TG2), which, in the intestinal mucosa, is located mainly extracellularly in the subepithelial region, but is also found in the brush border. CD4+ T cells in the lamina propria recognize deamidated gluten peptides predominantly, presented by HLA-DQ2 or -DQ8 molecules on the cell surface of antigen-presenting cells (APCs). **b** | Immunofluorescence staining of TG2 (pink), HLA-DQ (green) and T cells (CD3; purple) in the small-intestine mucosa of an untreated coeliac-disease patient. Note that there is a close spatial relationship between TG2, APCs that express HLA-DQ and T cells just beneath the epithelium. Immunofluorescent image courtesy of H. Scott, Rikshospitalet.

Figure 1: Depiction of the intestinal mucosa during development of Celiac disease (Nature Rev. Immunology (2002) 2: 647-55)

1.1 Molecular target: HLA-DQ2 association

Gluten had been identified as the exogenous antigen promoting celiac disorder, but further studies are needed to understand the mechanism by which this antigen is recognized in the body. Celiac disease can be thought of as a multi-factorial disorder involving an environmental component such as a gluten-containing diet, but also includes a genetic association to certain HLA allele subtypes. HLA molecules are MHC (Major Histocompability Complex) class II molecules presented on cell membranes that interact with peptide fragments referred to as epitopes. This epitope-MHC complex acts as an antigen-presentation signal to T cells. Almost all affected celiac patients have genotype

for the HLA-DQ2 and/or HLA-DQ8 allele. In the European white population, common haplotype alleles found in celiac patients are HLA-DQA1*05 and DQB1*02 for DQ2 molecules, whereas for DQ8 molecules, HLA-DQA1*03 and DQB1*0302 alleles are found. Without these allele HLA haplotypes, there is no risk of celiac disorder. Although, in general, the HLA-DQ2 or DQ8 alleles are deemed necessary, it is not sufficient for the development of celiac disease. MHC is a set of linked genes found among a 3.5 million base pair region on the short arm of human chromosome 6 (Hourigan, 2006). Class II MHC molecules consist of a heterodimeric complex of a two-domain 32-34-kDa α-chain and a two-domain 29-32-kDa β-chain. The highest risk for disease development is from individuals who express HLA-DQ2 dimers in cis or trans (HLA-DR3/DQ2 homozygous or HLA-DR3/7DQ2). In 1993, a paper by Lundin had shown the proliferative response of $CD4^{+}CD25^{+}$ T lymphocytes from small intestinal biopsies of HLA-$DQ2^{+}$ adult celiac disease patients stimulated with gliadin (Lundin, 1993). Gliadins are digested, alcohol-soluble peptide fragments from wheat gluten, which have been identified to be epitopes for HLA-DQ antigen-presentation. The proliferative T-lymphocyte response can be inhibited by blocking HLA-DQ2 with anti-HLA-DQ2 antibodies. It was demonstrated by Yvonne Van de Wal and collaborators that HLA-DQ2 peptide-binding motif had a preference for negatively charged residues at several positions (Van de Wal, 1998).

1.2 HLA-DQ2 epitope: Wheat gluten peptides

The immunogenic epitope binding to HLA-DQ2 is located within the p56-75 region of A-gliadin. A-gliadin is a peptide fragment of the wheat gluten protein. In celiac patients, the recognition of different epitopes from different gliadins is found with

the various T cell clone population. It has been assumed that the N-terminal part of α-I gliadin is able to promote disease activity (Weiser, 1984; de Ritis, 1988). From wheat cultivar Scout 66, the overlapping peptides in the 58 N-terminal amino acids region were found to bind DQ2, but showed very weak or no binding to DR3. The α-I gliadin 21-40 peptide bound to DQ2 with the highest affinity (Johansen, 1996). However, the N-terminal overlapping α-I gliadin peptides were shown to have no stimulatory effects on any of their assayed gliadin specific TCC populations from small intestinal mucosa of CD patients. These peptides showed negligible inhibition to TCC reactivity in the presence of stimulatory α-I gliadin 31-49 peptide. Through incremental single amino acid deletions from the N-terminal or the C-terminal end of the α-I gliadin 31-49 peptide, the truncated versions of this peptide was shown to be able to maintain binding capacity. However, the truncated peptides yielded different levels of T cell stimulation compared to the native α-I gliadin 31-49 peptide. It was observed that having proline on either the N-terminal or C-terminal end of the truncations appeared to reduce the binding and TCC stimulation. The moderate to weak affinity binding of these truncations could be offset by the unfavorable interaction of having a terminal proline in the epitope. Using fixed APCs to stimulate TCC RNnTα33 (T cell clone used in the study), the incubation of α-I gliadin 31-49 peptide with fixed APCs at pH 4.9 was significantly better in stimulating TCC RNnTα33 compared to incubating the peptide at pH 7.4 condition. There was a correlation between the binding affinity of a non-stimulatory peptide to DQ2 on antigen presenting cells and its ability to inhibit TCC reactivity in the presence of α-I gliadin 31-49 peptide. Moderate to low affinity non-stimulatory peptides generally exhibit poor inhibition to TCC reactivity. Together, this study addresses two closely related issues

regarding the T-cell-mediated immunopathogenesis of CD. First, there is a wide range affinity of disease-associated DQ2 binding to various gliadin peptide fragments that can either illicit stimulatory or inhibitory effects on TCC reactivity. Second, there may be a complication behind gut-derived gliadin-specific TCC in epitope heterogeneity. TCC reactivity patterns may be dependent on the epitope cocktail rather than one specific epitope recognition. It is unclear how the T cell activation from this epitope heterogeneity would lead to the pathogenesis of CD.

1.2.1 Immunogenic Gluten peptide: α-I gliadin epitope

The α-I gliadin epitope, QLQPFPQPELPY, has been shown in a crystal structure to have the first N-terminal proline binding in the P1 pocket of the HLA-DQ2 nonamer binding register. The crystal structure was in agreement with the characteristic nonamer epitope binding pocket of class II MHCs, although studies have shown that the three amino acids prior to the N-terminal proline does play a role in the binding affinity via peptide backbone interactions. Structural information of the HLA-DQ2 suggested that positions 70 (Arg) and 71 (Lys) of the β-chain create a preferred binding motif for negatively charged peptide residues at the P4, P6, and P7 pockets. Consistent with the role of tissue transglutaminase (TG2) in the increase of gliadin immunogenicity (Hourigan, 2006), the deamidation of the gliadin substrate at position 6 Gln to Glu improves binding to HLA-DQ. The negatively charged carboxyl side-chain participates in an extensive hydrogen-bonding network. Due to the proline-rich sequence of α-I gliadin, this epitope is rather protease-resistant. Therefore, α-I gliadin is considered an

effective and potent antigen due to its stability and moderate, but high specificity in HLA-DQ2 binding.

1.2.2 Cellular Response Modulations from Gliadins

The effects of gliadin fragments have a complex influence on the oral tolerance of celiac patients. Not only does gliadin serve as antigen for HLA-DQ2 presentation, but studies have shown that gliadin can induce phenotypic and functional maturation of dendritic cells (subset of antigen-presenting cells for T cell repertoire). Some of these influences include up-regulation of maturation markers (CD80, CD83, CD86, and HLA-DR molecules), increased secretion of chemokines/cytokines (i.e. IL-6, IL-8, IL-10, and TNF-α), phosphorylation of cell growth MAPK signal pathways, and down-regulation of mannose receptor-mediated endocytosis.

1.2.3 Biological Toxicity of Gliadins

A toxic epitope mapped to p31-49 of A-gliadin was found to be responsible for the rapid villous atrophy seen in celiac lesions. Jejunal biopsy of celiac patients after infusion of 200 mg of the p31-49 peptide resulted in histological changes within six hours of infusion (Sturgess, 1994). Later, it was shown that the p31-49 peptide induced the expression of the non-classical MHC molecule MICA on the cell surface of villous epithelium. The effect of p31-49 peptide on the upregulation of MICA was demonstrated to be mediated by cytokine IL-15. Mononuclear cells or enterocytes produces IL-15 in response to the p31-49 peptide. The surface levels of MICA appeared to correlate with the clinical severity of the disease. MICA serves as a ligand for the NKG2D receptor.

Resident intraepithelial lymphocytes in the gut lumen of celiac patients express NKG2D receptors that can interact with MICA on the epithelial cells resulting in lysing of the epithelial cells.

1.3 MHC Peptide Blocker

The initial onset of celiac disease is presumed to be associated with ingested gliadin binding to HLA-DQ molecules on antigen-presenting cells that leads to priming of T lymphocytes towards an autoimmune response. By blocking this occurrence after ingestion of gliadin, the adverse reaction of an autoimmune response can be inhibited in celiac individuals. Studies on NOD mice have tested the peptide blocking potential in class II MHCs to prevent autoimmune diabetes. In these studies, investigators were able to demonstrate, through screening for a synthetic peptide, competitive inhibition in antigen presentation of A^{g7} molecule *in vitro*. They could inhibit the priming for A^{g7}-restricted T cell responses *in vivo* and delay the development of spontaneous autoimmune diabetes in the NOD mice (Vaysburd, 1995). It is noteworthy that in such studies or any studies involving the MHC association of an autoimmune disorder, it is necessary to have an identifiable antigen before any kind of MHC blockade studies can be conducted. Rather than screening for novel peptides as potential MHC peptide blockers (Anderson, 2006), known epitopes for HLA-DQ2 were studied with the intention in developing a rational design peptide blocker (Johansen, 1996). Fortunately, structural data have been obtained for antigen-bound HLA-DQ2 molecule. Crystal structure shows the α- and β-chains forming a heterodimeric HLA-DQ2 molecule with an α-I gliadin epitope bound to its MHC binding groove (Kim, 2004).

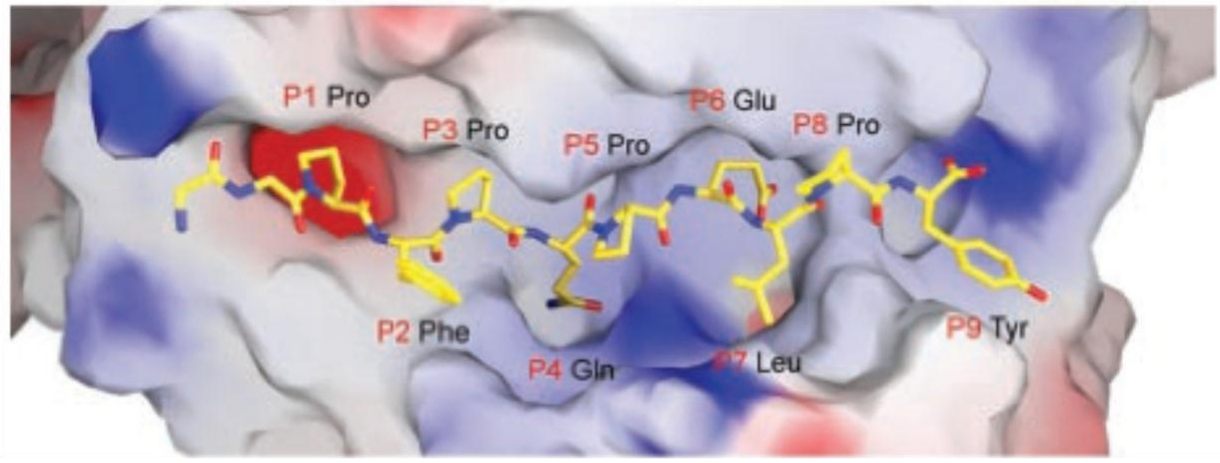

Figure 2: Crystal structure of the α-I gliadin epitope bound to the binding groove of the HLA-DQ2 molecule. *PNAS (2004) 101(12):4175-79*

1.3.1 α-I gliadin-based Rational Design

Although peptides have been identified that competitively bind to HLA-DQ2 with no immunogenicity, these peptides may lack the protease-resistance or the high specificity of the native antigen, α-I gliadin. Since α-I gliadin has been already studied to some extent, it was taken to be a model template sequence in developing a class II MHC blocker. According to the crystal structure of the α-I gliadin -HLA-DQ2 complex, P2 residue (phenylalanine) side-chain is solvent exposed (Kim , 2004). In order to implement some degree of rational design, the P2 residue was chosen as a substitution position. The rationale behind a single amino acid substitution at the P2 position is to obtain an α-I gliadin analog that will have similar binding affinity to the original α-I gliadin and block the T cell recognition to MHC presentation. The incentive for a similar affinity binding α-I gliadin analog will be discussed later (see section 1 4 on Multivalent Principle), whereas the MHC blockade strategy is accomplished through inhibition of T cell recognition.

1.3.2 Important Factors in Construction of MHC Peptide Blocker

MHC blockade of HLA-DQ2 with a peptide blocker should prevent the presentation of gluten peptides to gliadin-specific T cells, but also not be recognizable by any other T cell clones that may arise due to hypersensitivity. To ensure this, peptide blocker should contain relatively big side-chains so that no T cell receptor can dock onto HLA-DQ2-peptide blocker complex due to steric hindrance. Since MHC peptide blockers must persist through the digestive tract in order to target the HLA-DQ2 molecules on antigen presenting cell surface, they not only need to have high-affinity at concentration levels in the intestinal lamina propria, but also have proteolytic stability against the digestive enzymes in the intestinal tract.

1.3.3 Mode of Action in MHC Blockade

In a simplistic model, MHC blockers should exhibit binding affinity to MHC class II molecules that could out-compete the antigenic peptide. Hence, such a blocker can down-regulate the moiety of MHC class II complexes on antigen-presenting cells from being immunogenic. However, it is known that clusters of T cell receptor (TCR)/CD3 complexes form in parallel with clusters of agonist class II MHC/peptide complexes on the surface of antigen presenting cells (Chmielowski, 2002). An alternative model for inhibition of T cell recognition is the redistribution of agonist and null class II MHC/ peptide complexes with antagonist peptides affecting the interface of antigen presenting cells with $CD4^+$ T cells; more specifically naïve T cells. In this alternative model, the inhibition of T cell recognition is not so much involving the cumulative effect of independent single blocking events with MHC blockers on MHC-

peptide immune complexes. Rather, it is a redistribution or the change in characteristics of a cluster/population of MHC-peptide immune complexes that affects the interface compatibility with a T cell. This would imply that inhibition of T cell recognition requires interfering with the intrinsic ability of agonist peptide/MHC complexes from forming appropriate interfaces for T cell recognition. Moreover, such an inhibition would require more than just independent MHC blocking events, which is less likely to affect neighboring MHC molecules from undergoing proper interface formation with agonist peptides. Therefore, the two models aforementioned suggest that the effectiveness of MHC blockade occurs in two-fold: competitive binding of a blocker peptide to its targeted MHC over the antigenic peptide and a multi-level inhibitory mechanism that can account for the intrinsic surface dynamics of multiple antigenic peptide/MHC complexes to form favorable interfaces for T cell docking. A MHC blockade approach should give importance for targeting MHC clusters rather than individual MHC molecules.

1.4 Multivalency Principle

In keeping with an effective class II MHC blockade approach, a multivalency strategy was implemented in testing MHC blockade on HLA-DQ2 blockade. Studies have shown that clustered epitopes in a multivalent fashion can increase the binding affinity towards its target receptor. This increase in binding affinity can be attributed to a "bind and slide" or internal diffusion mechanism. Essentially, the first micro-affinity constant of a multivalent ligand can undergo recapture with the receptor before complete

dissociation of the complex. Effectively, the off rate is reduced and overall binding affinity of the multivalent ligand-receptor interaction is increased.

Thermodynamically, the free energy of binding for a multivalent ligand is the sum of favorable energy of each binding monomer unit, a favorable entropic contribution due to fewer rotational and translation degrees of freedom lost in binding when previous monomer units are already bound, and an unfavorable term as a result of strain or distortion in the multivalent ligand or receptor when achieving the bound state (Dam, 2008). Minimizing this strain or distortion in bound state between a multivalent ligand and its receptors is critical to maximizing the favorable free energy of binding.

In principle, a multivalent-peptide blocker having an increased binding affinity towards HLA-DQ2 can competitively bind over the agonist, α-I gliadin even though the "monomeric" peptide blocker may have similar binding affinity compared to the antigenic α-I gliadin. In addition, the structural architecture from the binding interaction between a multivalent-peptide blocker to HLA-DQ2 can result in a steric occlusion of the MHC surface to T cell recognition. Thus, a multivalent-peptide blocker with increased binding affinity, steric blocking potential, and multiple MHC targeting can fulfill the criteria of an effective and specific HLA-DQ2 blocker.

Synthetic peptide dendrimers are known examples of utilizing the multivalency principle for therapeutic treatments. Synthetic peptide dendrimers have been shown to prevent the development of experimental allergic encephalomyelitis in SJL mice with pre-treatment before the immunization of monomeric encephalitogenic peptide. This

study demonstrates that multiple antigen peptides (MAPs) can be used to elicit robust immune response over monomeric forms of a peptide to prevent autoimmune disease progression (Wegmann, 2008). In Section 1.4.4, the formation of multimer constructs using PAMAM core dendrimers will be discussed.

1.4.1 Maleimide Peptide Cross-linking

Maleimide is a five-member ring compound that contains an unsaturated imide. It can be formed by treating maleic anhydride with an amine derivativefollowed by dehydration. Maleimides that are connected by a molecular unit are useful cross-linking reagents utilized in polymer chemistry. A common method in formation of a maleimide cross-linking reagent undergoes N-alkylation of the imide under Mitsunobu condition. The electrophilic nature of the double bond in the maleimide is a major culprit behind lower yields when attempting to synthesize maleimide-based cross-linkers. By combining Mitsunobu reaction with reversible Diels-Alder reaction (for reversible protection of the double bond in maleimides), 1,3,5-tris(hydroxymethyl)benzene as a trifunctional core molecular unit reacts with the imide of the maleimide to produce a homotrifunctional maleimide based cross-linker (Farha, 2006).

Maleimides can serve as a core linker with chemoselectivity towards sulfhydryl groups. This selective reactivity is established by neutral or acidic pH. At this pH, thiol reactivity is 10^3 times faster than amine reactivity. The unsaturated maleimide has a dienophilic nature as well as being susceptible to Michael-addition reactions.

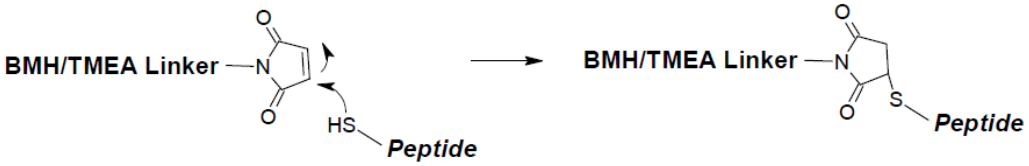

In principle, through protein or peptide engineering, thiol-containing cysteines can be rationally incorporated into target biomolecules to have predictable cross-linking by maleimide-containing cross-linkers. Several other applications have used multifunctional maleimides as an invaluable biochemical tool. Homobifunctional maleimides have been used as molecular rulers between cross-linked amino acids, to facilitate low- protein crystallization, to probe conformational states of proteins, and to enhance potency of protein therapeutics in development of enzyme-antibody conjugates. Two commercially available maleimide-based cross-linkers (Pierce) were used in the study of the multivalent principle: 1,4-bis(maleimido)butane (BMH), a dimer forming cross-linker with thioether linkages and Tris-[2-maleimidoethyl]amine (TMEA), a trimer forming cross-linker with thioether linkages.

1.4.2 Disulfide Peptide Cross-linking

Disulfide bonds are common chemical linkages found in protein tertiary structures. These chemical bonds are formed between two cysteine residues in the protein through oxidative reaction between the two sulfhydryl groups of the cysteine side chains. Although disulfide bonds are relatively stable at physiological pH, it is susceptible to a reductive reaction where the bond is hydrolsed into two separate sulfhydryl groups. A convenient chemical reaction that can yield a disulfide bond is through an activation of a sulfhydryl group. An "activated" sulfhydryl group can be obtained with pyridine-2-thione.

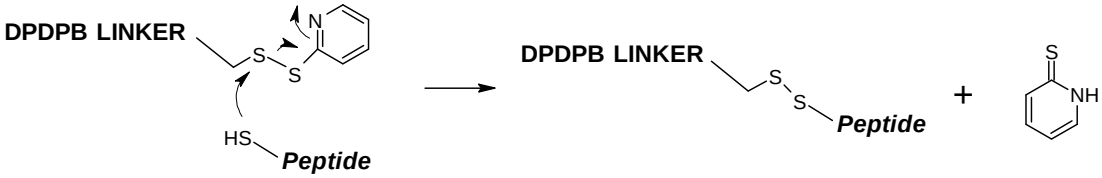

The electron-withdrawing pyridine ring results in a weak bond with the sulfhydryl group, which would be susceptible to nucleophilic attack. Another sulfhydryl-containing compound can undergo nucelophilic attack of the "activated" sulfhydryl group yielding a stable disulfide bond and release of the pyridine-2-thione. This reaction happens at neutral pH or a slightly basic pH with a reported ~60% yield efficiency (Cochran, 2000). Since the liberated pyridine-2-thione has an absorbance at 344 nm, the extent of reaction can be monitored using UV/Vis spectrometry.

The final epitope dimer is spaced by a crossbridge spacer arm of 19.9 angstroms. A commercially available cross-linker with "activated" sulfhydryl groups (Pierce) was used in the study of the multivalent principle: 1,4-di-[3'-(2'-pyridyldithio)propionamido]butane (DPDPB), a dimer forming cross-linker with disulfide linkages.

1.4.3 Vinylsulfone Peptide Cross-linking

An alternative chemical moiety that can form a stable sulfhydryl alkylation linkage, aside from the maleimide chemistry described earlier (1.4.1 Maleimide Peptide Cross-linking), is vinylsulfone groups. Vinylsulfone groups are susceptible to nucleophilic Michael addition reactions. The sulfone group provides electron resonance upon nucleophilic attack that stabilizes the transition state. The product formation such as a thioether bond is irreversible under the reaction conditions.

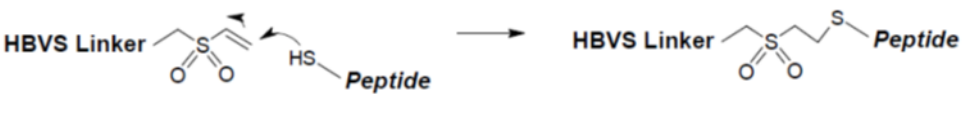

Vinylsulfone is selectively reactive with sulfhydryl groups at pH 7.2-9.2 (Pierce). However, at pH 9.5 and greater, vinylsulfone can react with amines and sulfhydryl groups leading to potentially unwanted side products. A mild basic condition of pH 8.0 with 2% N-methylimidazole in aqueous solution can provide sufficient sulfhydryl selectivity in the Michael addition to vinylsulfone. The two epitopes forming stable thioether linkages with the HBVS are spaced apart by 14.7 angstroms. A commercially available cross-linker with vinylsulfone moiety (Pierce) was used in the study of the multivalency principle: 1,6-hexane-bis-vinylsulfone (HBVS), a dimer forming cross-linker with thioether linkages.

1.4.4 G0 and G1 PAMAM Dendrimer Bifunctional Peptide Cross-linking

A tetrameric core was formed using succinimidyl-[(N-maleimidopropionamido)-tetraethyleneglycol] ester (NHS-PEO_4-Maleimide) and G0 polyamidomine (PAMAM) dendrimer [amide linkage and thioether linkage]. NHS-PEO_4-Maleimide is a heterofunctional linker with a succinimidyl-activated free acid group at one end and a thiol-reactive maleimide group at the other end. The free acid end is primed to react with an amine nucleophile to form an amide linkage and the maleimide will react with a sulfhydryl group to form a thioether linkage.

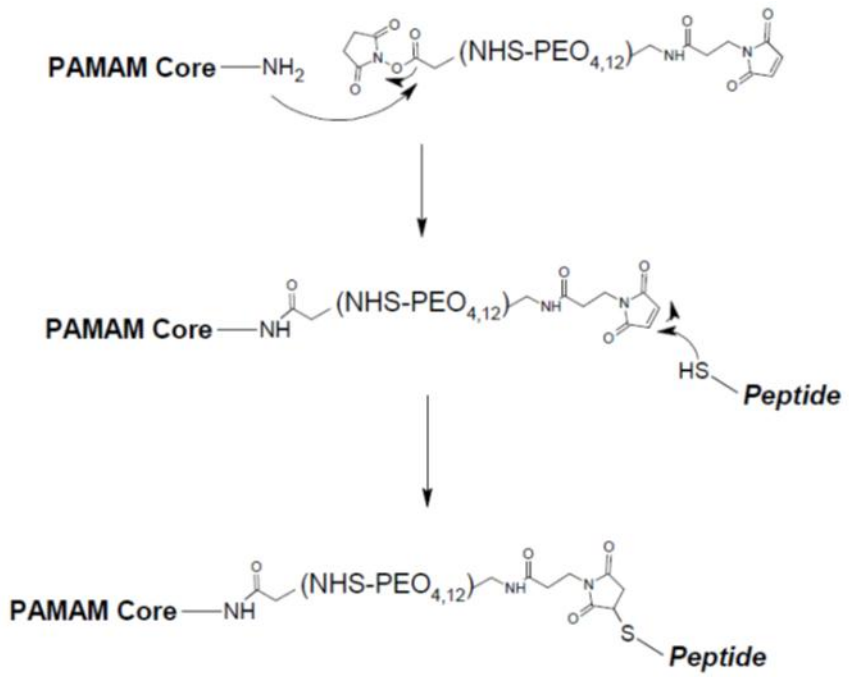

Although both ends of the heterofunctional linker are susceptible to nucleophilic attack by indiscriminate nucleophiles, it is possible to tune the selectivity for the respective ends by maintaining an optimal pH range and keeping a particular reaction order. The latter point suggests that amine reactivity with the succinimidyl-activated free acid should be performed first followed by the thiol addition to the maleimide. The reason that this sequence of selective reactions can occur is due to maintaining an optimal range of pH 7.0. At this pH range, amine reacts readily with the succinimidyl-activated free acid without non-selectively reacting with the maleimide group. Once the heterofunctional linker is devoid of the succinimidyl-activated free acid, then the thiol-reactive maleimide can react with the sulfhydryl containing ligand. Therefore, the tetrameric G0 PAMAM dendrimer core was first reacted with NHS-PEO_4-Maleimide linker followed by Michael addition to the maleimide by the sulfhydryl group of the

cysteine-containing epitope. The maximal spacing distance between two epitope linkages is 68.2 angstroms. Similarly, octamer formation was accomplished with succinimidyl-[(N-maleimidopropionamido)-dodecaethyleneglycol] ester (NHS-PEO_{12}-Maleimide) and G1 polyamidomine (PAMAM) dendrimer (maximal spacing distance between two epitope linkages is 125.8 angstroms).

1.5 Solid Phase Peptide Synthesis (SPPS)

Peptides were synthesized using standard Fmoc solid phase synthesis. Solid phase synthesis on polymeric resin support, developed by Merrifield, is a common chemical strategy to perform chemical couplings while minimizing the need to perform reaction workup/purification steps after each subsequent coupling step. In the case of peptide synthesis, the procedure is a series of repetitive steps of amino acid coupling and selective removal of the α-carbon amine protection group. The basic principle underlying solid phase peptide synthesis can be thought to consist of two main steps: activation/coupling of amino acid and deprotection of N-terminal amine of the growing peptide chain. The growing peptide chain is covalently linked to a resin linker that can be chemically cleaved under specific conditions (i.e. basic or acidic). During peptide synthesis, the added amino acids are orthogonally protected by stable chemical moieties at the α-carbon amine and the potentially reactive side chain functional group. The α-carbon amine is typically protected by either butyloxycarbonyl (BOC) group or fluorenylmethoxycarbonyl (FMOC) group. Depending on whether the chemical stability of the peptidyl-linker is stable in basic or acidic conditions, BOC or FMOC protection would be used, respectively. The only possible functional group left on the amino acid

that is unprotected and allowed to react is the carboxylic acid group. This carboxylic acid group of the subsequent amino acid would undergo a coupling reaction with a free amine of the growing peptide chain. However, a carboxylic acid group does not react readily with a free amine to release an H_2O molecule. Therefore, the carboxylic acid group is chemically activated by reacting with a good leaving group. Upon activation, the free amine of the growing peptide chain can undergo nucleophilic attack of the activated carboxylic acid to form a stable peptidyl bond and with release of the leaving group. After coupling of the amino acid, the peptide chain becomes protected at the N-terminal amine by either a BOC or FMOC group. In order to prime the peptide chain for the next amino acid coupling step, the N-terminal amine protection is removed (BOC removal can be done with hydrogen fluoride/or trifluoroacetic acid and Fmoc removal is accomplished by piperidine solution). Once the N-terminal amine protection group is removed, the growing peptide chain is ready for another cycle of amino acid coupling. When the intended peptide sequence is made with the final N-terminal amine deprotected, the peptide would be isolated by cleaving it off the resin-bound support. Under the cleavage condition, which is orthogonal to the repetitive conditions of amino acid coupling and N-terminal amine deprotection, the chemical moieties of the side-chain protection are simultaneously removed. Finally, after synthesis, theThe final result product is to have obtained the desired peptide sequence in solution. However, due to the limited efficiencies in amino acid coupling and protection group removal, it is necessary to isolate the desired peptide from the crude cleavage mixture using a purification method (Chan and White, 2000).

Step 1: Activation of free amino acid for coupling

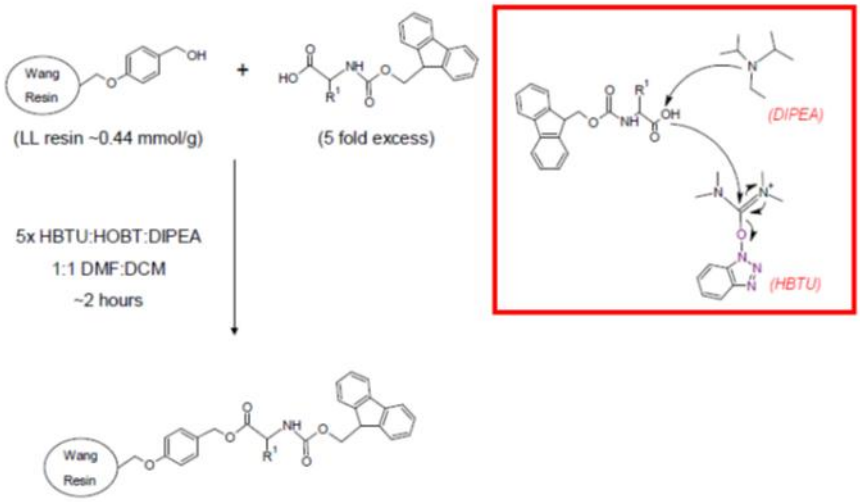

Step 2: Removal of protection group on free amine

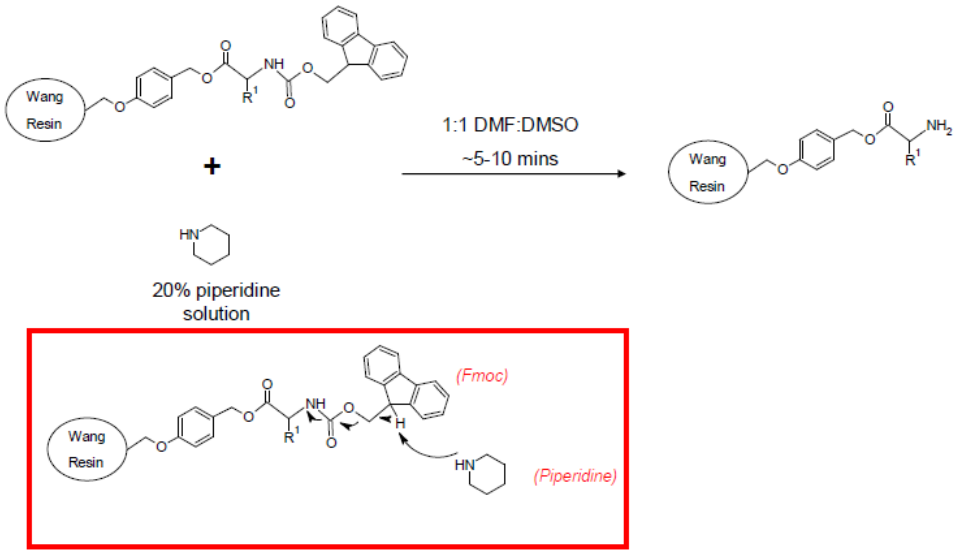

Step 3 (after repetitions of step 1 and 2): Cleavage of peptide off resin and isolation of peptide

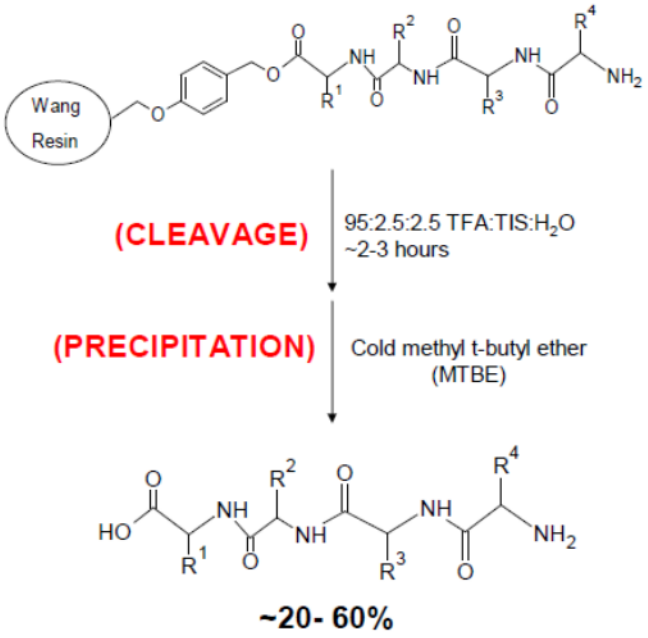

1.6 Specific Aim of Study

The primary objective is to inhibit HLA-DQ2 antigen presentation. Inhibition of antigen presentation will minimize the immunogenic response from T cell recognition and proliferation. To achieve competitive inhibition of antigen presentation, a multivalent approach is taken. A peptide is first identified which bind to HLA-DQ2, but does not illicit an immunogenic response. This peptide will be incorporated as a ligand into various multimers (i.e. dimers, trimers, tetramers, and octamers) forming a multivalent library set. The multivalent constructs are subjected to T cell proliferation assays and antigen presentation inhibition assays to validate the multivalent strategy. It is predicted that the increase in valency of the multivalent constructs will result in enhanced

binding affinity towards HLA-DQ2 through increase local concentration effects and clustering effects. Both effects will lead to competitive inhibition of HLA-DQ2 binding to native epitopes, Inhibition of HLA-DQ2 antigen presentation through competitive multivalent inhibitors can serve as an effective therapeutic for celiac disease.

CHAPTER 2: Materials and Methods

2.1 Synthesis of Peptides/MAPs on Solid-phase Support

Fmoc-protected amino acids and LL Wang resin (100-200 mesh) were from Novabiochem, Merck chemicals. All other solvents and reagents used for solid phase synthesis were from Sigma Aldrich.

2.1.1 Synthesis of NH_2-CGASGPFPQPELPYG, NH_2-GASGPCPQPELPYG, and NH_2-GASGPFPQPELPYGC

LL Wang resin (0.30-0.50 mmol/g resin) was swelled in dichloromethane (DCM) for at least two hours before transferring resin in DCM to a fritted glass filter (<100 mesh) reaction vessel (under vacuum filtration). Resin was re-suspended with dimethylformamide (DMF)/filtered five times. Resin re-suspended in DCM/filtered once. The subsequent Fmoc-amino acid, 2-(1H-Benzotriazole-1-yl)-1,1,3,3-tetramethylaminium hexafluorophosphate (HBTU), and hydroxybenzotriazole (HOBT, omitted in the first amino acid coupling reaction) dissolved in 1:1 DMF:DCM with final addition of diispropylethylamine to mixture before adding to the resin bed (amino acid, HBTU, HOBT, and DIPEA were in five fold excess relative to resin). Reaction vessel was placed on a shaker at ambient temperature and left for 2 hours. Reaction vessel (under vacuum filtration) washed with DMF five times and once with DCM. 20%

piperidine in DMF added to the resin bed and incubated for 2 minutes. Deprotection solution removed under vacuum filtration and washed with DCM. Deprotection repeated once more. Resin bed was washed with DMF five times and once with DCM. The next coupling reaction was carried out in a reiterative manner. The coupling reaction and deprotection reaction was followed until the completion of the intended peptide sequence. The peptide bound resin was re-suspended in DMF and pipette transferred into 50 mL falcon tube. DMF solvent was micro-pipette aspirated from the peptide bound resin. DCM added to the peptide bound resin to remove residue DMF solvent. DCM was micro-pipette aspirated from the peptide bound resin. A cleavage solution of 95:2.5:2.5 TFA:TIS:H_2O added to the resin in the 50 mL falcon tube. Tube was placed on a shaker at ambient temperature and left for 3 hours. Cleavage solution with resin was gravity filtrated through Whatman filter paper. Resin was rinsed twice with TFA cleavage solution. Filtrate was added drop-wise into 100 mL cold methyl tert-butyl ether (MTBE). Precipitate ether solution was aliquoted into two 50 mL falcon tube. Tubes were centrifuged at 4000 rpm for 10 minutes. Supernatant was discarded and pellets were air-dried overnight. Pellets were dissolved in 1:1 acetonitrile:water and frozen in -80 ^{0}C then lyophilized for 2-3 days.

2.1.2 Synthesis of NH_2-GASGPFPQPELPYG MAPs (multiple antigen peptides)

The same procedure was followed as the above solid-phase peptide synthesis, but with a pre-loaded resin rather than an empty Wang resin. A pre-loaded Fmoc-β-alanine-Wang resin (100-200 mesh) was treated with 20% piperidine in DMF to remove the Fmoc protection of the β-alanine amine instead of coupling the first amino acid. After

deprotection of the amine, $(Fmoc)_2$-lysine amino acid derivative was coupled to the resin (the double Fmoc-protection yields two free amine groups after Fmoc removal). The next iteration of amino acid coupling using $(Fmoc)_2$-lysine amino acid provided a branched core of four amine groups. The remaining synthesis followed the standard solid-phase peptide synthesis procedure as described above to obtain the desired sequence. (Note: one modification made to the solid-phase peptide synthesis for the MAPs construct was after each amino acid coupling and wash, ~10-20% acetic anhydride in 1:1 DMF:DCM was added to the resin and incubated for 5-10 minutes before proceeding to another wash and Fmoc removal step. This additional step ensures that any free amine groups left uncoupled from the previous amino acid coupling step will be acetylated. Hence, this minimizes further side reactions that would produce side products of comparable molecular weights to the end product and complicating the purification process.) (Refer to section 2.4.13 for purity and actual yields of this synthesis)

2.2 HPLC Purification *(analytical and crude isolation)*

Crude purification was performed with a LC-10 AT VP, class VP HPLC instrument using Phenomenex C18 Luna hydrophobic column and Phenomenex Biosep S3000 size exclusion column (octamer isolation). Analytical HPLC was performed with a Amersham Ettan LC HPLC instrument using Phenomenex C18 Luna hydrophobic column (purity deterimination).

2.3 Analytical Mass Spectrometry

Molecular mass determination was performed by using LCMS 2010 EV electron spray ionization MS and MALDI TOF -Voyager-DE™ STR Biospectrometry™ Workstation.

2.4 Synthesis of Multivalent Constructs

2.4.1 Synthesis of CGASGPFPQPELPYG DPDPB Dimer *(N-terminus linked)*

A solution of 1,4-Di-[2'-pyridyldithio)propionamido]butane (DPDPB) prepared by dissolving 1.5 mg DPDPB in 100 uL DMSO. 11.5 mg CGASGPFPQPELPYG peptide was dissolved in 400 uL DMSO. DPDPB solution was added to the peptide solution, and left the reaction for 12 hours. Reaction mixture was injected directly into semipreparative C_{18} reverse-phase HPLC column using water-acetonitrile gradient in 0.05-0.04% (v/v) TFA. Purified product peak collected and lypholized as dry sample. Mass determination was confirmed by MALDI-TOF MS and purity check by analytical C_{18} reverse-phase HPLC. Reported 98.5% pure CGASGPFPQPELPYG DPDPB dimer construct was stored at -80^{o} C. Average yields obtained were 31%.

2.4.2 Synthesis of GASGPCPQPELPYG DPDPB Dimer *(P2-residue linked)*

A solution of 1,4-Di-[2'-pyridyldithio)propionamido]butane (DPDPB) prepared by dissolving 1.6 mg DPDPB in 100 uL DMF. 18.2 mg GASGPCPQPELPYG peptide was dissolved in 400 uL DMF. DPDPB solution was added to the peptide solution, and left the reaction for 12 hours. Reaction mixture was injected directly into semipreparative C_{18} reverse-phase HPLC column using water-acetonitrile gradient in

0.05-0.04% (v/v) TFA. Purified product peak collected and lypholized as dry sample. Mass determination was confirmed by MALDI-TOF MS and purity check by analytical C_{18} reverse-phase HPLC. Reported 97.7% pure GASGPCPQPELPYG DPDPB dimer construct was stored at -80^{o} C. Average yields obtained were 58%.

2.4.3 Synthesis of GASGPFPQPELPYGC DPDPB Dimer *(C-terminus linked)*

A solution of 1,4-Di-[2'-pyridyldithio)propionamido]butane (DPDPB) prepared by dissolving 1.5 mg DPDPB in 100 uL DMF. 11.5 mg GASGPFPQPELPYGC peptide was dissolved in 400 uL DMF. DPDPB solution was added to the peptide solution, and left the reaction for 12 hours. Reaction mixture was injected directly into semipreparative C_{18} reverse-phase HPLC column using water-acetonitrile gradient in 0.05-0.04% (v/v) TFA. Purified product peak collected and lypholized as dry sample. Mass determination was confirmed by MALDI-TOF MS and purity check by analytical C_{18} reverse-phase HPLC. Reported 97.4% pure GASGPFPQPELPYGC DPDPB dimer construct was stored at -80^{o} C. Average yields obtained were 46%.

2.4.4 Synthesis of CGASGPFPQPELPYG BMH Dimer *(N-terminus linked)*

A solution of 1,4-bis(maleimido)butane (BMH) prepared by dissolving 0.8 mg BMH in 100 uL acetonitrile. 18.0 mg CGASGPFPQPELPYG peptide was dissolved in 390 uL distilled water with 10 uL acetic acid. BMH solution was added to the peptide solution, and left the reaction for 12 hours. Reaction mixture was injected directly into semipreparative C_{18} reverse-phase HPLC column using water-acetonitrile gradient in 0.05-0.04% (v/v) TFA. Purified product peak collected and lypholized as dry sample. Mass determination was confirmed by MALDI-TOF MS and purity check by analytical

C_{18} reverse-phase HPLC. Reported 96.5% pure CGASGPFPQPELPYG BMH dimer construct was stored at -80^{o} C. Average yields obtained were 30%.

2.4.5 Synthesis of GASGPCPQPELPYG BMH Dimer *(P2-residue linked)*

A solution of 1,4-bis(maleimido)butane (BMH) prepared by dissolving 0.5 mg BMH in 100 uL acetonitrile. 10.9 mg GASGPCPQPELPYG peptide was dissolved in 390 uL distilled water with 10 uL acetic acid. BMH solution was added to the peptide solution, and left the reaction for 12 hours. Reaction mixture was injected directly into semipreparative C_{18} reverse-phase HPLC column using water-acetonitrile gradient in 0.05-0.04% (v/v) TFA. Purified product peak collected and lypholized as dry sample. Mass determination was confirmed by MALDI-TOF MS and purity check by analytical C_{18} reverse-phase HPLC. Reported 98.2% pure GASGPCPQPELPYG BMH dimer construct was stored at -80^{o} C. Average yields obtained were 48%.

2.4.6 Synthesis of GASGPFPQPELPYGC BMH Dimer *(C-terminus linked)*

A solution of 1,4-bis(maleimido)butane (BMH) prepared by dissolving 0.8 mg BMH in 100 uL acetonitrile. 18.0 mg GASGPFPQPELPYGC peptide was dissolved in 390 uL distilled water with 10 uL acetic acid. BMH solution was added to the peptide solution, and left the reaction for 12 hours. Reaction mixture was injected directly into semipreparative C_{18} reverse-phase HPLC column using water-acetonitrile gradient in 0.05-0.04% (v/v) TFA. Purified product peak collected and lypholized as dry sample. Mass determination was confirmed by MALDI-TOF MS and purity check by analytical C_{18} reverse-phase HPLC. Reported 96.0% pure GASGPFPQPELPYGC BMH dimer construct was stored at -80^{o} C. Average yields obtained were 12%.

2.4.7 Synthesis of CGASGPFPQPELPYG HBVS Dimer *(N-terminus linked)*

A solution of 1,6-hexane-bis-vinylsulfone (HBVS) prepared by dissolving 0.3 mg HBVS in 50 uL acetonitrile. 7.3 mg CGASGPFPQPELPYG peptide was dissolved in 440 uL distilled water with 10 uL N-methylimidazole. HBVS solution was added to the peptide solution, and left the reaction for 12 hours. Reaction mixture was injected directly into semipreparative C_{18} reverse-phase HPLC column using water-acetonitrile gradient in 0.05-0.04% (v/v) TFA. Purified product peak collected and lypholized as dry sample. Mass determination was confirmed by MALDI-TOF MS and purity check by analytical C_{18} reverse-phase HPLC. Reported 96.8% pure CGASGPFPQPELPYG HBVS dimer construct was stored at -80^{o} C. Average yields obtained were 53%.

2.4.8 Synthesis of GASGPCPQPELPYG HBVS Dimer *(P2-residue linked)*

A solution of 1,6-hexane-bis-vinylsulfone (HBVS) prepared by dissolving 0.8 mg HBVS in 50 uL acetonitrile. 18.1 mg GASGPCPQPELPYG peptide was dissolved in 440 uL distilled water with 10 uL N-methylimidazole. HBVS solution was added to the peptide solution, and left the reaction for 12 hours. Reaction mixture was injected directly into semipreparative C_{18} reverse-phase HPLC column using water-acetonitrile gradient in 0.05-0.04% (v/v) TFA. Purified product peak collected and lypholized as dry sample. Mass determination was confirmed by MALDI-TOF MS and purity check by analytical C_{18} reverse-phase HPLC. Reported 97.5% pure GASGPCPQPELPYG HBVS dimer construct was stored at -80^{o} C. Average yields obtained were 35%.

2.4.9 Synthesis of GASGPFPQPELPYGC HBVS Dimer *(C-terminus linked)*

A solution of 1,6-hexane-bis-vinylsulfone (HBVS) prepared by dissolving 0.8 mg HBVS in 50 uL acetonitrile. 18.2 mg GASGPFPQPELPYGC peptide was dissolved in 440 uL distilled water with 10 uL N-methylimidazole. HBVS solution was added to the peptide solution, and left the reaction for 12 hours. Reaction mixture was injected directly into semipreparative C_{18} reverse-phase HPLC column using water-acetonitrile gradient in 0.05-0.04% (v/v) TFA. Purified product peak collected and lypholized as dry sample. Mass determination was confirmed by MALDI-TOF MS and purity check by analytical C_{18} reverse-phase HPLC. Reported 96.2% pure GASGPFPQPELPYGC HBVS dimer construct was stored at -80^{o} C. Average yields obtained were 39%.

2.4.10 Synthesis of CGASGPFPQPELPYG TMEA Trimer *(N-terminus linked)*

A solution of Tris-[2-maleimidoethyl]amine (TMEA) prepared by dissolving 0.5 mg TMEA in 100 uL acetonitrile. 11.0 mg CGASGPFPQPELPYG peptide was dissolved in 390 uL distilled water with 10 uL acetic acid. TMEA solution was added to the peptide solution, and left the reaction for 12 hours. Reaction mixture was injected directly into semipreparative C_{18} reverse-phase HPLC column using water-acetonitrile gradient in 0.05-0.04% (v/v) TFA. Purified product peak collected and lypholized as dry sample. Mass determination was confirmed by MALDI-TOF MS and purity check by analytical C_{18} reverse-phase HPLC. Reported 97.8% pure CGASGPFPQPELPYG TMEA trimer construct was stored at -80^{o} C. Average yields obtained were 40%.

2.4.11 Synthesis of GASGPCPQPELPYG TMEA Trimer *(P2-residue linked)*

A solution of Tris-[2-maleimidoethyl]amine (TMEA) prepared by dissolving 0.8 mg TMEA in 100 uL acetonitrile. 18.2 mg GASGPCPQPELPYG peptide was dissolved in 390 uL distilled water with 10 uL acetic acid. TMEA solution was added to the peptide solution, and left the reaction for 12 hours. Reaction mixture was injected directly into semipreparative C_{18} reverse-phase HPLC column using water-acetonitrile gradient in 0.05-0.04% (v/v) TFA. Purified product peak collected and lypholized as dry sample. Mass determination was confirmed by MALDI-TOF MS and purity check by analytical C_{18} reverse-phase HPLC. Reported 96.6% pure GASGPCPQPELPYG TMEA trimer construct was stored at -80^{o} C. Average yields obtained were 25%.

2.4.12 Synthesis of GASGPFPQPELPYGC TMEA Trimer *(C-terminus linked)*

A solution of Tris-[2-maleimidoethyl]amine (TMEA) prepared by dissolving 0.7 mg TMEA in 100 uL acetonitrile. 18.3 mg GASGPFPQPELPYGC peptide was dissolved in 390 uL distilled water with 10 uL acetic acid. TMEA solution was added to the peptide solution, and left the reaction for 12 hours. Reaction mixture was injected directly into semipreparative C_{18} reverse-phase HPLC column using water-acetonitrile gradient in 0.05-0.04% (v/v) TFA. Purified product peak collected and lypholized as dry sample. Mass determination was confirmed by MALDI-TOF MS and purity check by analytical C_{18} reverse-phase HPLC. Reported 96.0% pure GASGPFPQPELPYGC TMEA trimer construct was stored at -80^{o} C. Average yields obtained were 50%.

2.4.13 Synthesis of NH_2-GASGPFPQPELPYG MAPs (multiple antigen peptides)

Dried pellet was dissolved in 5-10% DMF in 70:30 H_2O: acetonitrile and injected directly into semipreparative C_{18} reverse-phase HPLC column using water-acetonitrile gradient in 0.05-0.04% (v/v) TFA. Purified product peak collected and lypholized as dry sample. Mass determination was confirmed by MALDI-TOF MS and purity check by analytical C_{18} reverse-phase HPLC. Reported 94.8% pure NH_2-GASGPFPQPELPYGC MAPs tetramer construct was stored at -80^o C. Average yields obtained were < 1%.

2.4.14 Synthesis of CGASGPFPQPELPYG G0 Tetramer *(N-terminus linked)*

A linker solution of succinimidyl-[(N-maleimidopropionamido)-tetraethyleneglycol] ester (NHS-PEO_4-Maleimide) prepared by dissolving 3.0 mg NHS-PEO_4-Maleimide in 200 uL acetonitrile and 100 uL distilled water. At 2 hour intervals, 2 uL of 20% G0 polyamidomine (G0 PAMAM) dendrimer in methanol was added into the linker solution. A total of 8 uL G0 PAMAM solution was added into the linker solution. 22.0 mg CGASGPFPQPELPYG peptide was dissolved into 400 uL distilled water and 100 uL acetonitrile with 14 uL acetic acid. Linker solution was added to the peptide solution, and left the reaction for 12 hours. Reaction mixture was injected directly into semipreparative C_{18} reverse-phase HPLC column using water-acetonitrile gradient in 0.05-0.04% (v/v) TFA. Purified product peak collected and lypholized as dry sample. Mass determination was confirmed by MALDI-TOF MS and purity check by analytical C_{18} reverse-phase HPLC. Reported 98.3% pure CGASGPFPQPELPYG G0 tetramer construct was stored at -80^o C. Average yields obtained were 7%.

2.4.15 Synthesis of GASGPCPQPELPYG G0 Tetramer *(P2-residue linked)*

A linker solution of succinimidyl-[(N-maleimidopropionamido)-tetraethyleneglycol] ester (NHS-PEO_4-Maleimide) prepared by dissolving 6.0 mg NHS-PEO_4-Maleimide in 200 uL acetonitrile and 100 uL distilled water. At 1 hour intervals, 2 uL of 20% G0 polyamidomine (G0 PAMAM) dendrimer in methanol was added into the linker solution. A total of 12 uL G0 PAMAM solution was added into the linker solution. 38.8 mg GASGPCPQPELPYG peptide was dissolved into 400 uL distilled water with 14 uL acetic acid. Linker solution was added to the peptide solution, and left the reaction for 6 hours. Reaction mixture was injected directly into semipreparative C_{18} reverse-phase HPLC column using water-acetonitrile gradient in 0.05-0.04% (v/v) TFA. Purified product peak collected and lypholized as dry sample. Mass determination was confirmed by MALDI-TOF MS and purity check by analytical C_{18} reverse-phase HPLC. Reported 95% pure GASGPCPQPELPYG G0 tetramer construct was stored at -80^o C. Average yields obtained were 28%.

2.4.16 Synthesis of GASGPFPQPELPYGC G0 Tetramer *(C-terminus linked)*

A linker solution of succinimidyl-[(N-maleimidopropionamido)-tetraethyleneglycol] ester (NHS-PEO_4-Maleimide) prepared by dissolving 6.0 mg NHS-PEO_4-Maleimide in 200 uL acetonitrile and 100 uL distilled water. At 3 hour intervals, 2 uL of 20% G0 polyamidomine (G0 PAMAM) dendrimer in methanol was added into the linker solution. A total of 6 uL G0 PAMAM solution was added into the linker solution. 35.3 mg GASGPFPQPELPYGC peptide was dissolved into 400 uL distilled water with 14 uL acetic acid. Linker solution was added to the peptide solution, and left the reaction

for 6 hours. Reaction mixture was injected directly into semipreparative C_{18} reverse-phase HPLC column using water-acetonitrile gradient in 0.05-0.04% (v/v) TFA. Purified product peak collected and lypholized as dry sample. Mass determination was confirmed by MALDI-TOF MS and purity check by analytical C_{18} reverse-phase HPLC. Reported 95.6% pure GASGPFPQPELPYGC G0 tetramer construct was stored at -80^{o} C. Average yields obtained were 27%.

2.4.17 Synthesis of CGASGPFPQPELPYG G1 Octamer *(N-terminus linked)*

A linker solution of succinimidyl-[(N-maleimidopropionamdio)-dodecaethyleneglycol]ester (NHS-PEO_{12}-Maleimide) prepared by dissolving 6.0 mg NHS-PEO_{12}-Maleimide in 200 uL acetonitrile and 100 uL distilled water. At 2 hour intervals, 2 uL of 20% G1 polyamidomine (G1 PAMAM) dendrimer in methanol was added into the linker solution. A total of 10 uL G1 PAMAM solution was added into the linker solution. 30.0 mg CGASGPFPQPELPYG peptide was dissolved into 400 uL distilled water with 14 uL acetic acid. Linker solution was added to the peptide solution, and left the reaction for 12 hours. Reaction mixture was first purified using size-exclusion chromatography (SEC-3000 gel filtration column). Collected fraction was then injected into semipreparative C_{18} reverse-phase HPLC column using water-acetonitrile gradient in 0.05-0.04% (v/v) TFA. Purified product peak collected and lypholized as dry sample. Mass determination was confirmed by MALDI-TOF MS and purity check by analytical C_{18} reverse-phase HPLC. CGASGPFPQPELPYG G1 octamer construct was stored at -80^{o} C. Average yields obtained were 8%. No reported purity.

2.4.18 Synthesis of GASGPCPQPELPYG G1 Octamer *(P2-residue linked)*

A linker solution of succinimidyl-[(N-maleimidopropionamdio)-dodecaethyleneglycol]ester (NHS-PEO_{12}-Maleimide) prepared by dissolving 6.0 mg NHS-PEO_{12}-Maleimide in 200 uL acetonitrile and 100 uL distilled water. At 2 hour intervals, 2 uL of 20% G1 polyamidomine (G1 PAMAM) dendrimer in methanol was added into the linker solution. A total of 10 uL G1 PAMAM solution was added into the linker solution. 30.0 mg GASGPCPQPELPYG peptide was dissolved into 400 uL distilled water with 14 uL acetic acid. Linker solution was added to the peptide solution, and left the reaction for 12 hours. Reaction mixture was first purified using size-exclusion chromatography (SEC-3000 gel filtration column). Collected fraction was then injected into semipreparative C_{18} reverse-phase HPLC column using water-acetonitrile gradient in 0.05-0.04% (v/v) TFA. Purified product peak collected and lypholized as dry sample. Mass determination was confirmed by MALDI-TOF MS and purity check by analytical C_{18} reverse-phase HPLC. CGASGPFPQPELPYG G1 octamer construct was stored at -80^{o} C. Average yields obtained were 20%. No reported purity.

2.4.19 Synthesis of GASGPFPQPELPYGC G1 Octamer *(C-terminus linked)*

A linker solution of succinimidyl-[(N-maleimidopropionamdio)-dodecaethyleneglycol]ester (NHS-PEO_{12}-Maleimide) prepared by dissolving 12.0 mg NHS-PEO_{12}-Maleimide in 400 uL acetonitrile and 200 uL distilled water. At 2 hour intervals, 2 uL of 20% G1 polyamidomine (G1 PAMAM) dendrimer in methanol was added into the linker solution. A total of 20 uL G1 PAMAM solution was added into the linker solution. 50.0 mg GASGPFPQPELPYGC peptide was dissolved into 500 uL

distilled water with 14 uL acetic acid. Linker solution was added to the peptide solution, and left the reaction for 18 hours. Reaction mixture was first purified using size-exclusion chromatography (SEC-3000 gel filtration column). Collected fraction was then injected into semipreparative C_{18} reverse-phase HPLC column using water-acetonitrile gradient in 0.05-0.04% (v/v) TFA. Purified product peak collected and lypholized as dry sample. Mass determination was confirmed by MALDI-TOF MS and purity check by analytical C_{18} reverse-phase HPLC. GASGPFPQPELPYGC G1 octamer construct was stored at -80^{o} C. Average yields obtained were 14%. No reported purity.

2.5 Competitive Binding Assay

^{125}I-labeled peptide (30,000 cpm; 1-5 nM) were incubated with DQ2 (1 μM) overnight at 37^{o}C in the presence of a mixture of protease inhibitors. Various concentrations of the unlabeled peptides were added to inhibit binding of the ^{125}I-labeled peptide. DQ2 molecules and peptides were separated on Sephadex G-50 Superfine (Pharmacia Biotech) mini spin columns. The radioactivity was counted, and the concentrations of the competing peptides required to give 50% inhibition of binding of the indicator peptide (IC_{50}) were calculated (Qiao, 2004).

2.6 T Cell proliferation Assay

HLA-DR3/DQ2 homozygous Epstein-Barr virus transformed B-lymphoblastoid cell lines (CD114) were used as antigen-presenting cells. The cells were either γ-irradiated or fixed with 1% paraformaldehyde for 10 minutes or with 0.05% glutaraldehyde for 90 seconds using 0.2 M glycine to quench the reaction. The antigen

presenting cells were incubated with the appropriate peptides/multimer constructs overnight in 60 µL media containing 10% fetal bovine serum/2% human serum or 15% human serum, penicillin, and streptomycin at a cell density of 2 x 10^6 cells/mL in 96-well plates. The next day, the volume was doubled to yield a cell density of 1 x 10^6 cells/mL, 50 µL of which was placed into a U-bottom 96-well plate. An equal volume of T cells (50 µL of 1 x 10^6 cells/mL) was added to each well, and cells were incubated at 37^{o}C and 5% CO_2 for 48 hours, at which time 0.5 µCi/well of [methyl-^{3}H] thymidine (Amersham, TRK120) or 1 µCi/well of [methyl-^{3}H] thymidine (Hartmann Analytic) was added. Cells were incubated for an additional 12-14 hours and then frozen. After thawing, incorporated thymidine was collected on a filter mat (Wallac), using a Tomtec cell harvester, and counted using a Wallac 1205 Betaplate or Wallac 1450 MicroBeta TriLux liquid scintillation counter (Xia, 2006).

CHAPTER 3: Results and Discussion

3.1 Competitive Binding Assay on α-I gliadin Analogs

GASGPFPQPELPYG (RY111) was chosen as the monomer for the multivalent library constructs. The binding affinity of this peptide has a moderate IC50 among the range of IC50's exhibited from the α-I gliadin analog set (Table 1). A moderate binding affinity is desired because increases in binding affinity through a multivalency effect can be better observed with moderate binding affinity.

	17.01.2008	23.01.2008	28.01.2008
	10-fold IC50 (µM)	3-fold IC50 (µM)	3-fold IC50 (µM)
P1886 GASGPFPQPELPYG = RY111	0,8	1,3	0,8
P1887 GASGPAPQPELPYG =	0,5	1	0,8
P1888 GASGPEPQPELPYG =	5,8	<1,67	0,6
P1889 GASGPRPQPELPYG =	1,3	2,2	1,7
P1890 GASGPWPQPELPYG= RY115	0,8	1,3	0,8
P1281 LQPFPQPELPY	2,9	4,8	2,7
P198 KPLLIIAEDVEGEY	0,1	0,06	0,06

Table 1: Above α-I gliadin analogs were tested for binding to HLA-DQ2 molecules in a competitive binding assay with the IC50 values (µM) given for 10-fold and 3-fold titrations. P1281 is the positive control peptide and P198 is the negative control peptide. *(Courtesy of Ludwig Sollid and Elin Bergseng)*

3.2 T cell Proliferation Assay on α-I gliadin Analogs

None of the α-I gliadin analog peptides illicit an immunogenic response in a T cell proliferation assay using T cell clone (TCC 380.E37).

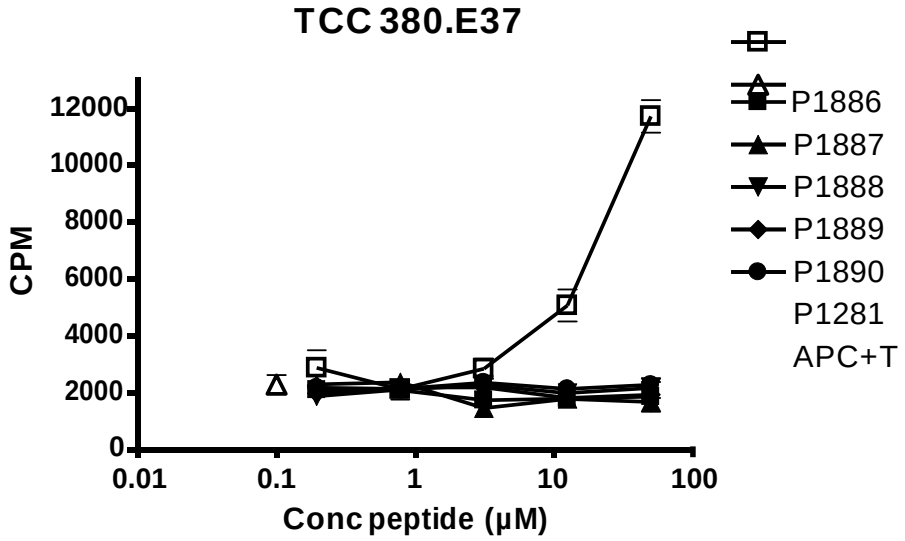

P1886 GASGPEPQPELPYG (RY111)
P1887 GASGPAPQPELPYG (RY112)
P1888 GASGPEPQPELPYG (RY113)
P1889 GASGPRPQPELPYG (RY114)
P1890 GASGPWPQPELPYG (RY115)
P1281 LQPFPQPELPY

Figure 3: T cell proliferation assay on the α-I gliadin analog peptides at various concentrations. No immunogenic response from any of the peptides for the DQ2-α-I-specific T cell clone (TCC 380.E37). P1281 is a positive control. *(Courtesy of Ludwig Sollid and Elin Bergseng)*

3.3 Multivalent Library/ Purity and Yield

Monomer:

RY-111

RY-211

RY-311

Dimer:

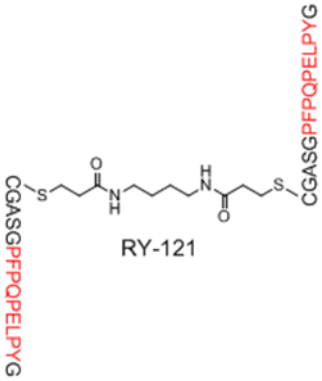

RY-121

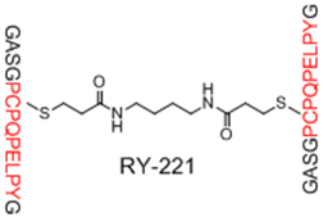

RY-221

GASGPFPQPELPYGC
S
O
N
H
N
H
O
S
GASGPFPQPELPYGC
RY-321

CGASGPFPQPELPYG
S
O
N
O
O
N
O
S
CGASGPFPQPELPYG
RY-122

GASGPCPQPELPYG
S
O
N
O
O
N
O
S
GASGPCPQPELPYG
RY-222

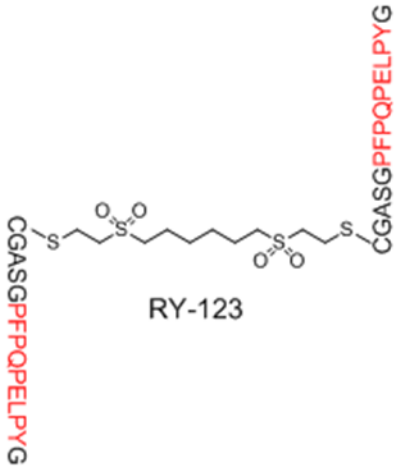
CGASGPFFPQPELPYG
CGASGPFFPQPELPYG
RY-123

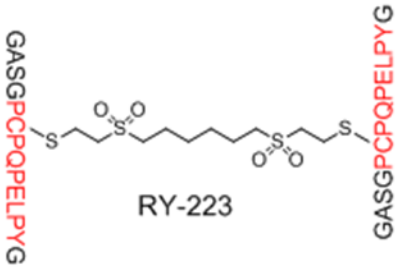
GASGPCPQPELPYG
GASGPCPQPELPYG
RY-223

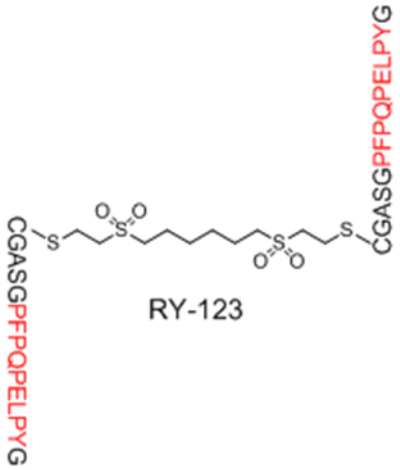
CGASGPFFPQPELPYG
CGASGPFFPQPELPYG
RY-123

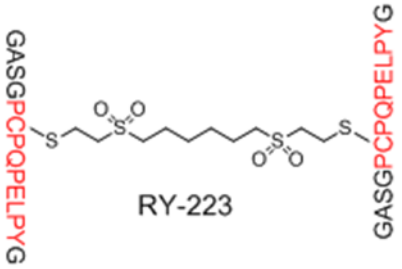
GASGPCPQPELPYG
GASGPCPQPELPYG
RY-223

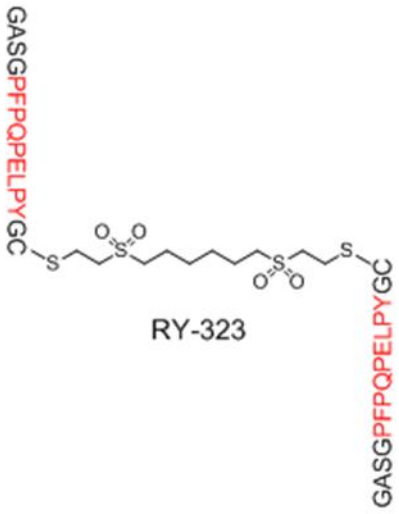
GASGPFFPQPELPYGC
GASGPFFPQPELPYGC
RY-323

Trimer:

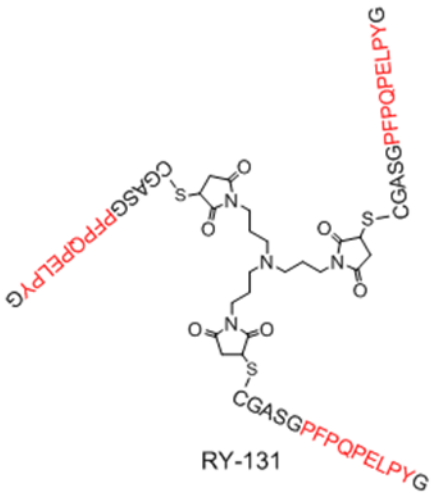

RY-131

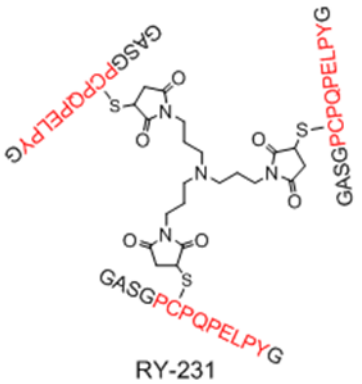

RY-231

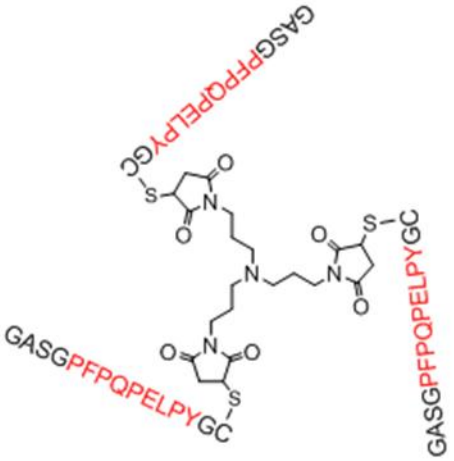

RY-331

Tetramer:

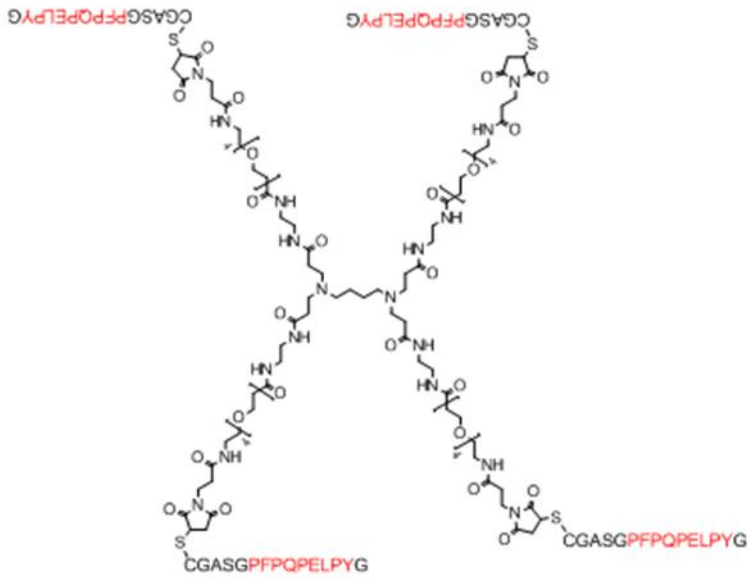

RY-141

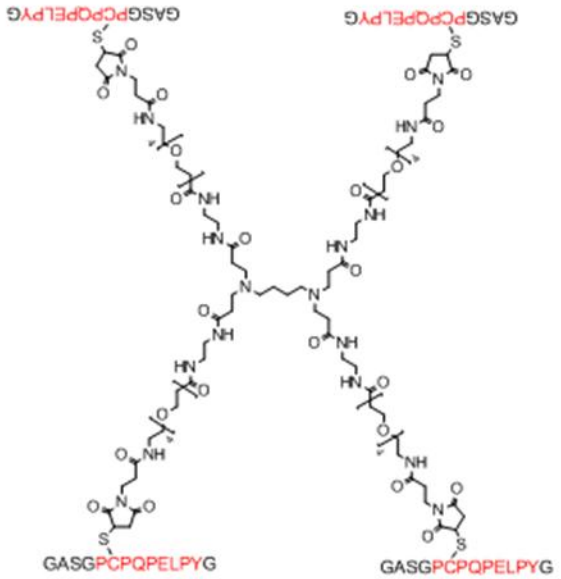

RY-241

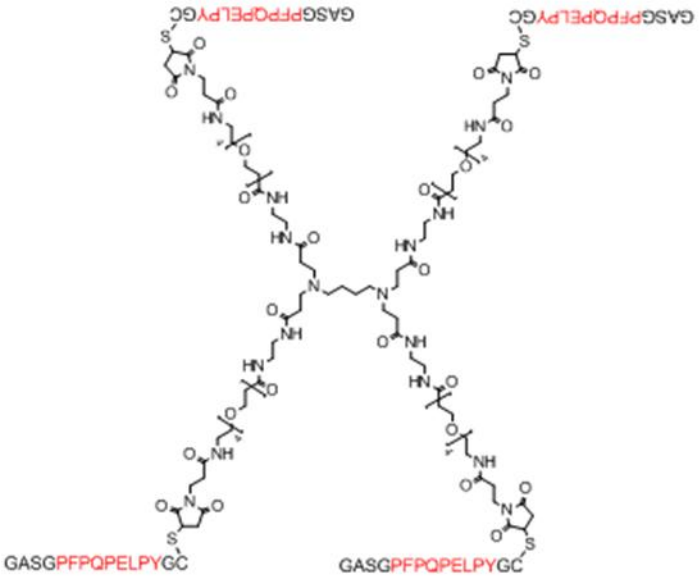
GASGPFPQPELPYGC
GASGPFPQPELPYGC
GASGPFPQPELPYGC
GASGPFPQPELPYGC

RY-341

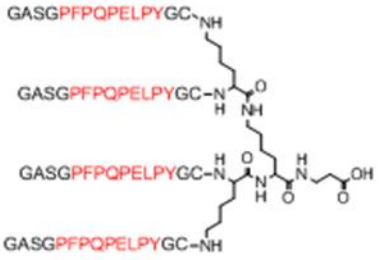
GASGPFPQPELPYGC
GASGPFPQPELPYGC
GASGPFPQPELPYGC
GASGPFPQPELPYGC

RY-441

Octamer:

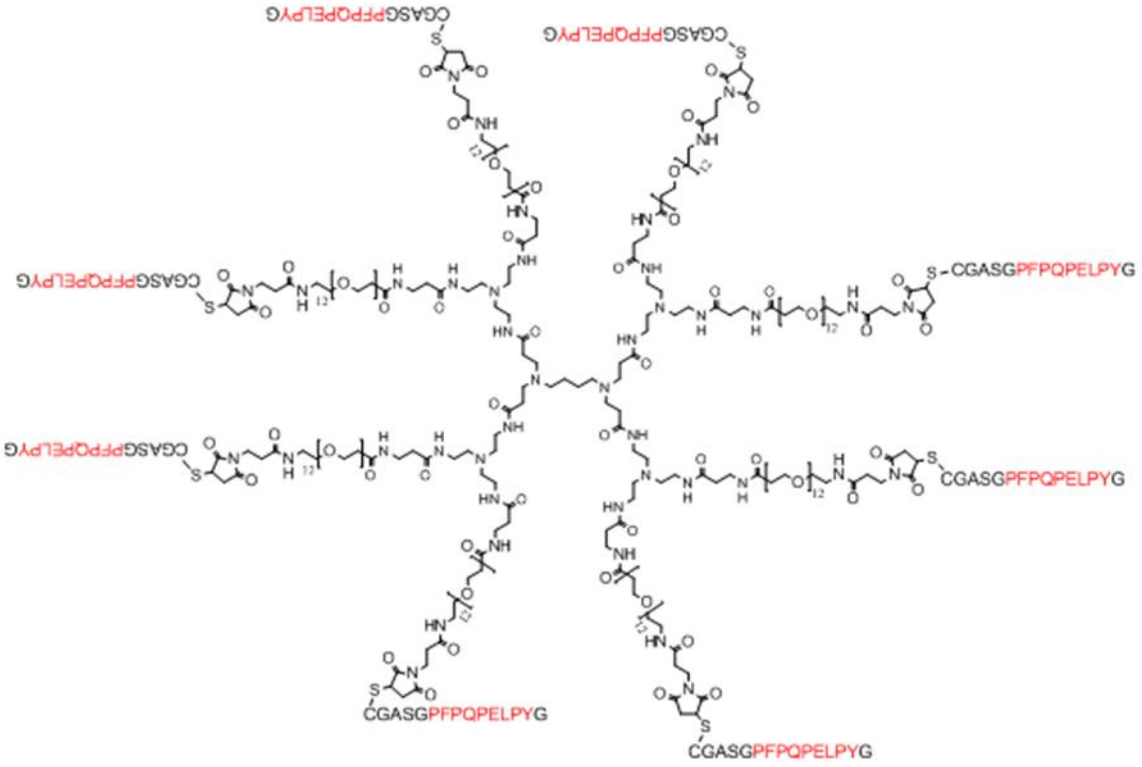

RY-181

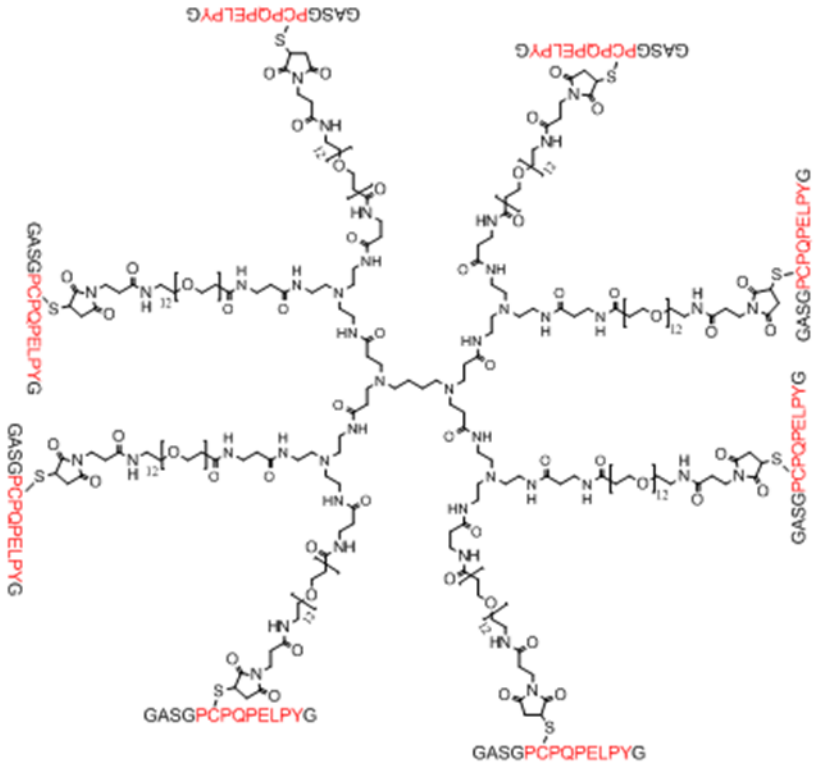

RY-281

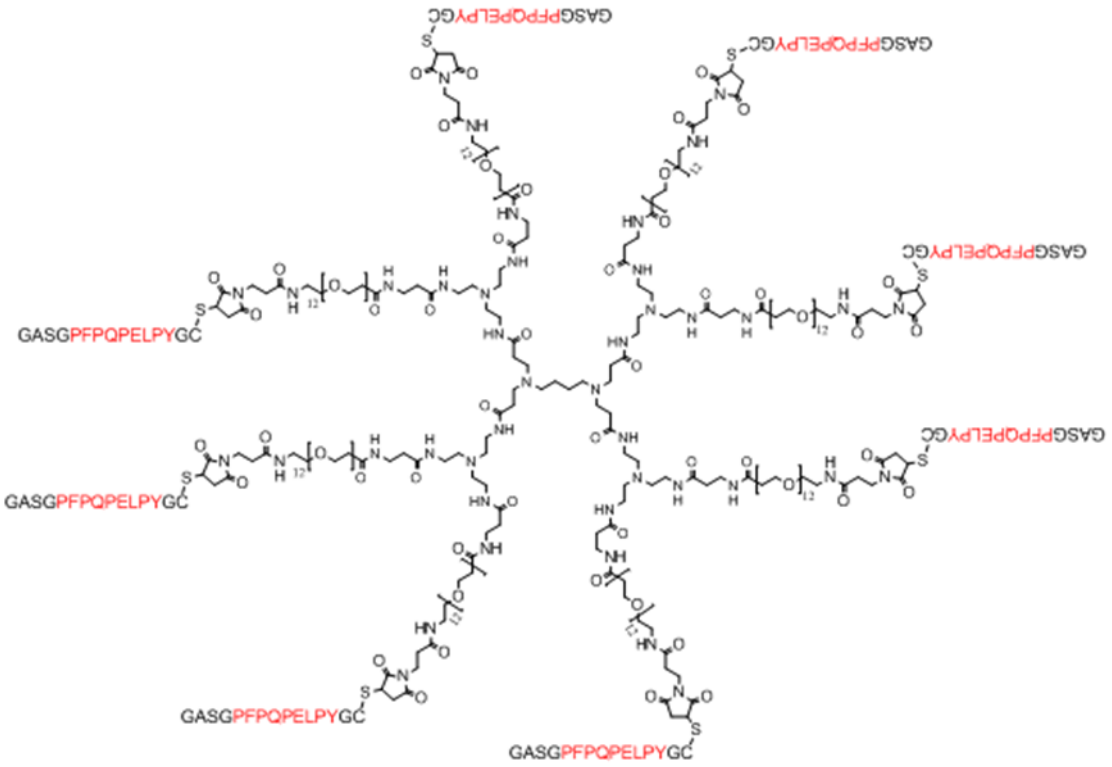

RY-381

Figure 4: Multivalent Library Set

	Construct #	*Molar abs. at 280nm ε (cm^{-1} M^{-1})	Calculated M.W.	Experimental M.W.	Percentage Yield	Purity (%)	
Monomer	RY-111	1,490	1,574.68	1,575.71	~30%	98	
	RY-211	1,490	1,427.61	1,428.64	~30%	98	
	RY-311	1,490	1,574.68	1,575.74	~30%	97	
Dimer	RY-121	3,230	3,298.06	3,298.68	31%	98	
	RY-122	2,980	3,313.65	3,336.31	30%	97	
	RY-123	2,980	3,303.74	3,307.65	53%	97	
	RY-221	3,230	3,003.92	3,004.21	58%	98	
	RY-222	2,980	3,020.29	3,020.23	48%	98	
	RY-223	2,980	3,009.60	3,013.10	35%	98	
	RY-321	3,230	3,298.06	3,293.90	46%	97	
	RY-322	2,980	3,313.65	3,311.17	12%	96	
	RY-323	2,980	3,303.74	3,300.20	39%	96	
Trimer	RY-131	4,470	4,942.40	4,956.86	40%	99	
	RY-231	4,470	4,501.19	4,507.44	25%	97	
	RY-331	4,470	4,942.40	4,939.64	50%	96	
Tetramer	RY-141	5,960	8,179.40	8,178.66	7%	98	
	RY-241	5,960	7,591.12	7,588.95	28%	95	
	RY-341	5,960	8,179.40	8,177.09	27%	96	
	RY-441	5,960	6,064.19	6,067.02	< 1%	95	
Octamer	RY-181	11,920	19,574.48	19,589.54	8%	N/A	
	RY-281	11,920	18,397.90	18,039.71	20%	N/A	
	RY-381	11,920	19,574.48	19,585.94	14%	N/A	

Table 2: Percentage Yield and purity of the multivalent library set, including calculated, experimental M.W. and molar absorptivity (ε).

3.4 Biological Assay on Multivalent Library

3.4.1 T cell Proliferation Assay on Multivalent Library

Irradiated $CD114^+$ antigen-presentation cells (APCs) were incubated with 10 μM of multivalent constructs, including the monomers. DQ2-α-I specific T cell clone (TCC 380.E2) proliferation is a measure of the immunogenicity of the antigen presentation. All the constructs in the library, except the GASGPC(t-butyl)PELPYG monomer (RY211), resulted in an immunogenic response (Figure 5). Interestingly, upon multimerization of RY211 monomer, there is increased immunogenicity. Furthemore,

this increase in immunogenicity relative to the monomer is not uniform across the various multivalent constructs. For example, of the three dimer constructs (RY221, RY222, and RY223), the dimer with the longest linker (19.9 Angstroms, DPDPB linker, RY221) has the highest immunogenicity. Whereas the dimer with the shortest linker (13 Angstroms, BMH linker, RY222) , shows the least increase in immunogenicity. This finding supports two assumptions: 1) the binding affinity of a multimer increases relative to a monomer and 2) the distance between two monomer epitopes in a dimer is critical to achieve enhanced binding. Moreover, the latter point may imply that the effect of increased affinity binding is not just simply due to an increase in "local concentration" of the epitopes, but rather simultaneous binding of the epitopes to mulitple targeted HLA-DQ2s (clustering effect). If we ignore the clustering effect, it can be assumed that the increase in valency of a construct will increase its binding affinity due to higher "local concentration". However, if clustering effect is added into the assumption, which is dependent on distance/orientation, increases in binding affinity cannot be evaluated on the basis of valency alone, but through both valency and optimal orientations. It is in this consideration that one can expect to see a construct of lower valency with optimal orientation having better binding affinity than a construct with higher valency but suboptimal orientation. For example, the DPDPB dimer (RY221) exhibits higher immunogenicty compared to the TMEA trimer (RY223). Despite the increase in valency from a dimer to a trimer, the trimer construct still has lower binding affinity. Additional examples are the tetramer (RY241) and octamer (RY281) constructs which exhibit similar immunogenicity as the DPDPB dimer (RY221). This can be partly explained through the clustering effect. The trimer has a less optimal orientation for simultaneous

binding compared to the dimer, resulting in a lower binding affinity. However, the tetramer and octamer binding affinities are similar to the dimer binding affinity because the opposing effects of increase in binding affinity due to valency and the less optimal binding orientation/clustering result may cancel each other out. Although the contribution of a higher valency in binding affinity is independent of the clustering effect, it is not possible to decipher the two effects independently in a T cell proliferation assay. The increase in binding affinity through an increase in valency without clustering effects can be masked by the steric hindrance of the multimer to T cell recognition. This would show up as "no effect" in a T cell proliferation assay. This is a limitation of using a T cell proliferation assay in studying multivalency effects.

An α-I gliadin, LQPFPQPELPY, peptide (P1281) at 10 μM was used as a control in the T cell proliferation assay. Other than GASGPFPQPELPYGC(t-butyl) (RY311) monomer, the control gave the highest immunogenicity response in the assay.

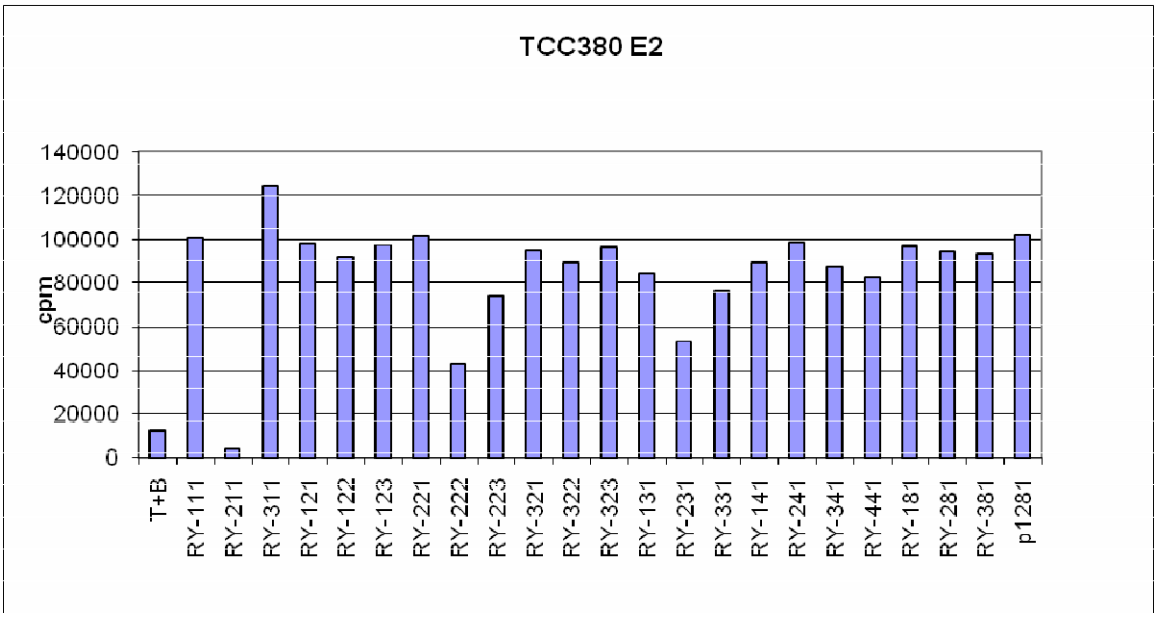

Figure 5: Recognition of multivalent constructs by DQ2-α-I specific T cell clone (TCC 380.E2). The peptides were tested at 10μM. P1281: LQPFPQPELPY *(Courtesy of Ludwig Sollid and Elin Bergseng)*

3.4.2 Antigen-Presentation Inhibition Assay with Multivalent Library Subset (irradiated APCs)

Irradiated $CD114^+$ antigen-presentation cells (APCs) were treated with 2.5 μM γ-I gliadin, PEQPQQSFPEQERP, epitope in the presence of varying concentrations of C(t-butyl)GASGPFPQPELPYG (RY111) –monomer, -dimer (RY121), -trimer (RY131), -tetramer (RY141), and –octamer (RY181) constructs. DQ2- γ-I specific T cell clone (TCC 423.1.3.8) proliferation was a measure of the multivalent blocking potential towards the antigen presentation of γ-I gliadin (Figure 6). This subset of constructs from the multivalent library did not block the γ-I gliadin presentation on irradiated APCs. T cell proliferation is the same across the different concentration of the multivalent constructs (RY111 monomer, RY121 dimer, RY131 trimer, and RY 141 tetramer, and RY181 octamer). There are several possibilities that can explain this result. The first is to realize that from Section 3.4.1, Figure 5, this subset of multivalent library constructs

overall illicit similar immunogenic response. The similar immunogenic response may imply that these constructs have similar binding affinities. With similar binding affinities, this subset of multivalent constructs would be expected to block the γ-I gliadin presentation in a similar fashion. Secondly, irradiated APCs can have biological processes such as endocytosis and MHC turnover that would interfere with the effects of blocking from the multivalent constructs. Endocytosis of the multivalent constructs can lead into endosomal-lysosomal degradation paths that render the constructs as metabolized remnants of non-binders toward HLA-DQ2. Alternatively, the multivalent constructs bind to HLA-DQ2 molecules on the cell surface, but due to MHC turnover, the blocking of antigen presentation with the multivalent constructs is non-effective.

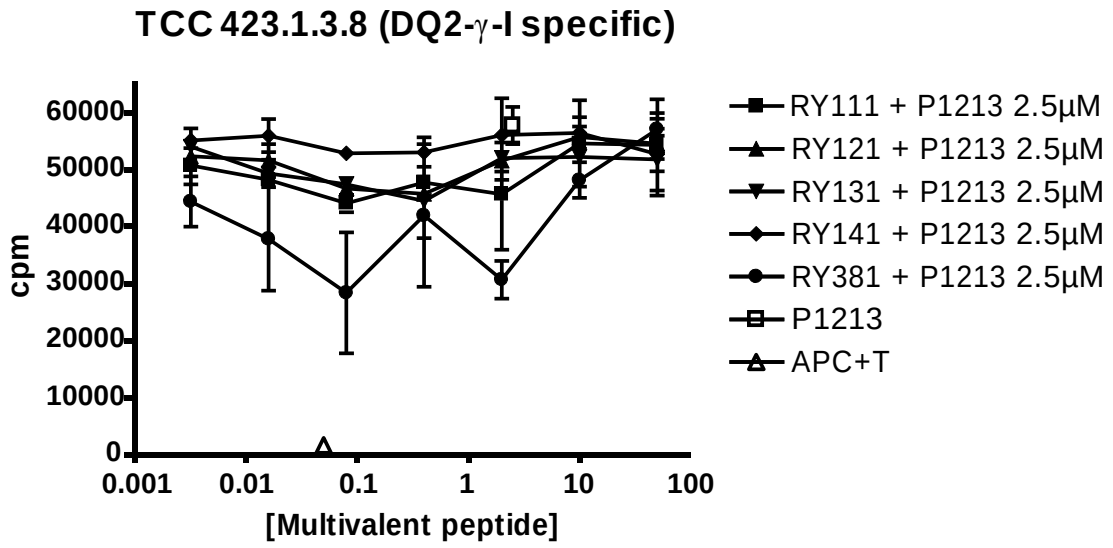

Figure 6: Inhibition of T-cell proliferation by the multivalent peptides. The T-cell clone 423.1.3.8 (specific for the DQ2-γ-I gliadin epitope) was stimulated with 2.5µM PEQPQQSFPEQERP (P1213, DQ2-γ-I gliadin epitope) in the presence of increasing concentration of multivalent peptides RY111, RY121, RY131, RY141 and RY381. APC: Irradiated CD114. *(Courtesy of Ludwig Sollid and Elin Bergseng)*

3.4.3 Antigen-Presentation Inhibition Assay with Multivalent Library Subset (fixed APCs)

Fixed $CD114^+$ antigen-presentation cells (APCs) were treated with 2 μM γ-IV gliadin, FSQPEQEFPQPQ, epitope in the presence of varying concentrations of GASGC(t-butyl)FPQPELPYG (RY211) –monomer, -dimer (RY221), -trimer (RY231), -tetramer (RY241), and –octamer (RY281) constructs. DQ2- γ-IV specific T cell clone (TCC 430.1.122) proliferation was a measure of the multivalent blocking potential towards the antigen presentation of γ-IV gliadin (Figure 7). Although this multivalent subset inhibited anitgen presentation of γ-IV gliadin compared to the monomer, there was no difference in inhibition between dimer, trimer, tetramer, and octamer. Since the inhibition is the same among the multimers, it is likely that the increase in local concentration is responsible for the inhibition rather than a clustering effect. The lack of effect due to clustering can be a result of non-optimal orientation of the multivalent construct as well as the fixed orientation of the HLA-DQ2 molecules. It would be of interest to observe the immunogenic response of TCC 380.E2 (T cells used in Section 3.4.1) towards this multivalent library subset using fixed APCs, since similar inhibition (Figure 7) would imply similar binding affinity. If this were true, the immunogenic response would be similar among this multivalent subset when using fixed APCs, unlike the differential immunogenic response profile seen with this same multivalent subset using irradiated APCs (Section 3.4.1, Figure 5).

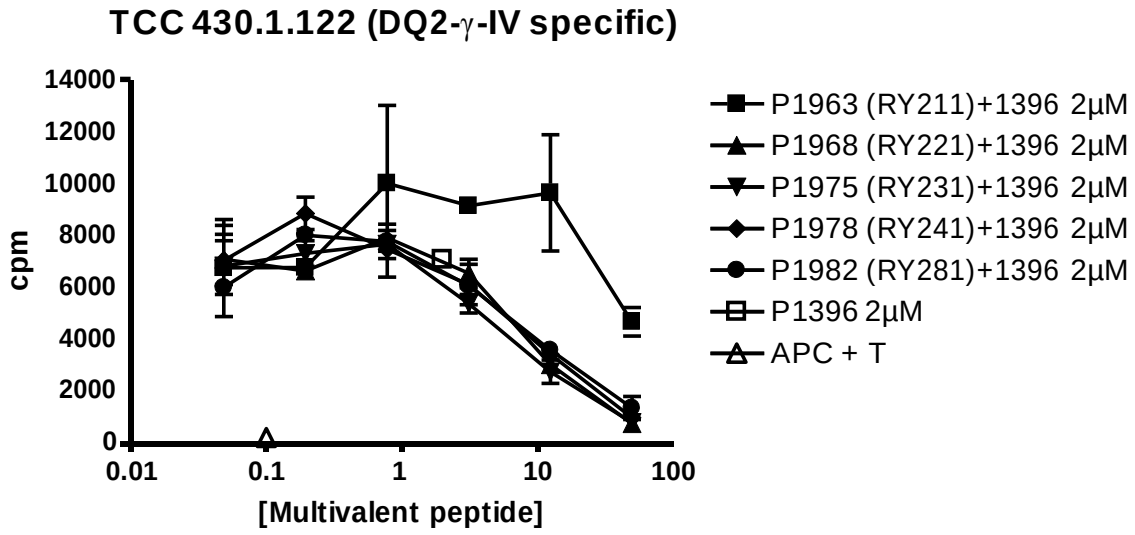

Figure 7: Inhibition of T-cell proliferation by the multivalent peptides. The T-cell clone 430.1.122 (specific for the DQ2-γ-IV gliadin epitope) was stimulated with 2µM FSQPEQEFPQPQ (P1396, DQ2-γ-IV gliadin epitope) in the presence of increasing concentration of multivalent peptides RY211, RY221, RY231, RY241 and RY281. APC: Fixed CD114. *(Courtesy of Ludwig Sollid and Elin Bergseng)*

3.5 Future Directions

Although this study did not demonstrate a positive correlation with increase in binding affinities and increase in valency, it did imply that a multimer has the capacity to enhance its binding affinity relative to the monomer (Section 3.4.3). It is speculated that a linear association was not observed due to non-optimal topologies of the multivalent constructs. The non-optimal orientations of the multivalent constructs prevent the clustering effect because the energy barrier for simultaneous ligand binding to HLA-DQ2 is too high. This can be addressed with rational design involving ligand spacing and orientation of the multivalent construct. Despite this supposed lack of clustering effect, the multivalent constructs still did not show any effect of increase in local concentration (through increases in valency) (Section 3.4.2). It is possible that the range of valencies (dimer, trimer, tetramer, and octamer) is not great enough to showcase the enhanced

binding due to increase in local concentration. In order to expand the range of valencies in the multivalent library, new synthetic chemical strategies must be explored. It is difficult to treat the effects of local concentration and clustering independently. An increase in local concentration by increasing valency has the potential of added clustering effects if the orientation/geometry of the multivalent construct is optimal for simultaneous ligand binding. Of course, this optimal orientation/geometry would certainly depend on the valency. When considering these issues, the study of the multivalency principle requires very careful rational design to ensure that the correct effects are being tested.

Another important point to consider is the biological assays used to observe the multivalency effect. The main biological assay used in this study is the T cell proliferation assay. This assay only measures the T cell proliferation response to antigen presentation. But antigen presentation is a multifaceted phenomenon that goes beyond the simple model of a lock and key interaction between a ligand and a receptor. MHC molecules can be turned over, peptides can be endocytosed and degraded, and MHC cluster moieties alter the T cell recognition (Wulfing, 2001). Furthermore, antigen presentation towards T cell recognition is T cell clone dependent. Thus, biochemical assays such as a competitive binding assay may be more suited, initially, to investigate the multivalency effect. After biochemical analyses, T cell proliferation assays can be used to validate the usefulness of such multivalent constructs.

There are several avenues for further investigation in the multivalent principle. These considerations include the stability of the constructs, optimizing linker lengths,

wider spectrum of valencies, and polyvalency. It is critical to evaluate the stability of the multivalent constructs because in the event of endocytoses and lysosomal fusion, these constructs are degraded into smaller constituents. This degradation pathway needs to be corrected for when attempts are made in quantifying the influence of valency on affinity binding. In regards to affinity binding, the issue of linker lengths plays a role in simultaneous ligand binding of a multivalent construct. By optimizing the linker lengths for a given valency, one can compare between valencies on its ability to competitively inhibit native epitopes. When showing the potential of the multivalent effect, it is important to demonstrate the difference in binding affinities with a wide range of valencies. A benefit of using higher valencies to show the multivalent effect is the opportunity to use lower doses to achieve similar levels of inhibition compared to constructs of lower valencies, but higher doses. Low doses and high activity are prime initiatives in developing therapeutics. Lastly, polyvalency is a topic of interest because it allows multiple targeting through different ligands. Polyvalency follows the same multivalency principle described previously, but instead of the principle applying to a single type of ligand, it is applicable to several different types of ligands on the same multivalent construct. For example, a multivalent construct can have multiple inhibitory peptides targeted for HLA-DQ2 and multiple ligands/peptides that can interact and block CTLA4 (co-stimulator of T cell activation). This results in a multi-level inhibition of HLA-DQ2 antigen presentation and T cell activation. Polyvalency can also provide insight on the multivalent effect. For instance, a multivalent construct can be optimized in linker length for a given valency in achieving a high affinity binding construct. One peptide can be substituted into this multivalent construct and analyzed for the affect on its binding affinity. With respect to this substituted peptide, binding

affinity could be enhanced through this polyvalent construct. Such a polyvalent construct proves useful when diverse T cell clone populations require minimal presence of any specific immunogen. In continuing the study of the multivalent principle beyond what has been presented here, the future endeavors should lie in the realm of optimization and better characterization of the binding kinetics in the multivalent library set.

REFERENCES

Anderson, RP et.al. "Antagonists and non-toxic variants of the dominant wheat gliadin T cell epitope in celiac disease" Gut (2006) 55: p. 485-491

Chan, WC., White, PD. "Fmoc solid phase peptide synthesis: a practical approach" Oxford University Press (2000)

Chmielowski, Bartosz et.al. "Presentation of antagonist peptides to naïve $CD4^+$ T cells abrogates spatial reorganization of class II MHC peptide complexes on the surface of dendritic cells" PNAS (2002) 99:23 p. 15012-15017

Cochran, Jennifer R. et.al. "A diverse set of oligomeric class II MHC-peptide complexes for probing T-cell receptor interactions" Chemistry & Biology (2000) 7: p. 683-696

Dam, Tarun K. "Effects of Clustered Epitopes in Multivalent Ligand-Receptor Interactions" Biochemistry (2008) 47:33 p. 8467

de Ritis, G. et.al. "In vitro (organ culture) studies of the toxicity of specific A-gliadin peptides in celiac disease" Gastroenterology (1988) 94: p. 41-49

Farha, Omar K. "Synthesis of a homotrifunctional conjugation reagent based on maleimide chemistry" Tetrahedron Letters (2006) 47: p. 2619-2622

Green, Peter H.R. et.al. "Celiac Disease" NEJM (2007) 357:17 p. 1731-1743

Hourigan, C.S. "The molecular basis of celiac disease" Clin. Exp. Med. (2006) 6: p. 53-59

Johansen, Bente H. et.al. "Binding of Peptides from the N-Terminal Region of α-Gliadin to the Celiac Disease-Associated HLA-DQ2 Molecule Assessed in Biochemical and T Cell Assays" Clin. Immunology and Immunopathology (1996) 79:3 p. 288-293

Johansen, Bente H. et.al. "Identification of a putative motif for binding of peptides to HLA-DQ2" International Immunology (1996) 8:2 p. 177-182

Kim, Chu-Young et.al. "Structural basis for HLA-DQ2-mediated presentation of gluten epitopes in celiac disease" PNAS (2004) 101:12 p. 4175-4179

Lundin, KE et.al. "Gliadin-specific, HLA-DQ(alpha 1*0501,beta 1*0201) restricted T cells isolated from the small intestinal mucosa of celiac disease patients" J Exp. Med. (1993) 178: p. 187-196

Sturgess, R. et.al. "Wheat peptide challenge in celiac disease" Lancet (1994) 343: p. 758-761

Van de Wal, Y et.al. "Selective deamidation by tissue transglutaminase strongly enhances gliadin-specific T cell reactivity" J Immunol. (1998) 161: p. 1585-1588
Vaysburd, Marina et.al. "Prevention of Insulin-dependent Diabetes Mellitus in Nonobese Diabetic Mice by Immunogenic but Not by Tolerated Peptides" J Exp. Med. (1995) 182: p. 897-902

Wegmann, Keith W. et.al. "Synthetic Peptide Dendrimers Block the Development and expression of Experimental Allergic Encephalomyelitis" J Immunology (2008) 181: p. 3301-3309

Wieser, H. et.al. "Amino-acid sequence of the coeliac active gliadin peptide B3142" Z. Lebensm.-Unters. Forsch. (1984) 179: p. 371-376

Wulfing, Christoph et.al. "Costimulation and endogenous MHC ligands contribute to T cell recognition" Nature Immunology (2001) 3: p. 42-47

Xia, Jiang et.al. "Inhibition of HLA-DQ2-Mediated Antigen Presentation by Analogues of a High Affinity 33-Residue Peptide from α2-Gliadin" J Am. Chem. Soc. (2006) 128: p. 1859-1867

PRESENTATIONS

Raymond T. Yan, Elin Bergseng, Kim Chu-Young "Multivalent Design toward Higher Affinity Therapeutic Blockers" AIC Chicago, IL November 2008 Poster/Oral Presentation

APPENDIX A: Analytical HPLC

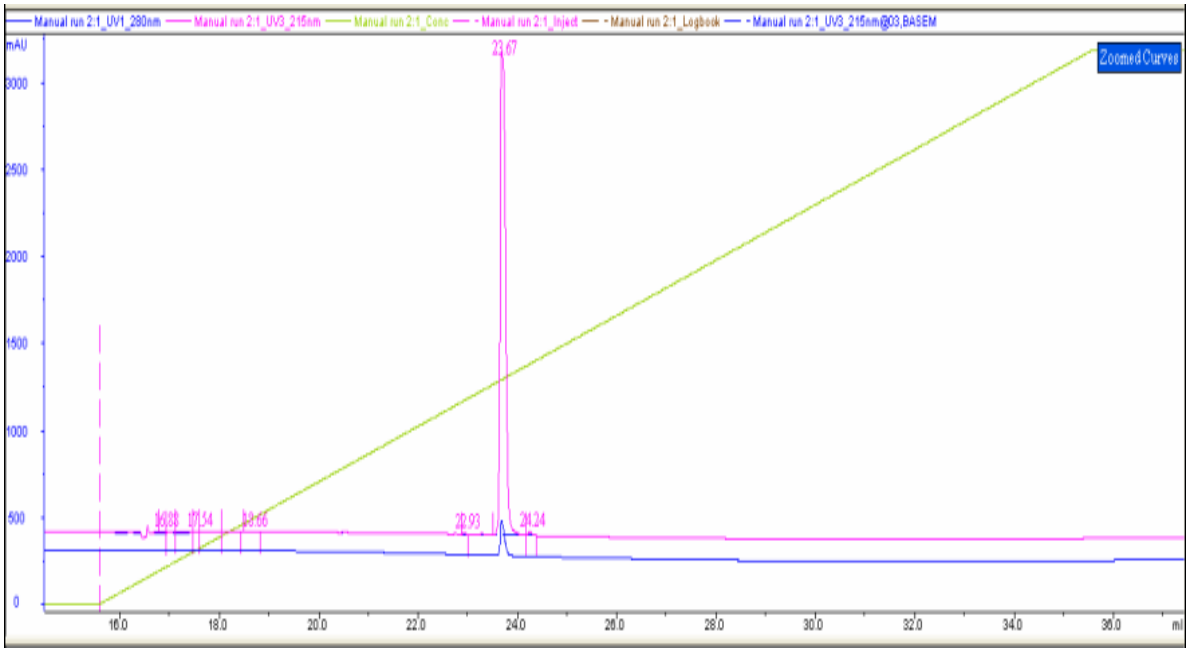

C(t-butyl)GASGPFPQPELPYG: 0 to 100% 80:20 ACN:H_2O w/ 0.04% TFA in 100 minutes at 0.2 mL/min.

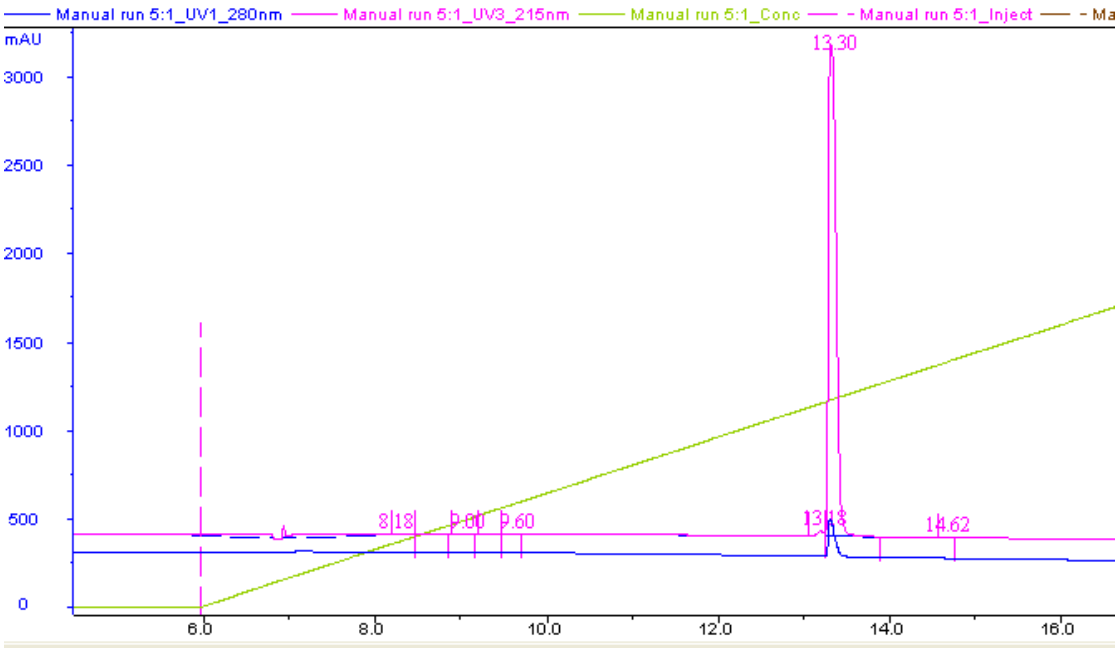

GASGPC(t-butyl)PQPELPYG: 0 to 100% 80:20 ACN:H_2O w/ 0.04% TFA in 100 minutes at 0.2 mL/min.

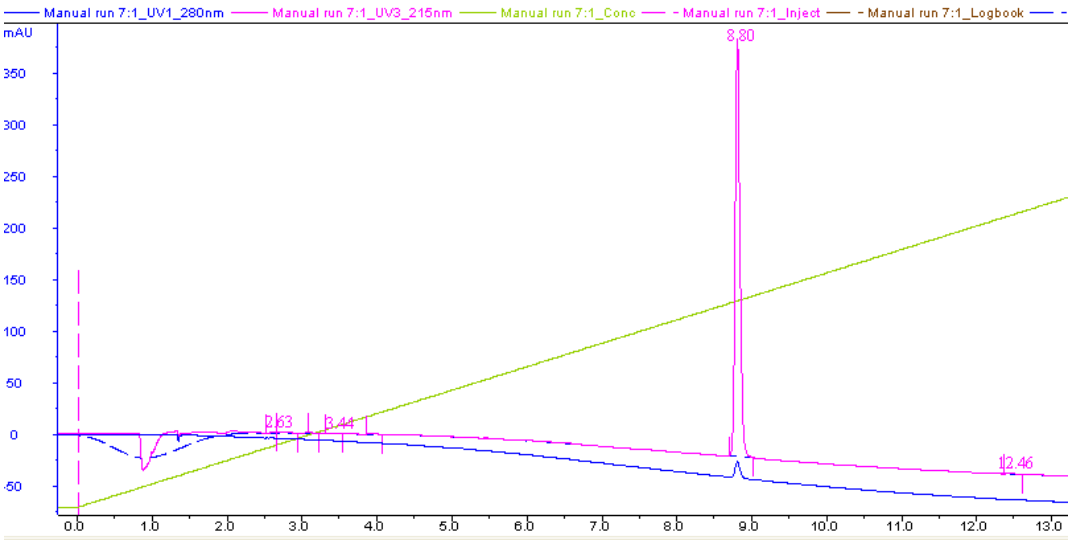

GASGPFPQPELPYGC(t-butyl): 0 to 100% 80:20 ACN:H_2O w/ 0.04% TFA in 100 minutes at 0.2 mL/min.

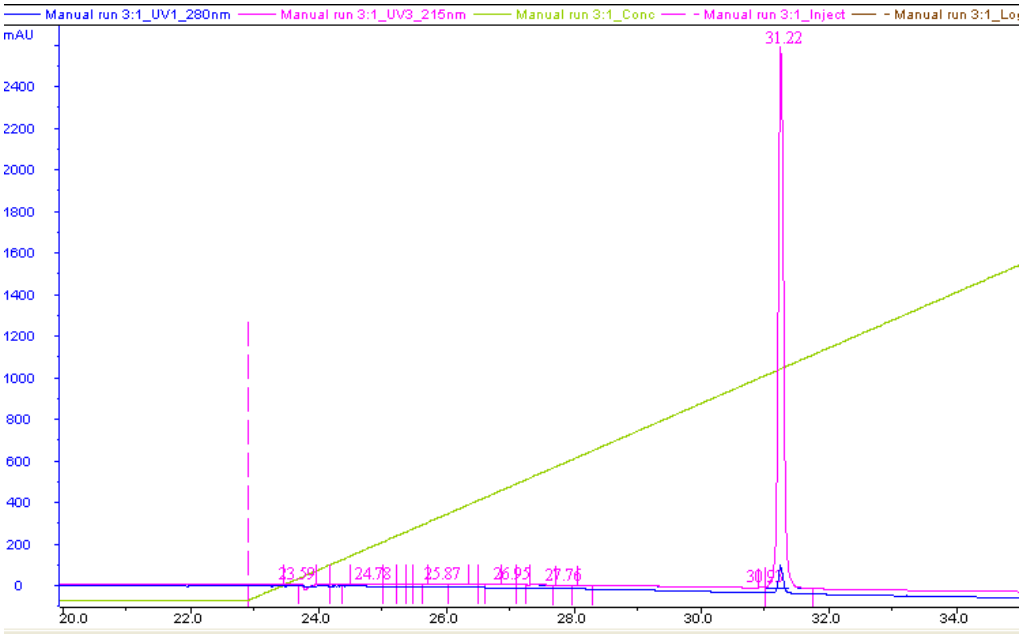

CGASGPFPQPELPYG DPDPB Dimer: 0 to 100% 80:20 ACN:H_2O w/ 0.04% TFA in 100 minutes at 0.2 mL/min.

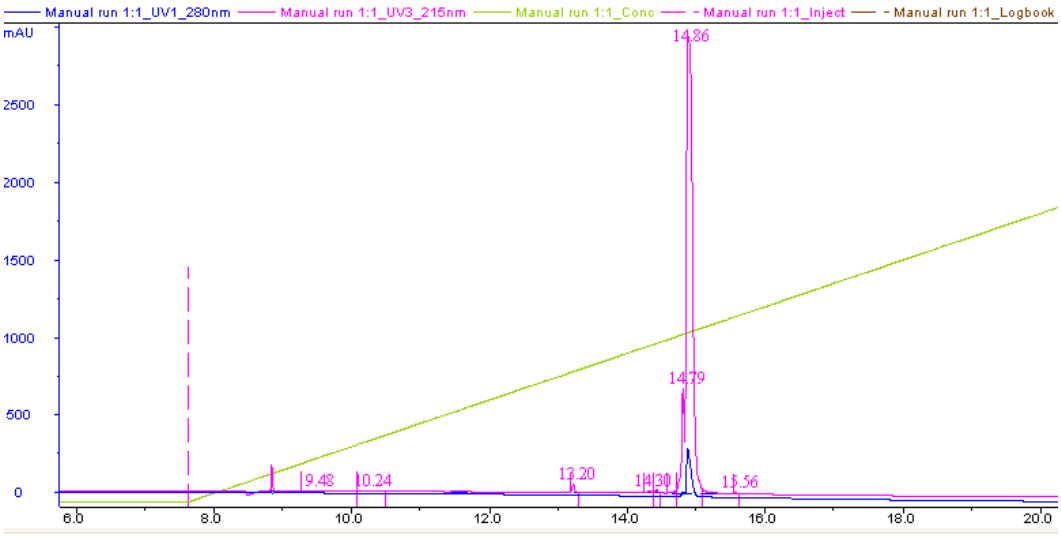

GASGPCPQPELPYG DPDPB Dimer: 0 to 100% 80:20 ACN:H_2O w/ 0.04% TFA in 100 minutes at 0.2 mL/min.

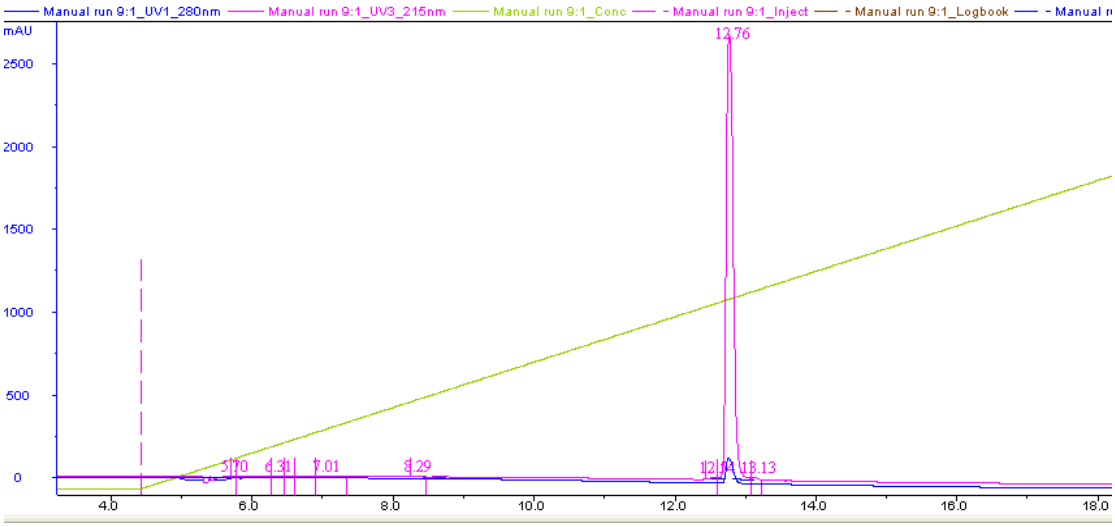

GASGPFPQPELPYGC DPDPB Dimer: 0 to 100% 80:20 ACN:H_2O w/ 0.04% TFA in 100 minutes at 0.2 mL/min.

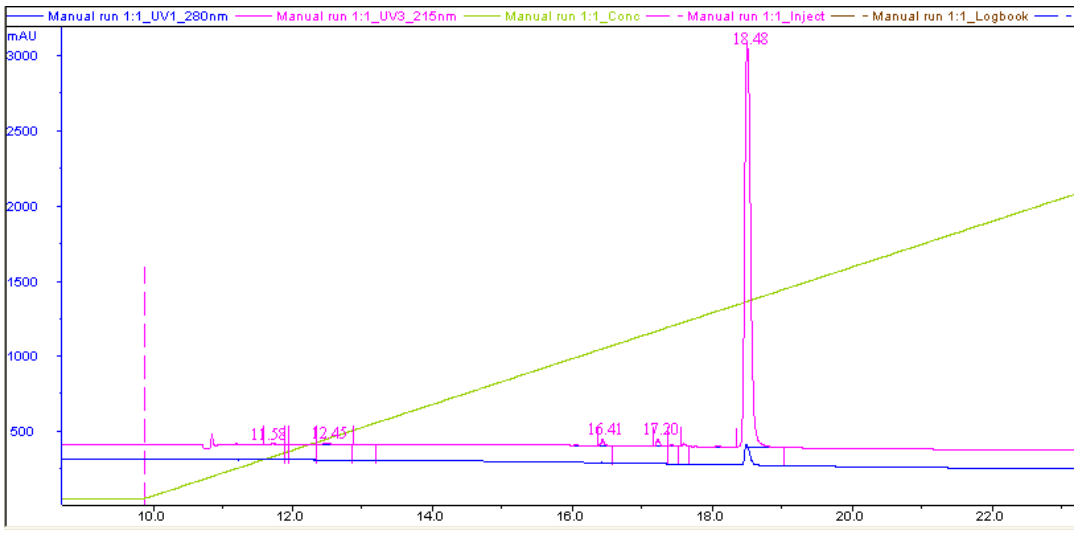

CGASGPFPQPELPYG BMH Dimer: 0 to 100% 80:20 ACN:H_2O w/ 0.04% TFA in 100 minutes at 0.2 mL/min.

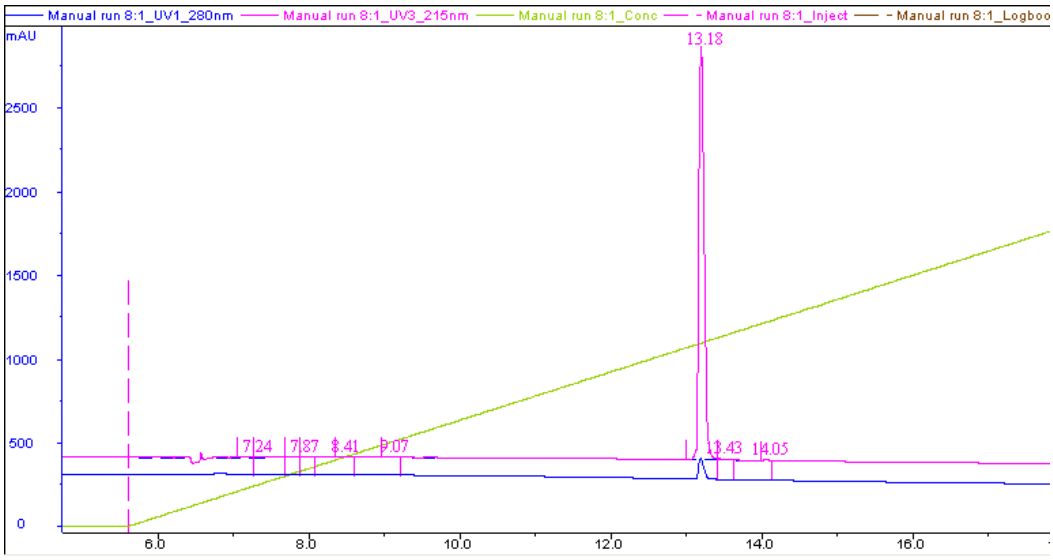

GASGPCPQPELPYG BMH Dimer: 0 to 100% 80:20 ACN:H_2O w/ 0.04% TFA in 100 minutes at 0.2 mL/min.

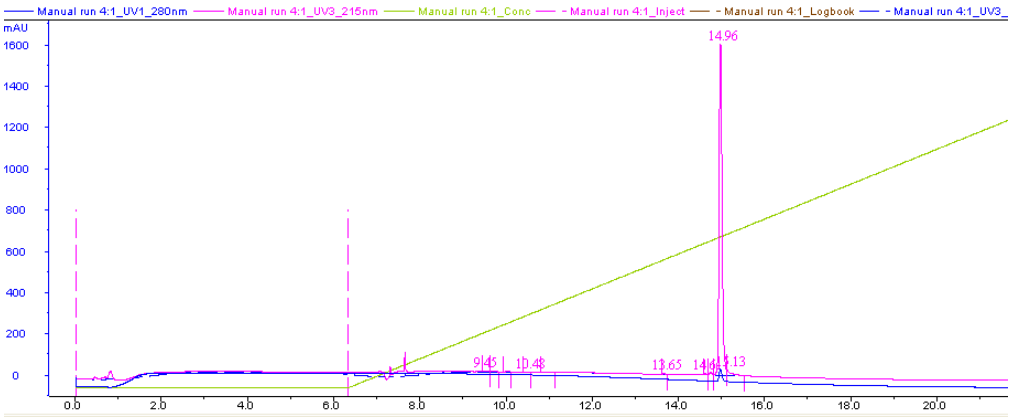

GASGPFPQPELPYGC BMH Dimer: 0 to 100% 80:20 ACN:H_2O w/ 0.04% TFA in 100 minutes at 0.2 mL/min.

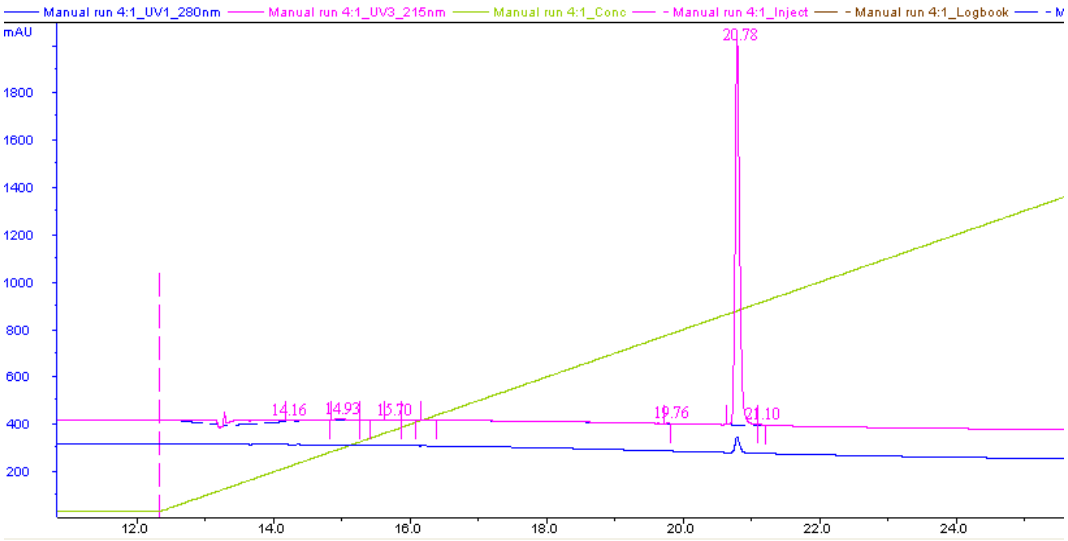

CGASGPFPQPELPYG HBVS Dimer: 0 to 100% 80:20 ACN:H_2O w/ 0.04% TFA in 100 minutes at 0.2 mL/min.

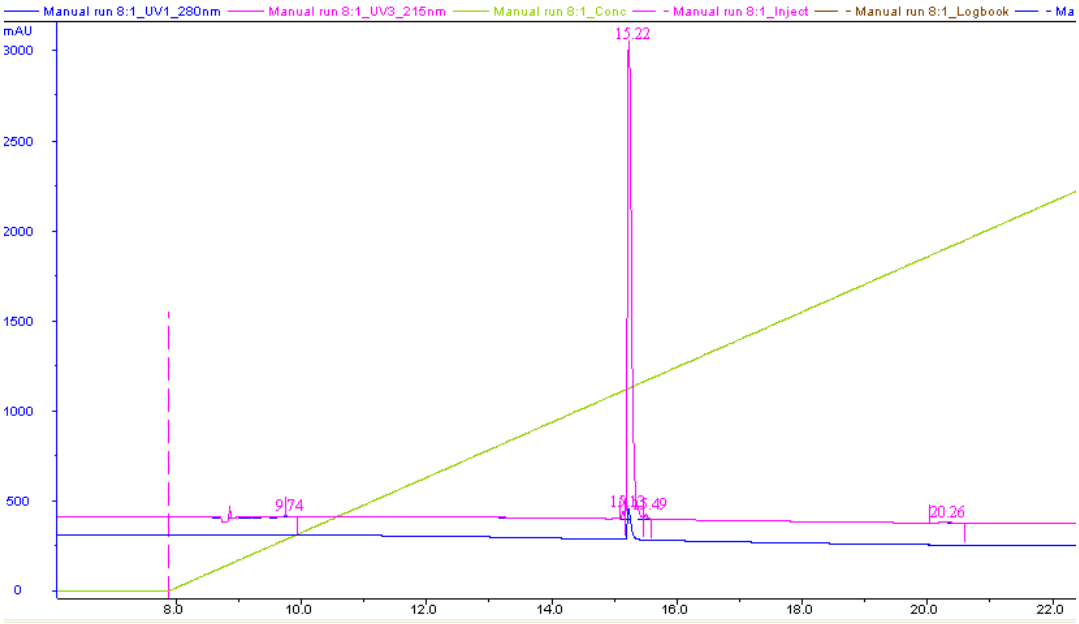

GASGPCPQPELPYG HBVS Dimer: 0 to 100% 80:20 ACN:H_2O w/ 0.04% TFA in 100 minutes at 0.2 mL/min.

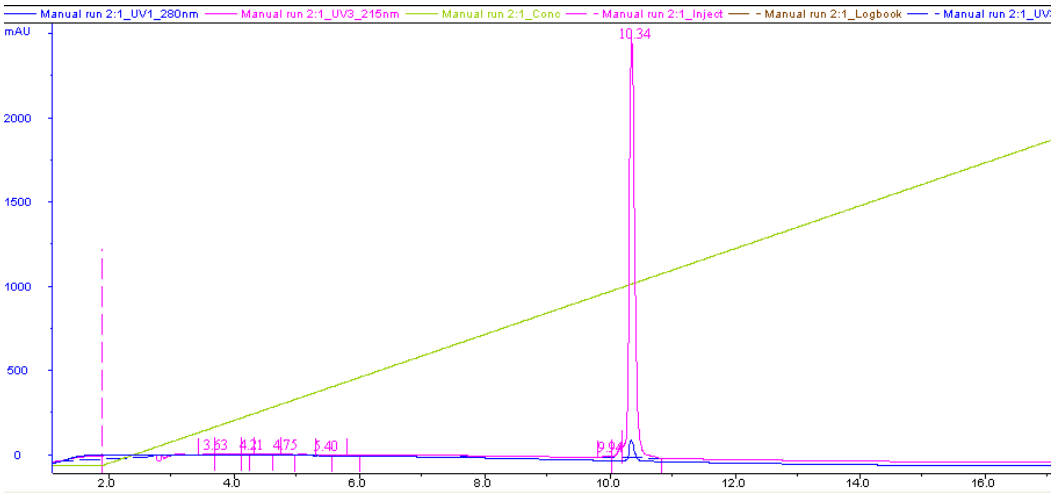

GASGPFPQPELPYGC HBVS Dimer: 0 to 100% 80:20 ACN:H_2O w/ 0.04% TFA in 100 minutes at 0.2 mL/min.

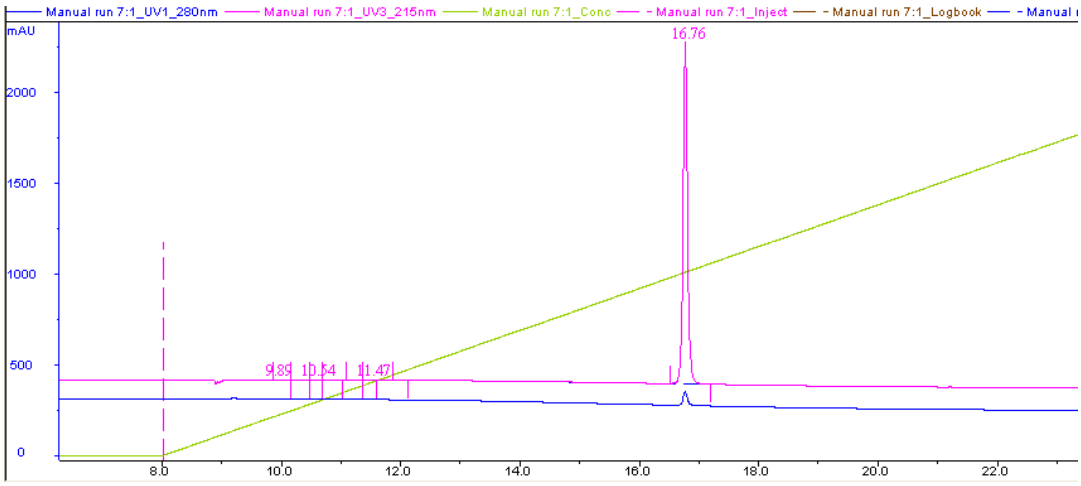

CGASGPFPQPELPYG TMEA trimer: 0 to 100% 80:20 ACN:H_2O w/ 0.04% TFA in 100 minutes at 0.2 mL/min.

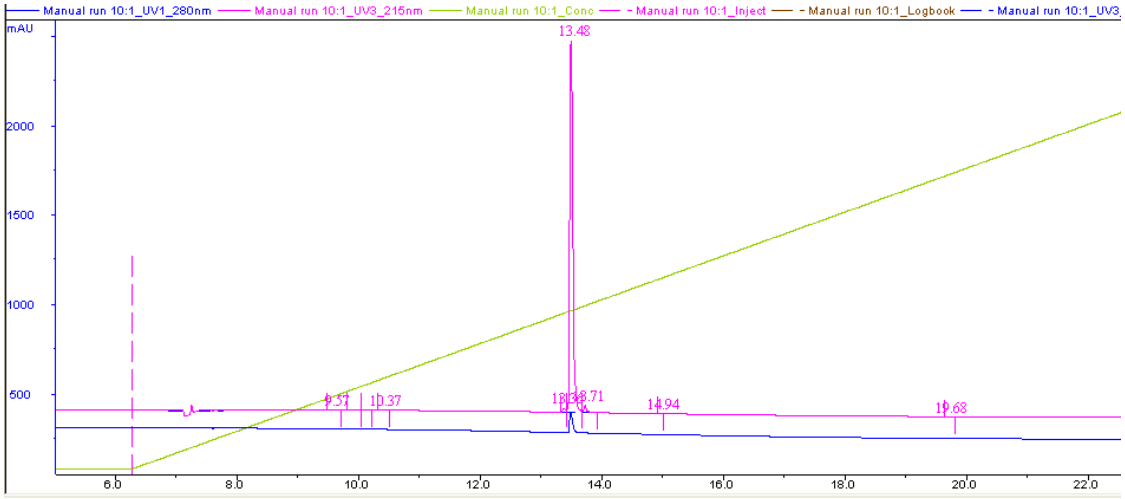

GASGPCPQPELPYG TMEA trimer: 0 to 100% 80:20 ACN:H_2O w/ 0.04% TFA in 100 minutes at 0.2 mL/min.

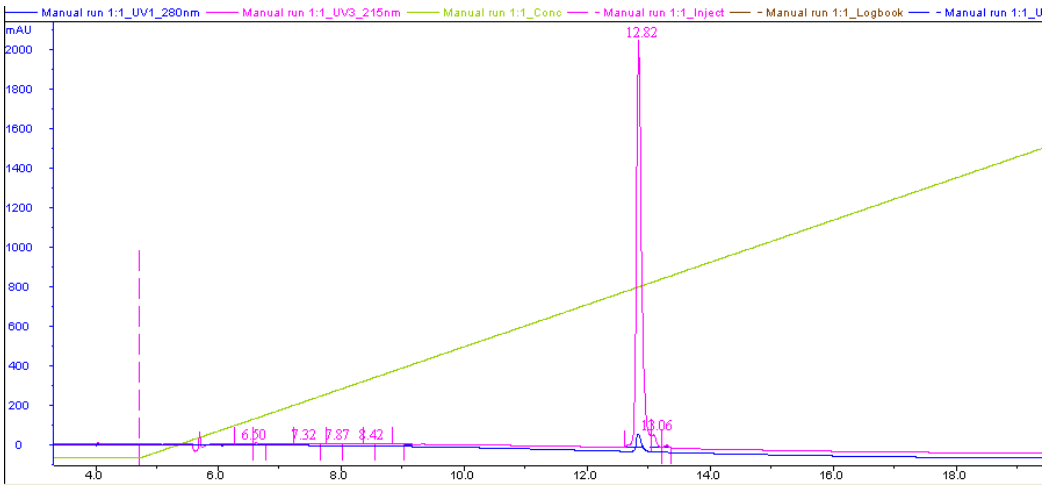

GASGPFPQPELPYGC TMEA trimer: 0 to 100% 80:20 ACN:H_2O w/ 0.04% TFA in 100 minutes at 0.2 mL/min.

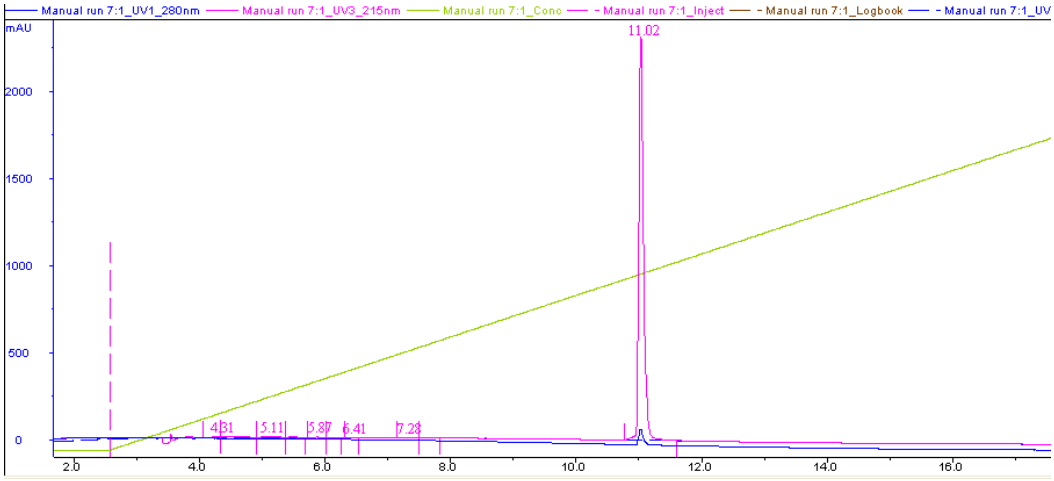

CGASGPFPQPELPYG G0 PAMAM tetramer: 0 to 100% 80:20 ACN:H_2O w/ 0.04% TFA in 100 minutes at 0.2 mL/min.

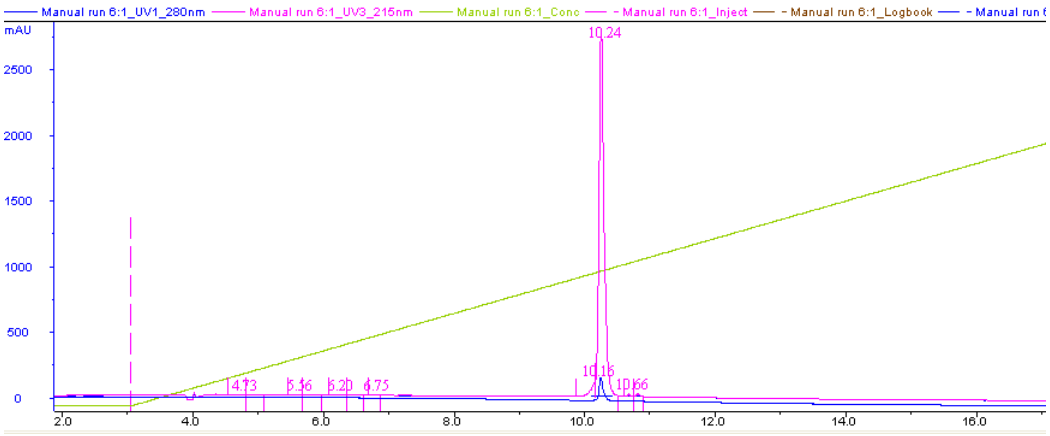

GASGPCPQPELPYG G0 PAMAM tetramer: 0 to 100% 80:20 ACN:H_2O w/ 0.04% TFA in 100 minutes at 0.2 mL/min.

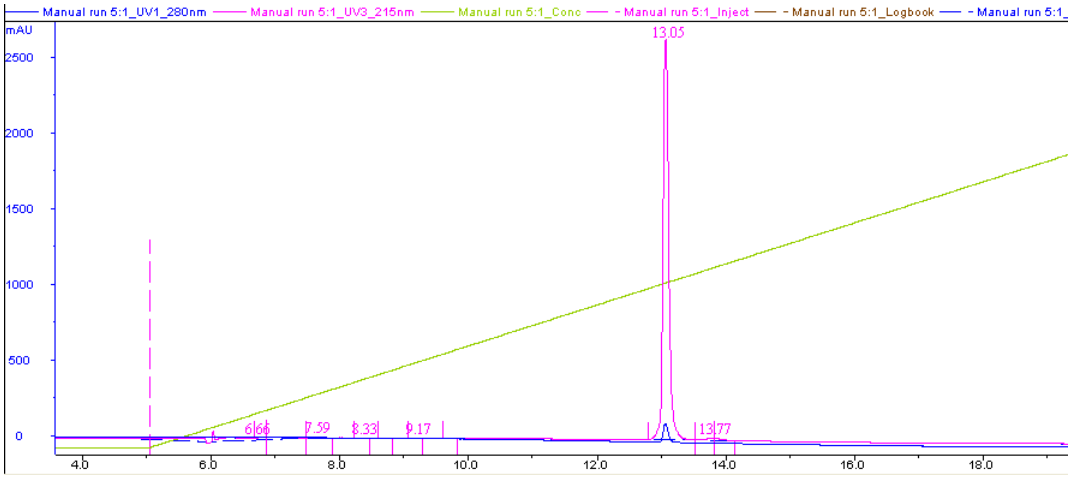

GASGPFPQPELPYGC G0 PAMAM tetramer: 0 to 100% 80:20 ACN:H_2O w/ 0.04% TFA in 100 minutes at 0.2 mL/min.

APPENDIX B: MALDI-TOF MS (Peak of interest are shown in subpanels)

NH_2-C(t-butyl)GASGPFPQPELPYG (RY 111)

Expected Molecular Weight: 1574.68

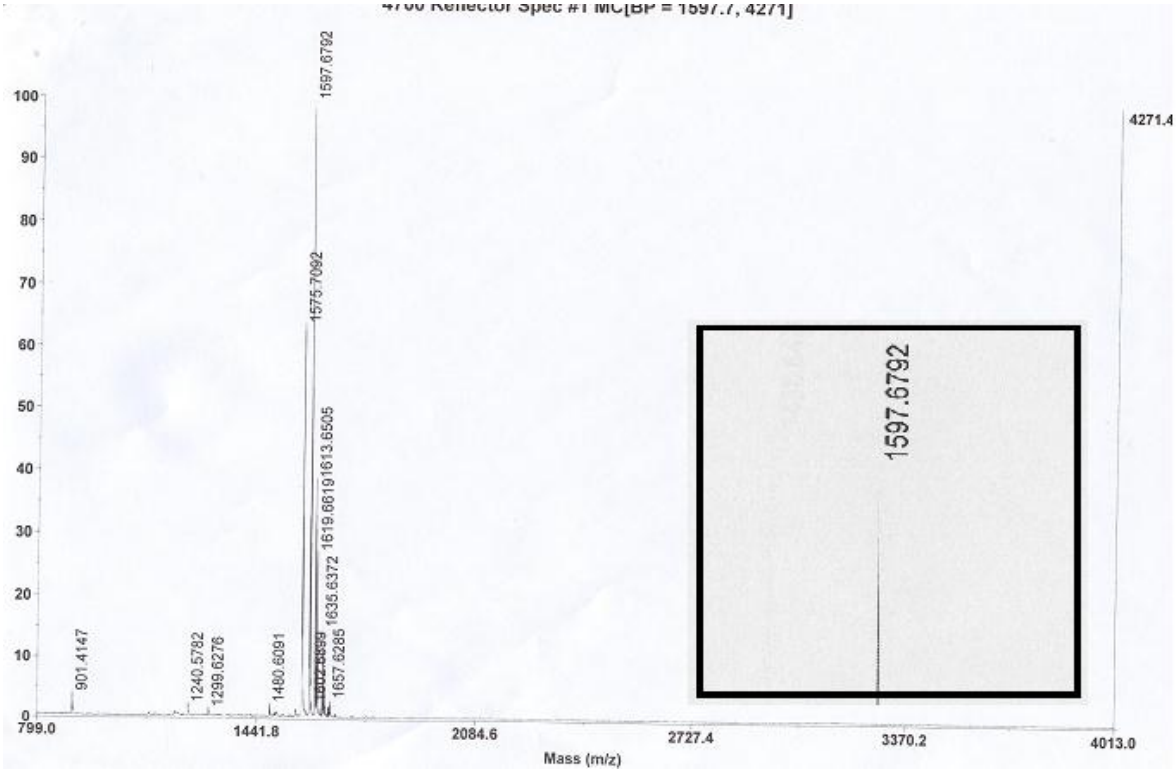

NH_2-GASGPC(t-butyl)PQPELPYG (RY 211)

Expected Molecular Weight: 1427.61

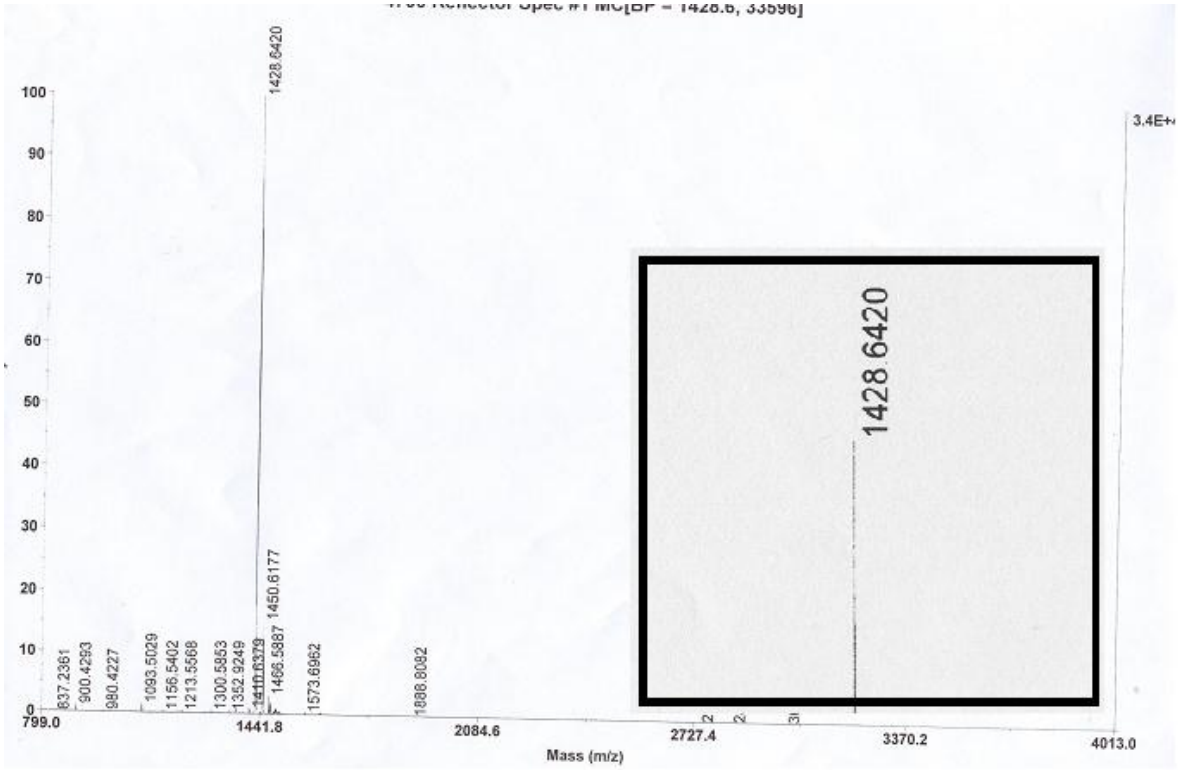

NH_2-GASGPFPQPELPYGC(t-butyl) (RY 311)

Expected Molecular Weight: 1574.68

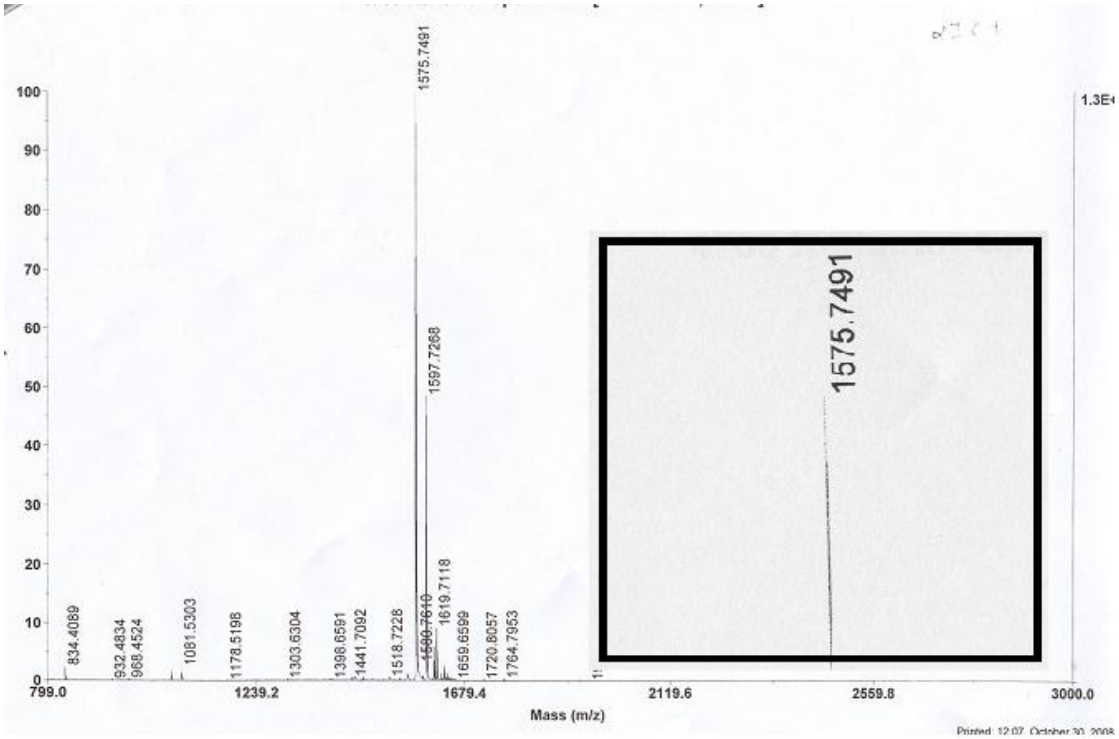

NH_2-CGASGPFPQPELPYG DPDPB Dimer (RY 121)

Expected Molecular Weight: 3298.06

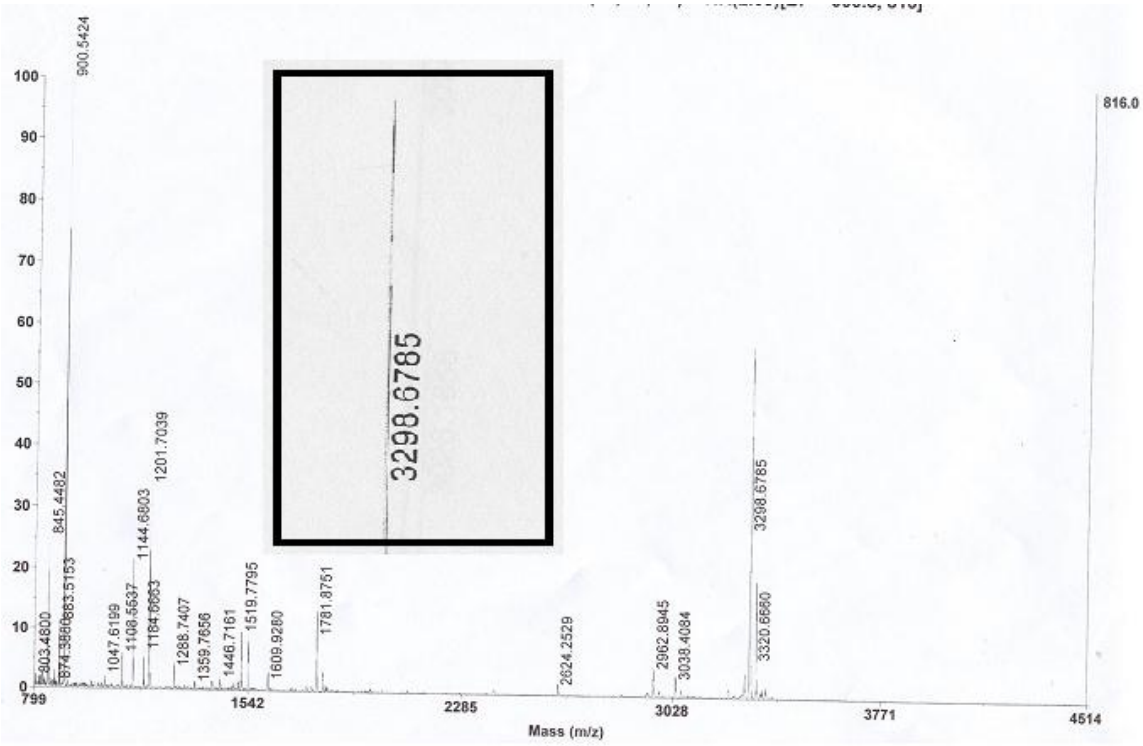

NH_2-GASGPCPQPELPYG DPDPB Dimer (RY 221)

Expected Molecular Weight: 3003.92

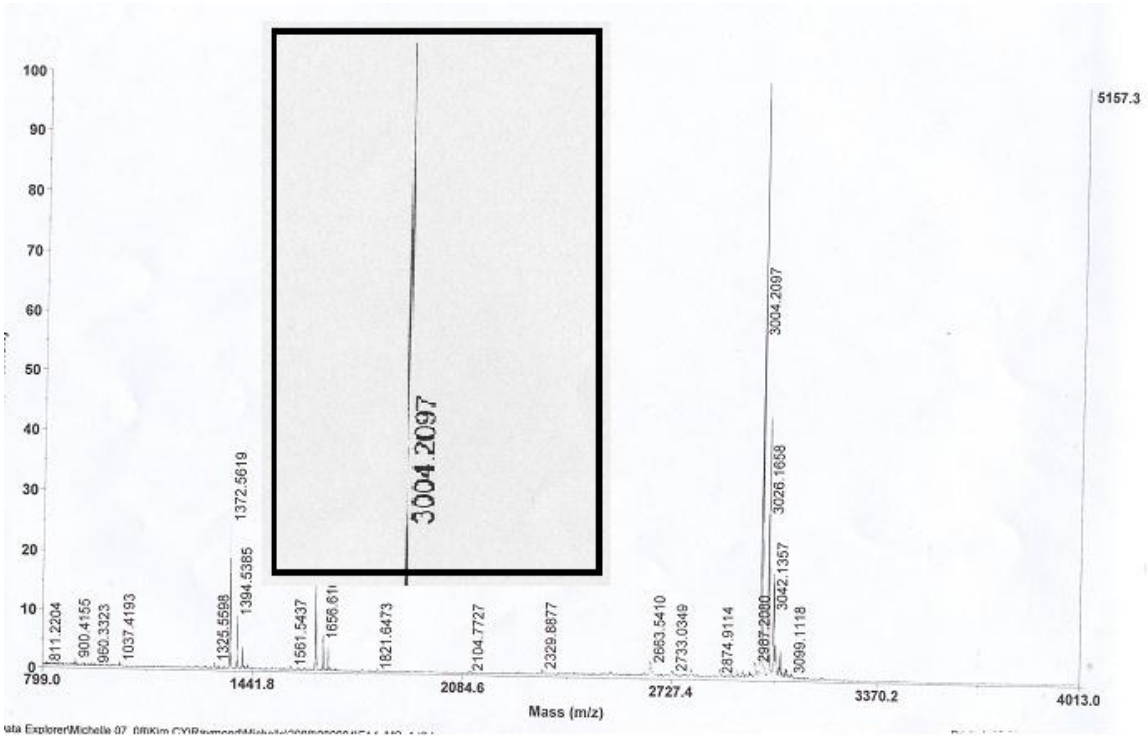

NH_2-GASGPFPQPELPYGC DPDPB Dimer (RY 321)

Expected Molecular Weight: 3298.06

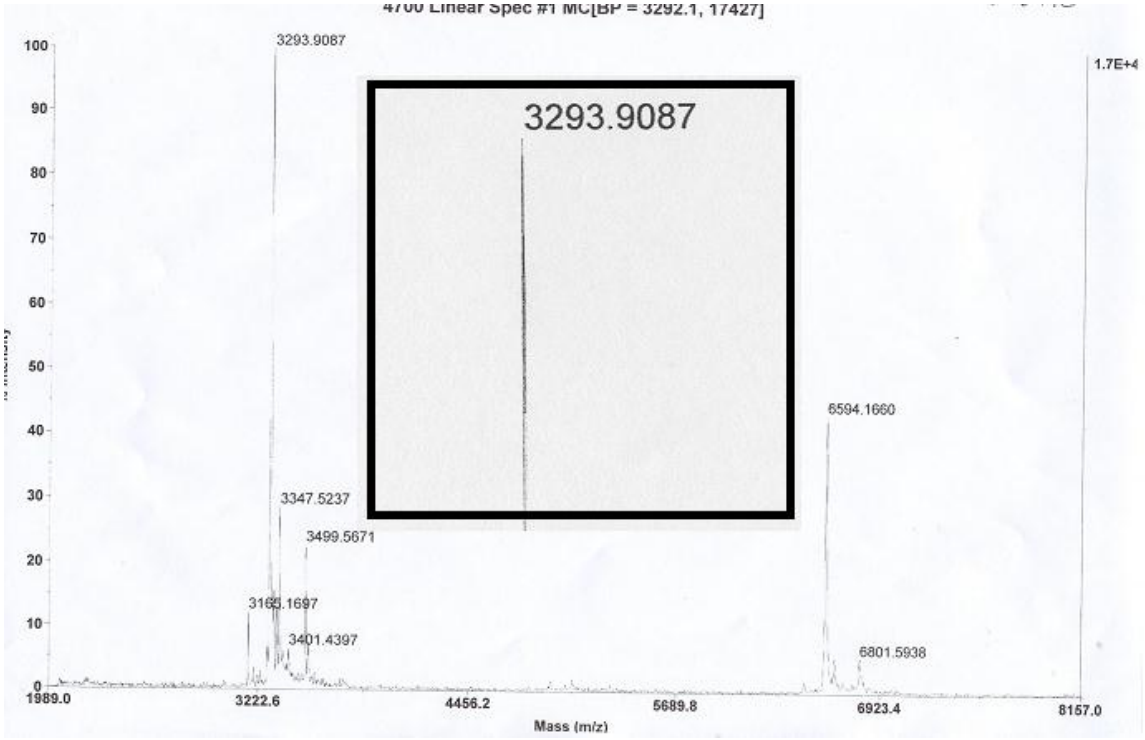

NH_2-CGASGPFPQPELPYG BMH Dimer (RY 122)

Expected Molecular Weight: 3313.65

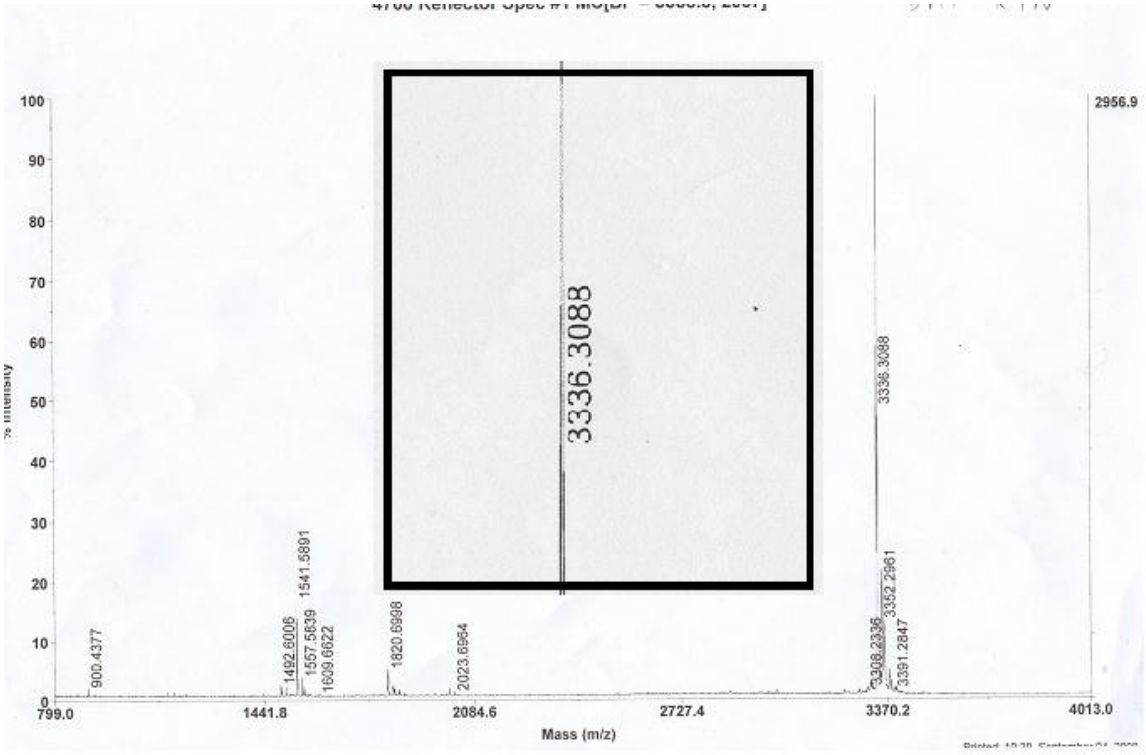

NH_2-GASGPCPQPELPYG BMH Dimer (RY 222)

Expected Molecular Weight: 3020.29

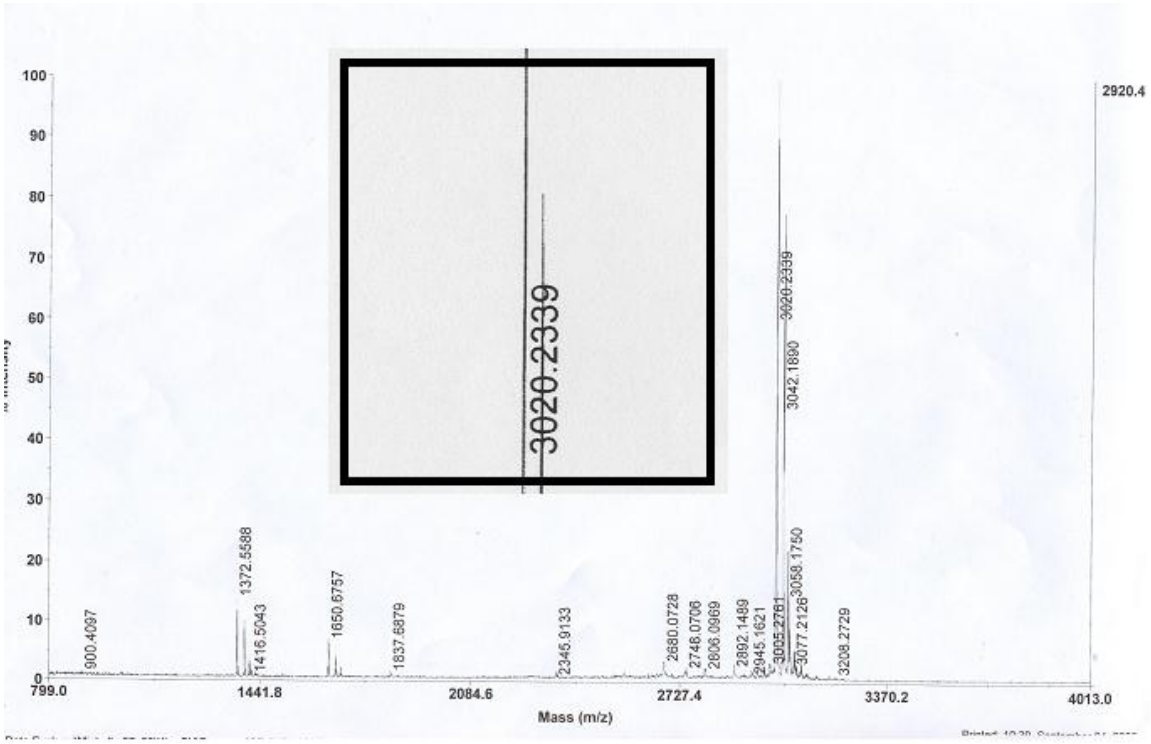

NH_2-GASGPFPQPELPYGC BMH Dimer (RY 322)

Expected Molecular Weight: 3313.65

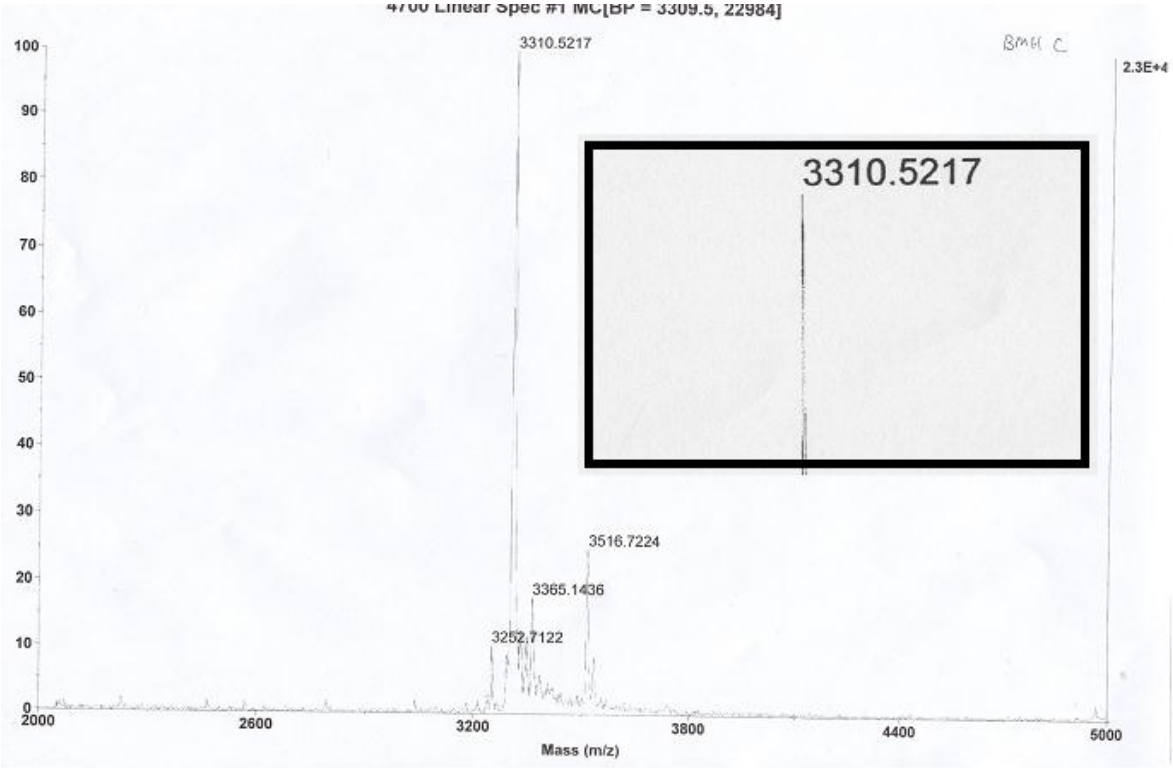

NH_2-CGASGPFPQPELPYG HBVS Dimer (RY 123)

Expected Molecular Weight: 3303.74

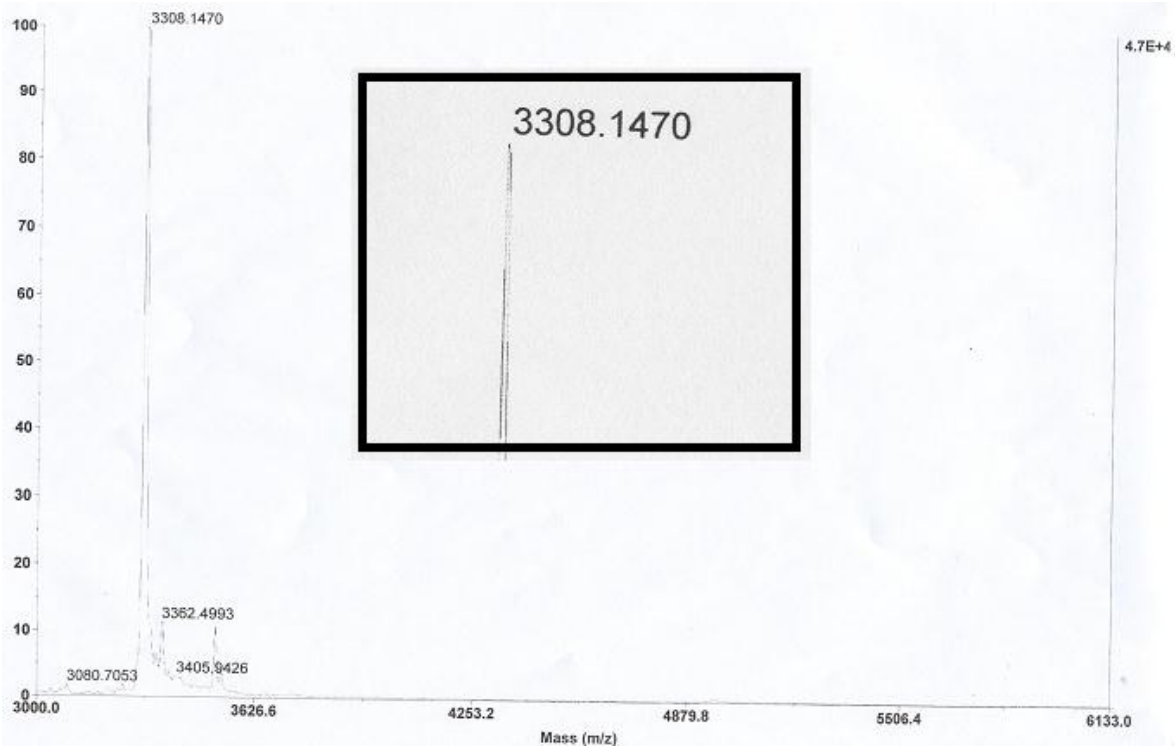

NH_2-GASGPCPQPELPYG HBVS Dimer (RY 223)

Expected Molecular Weight: 3009.6

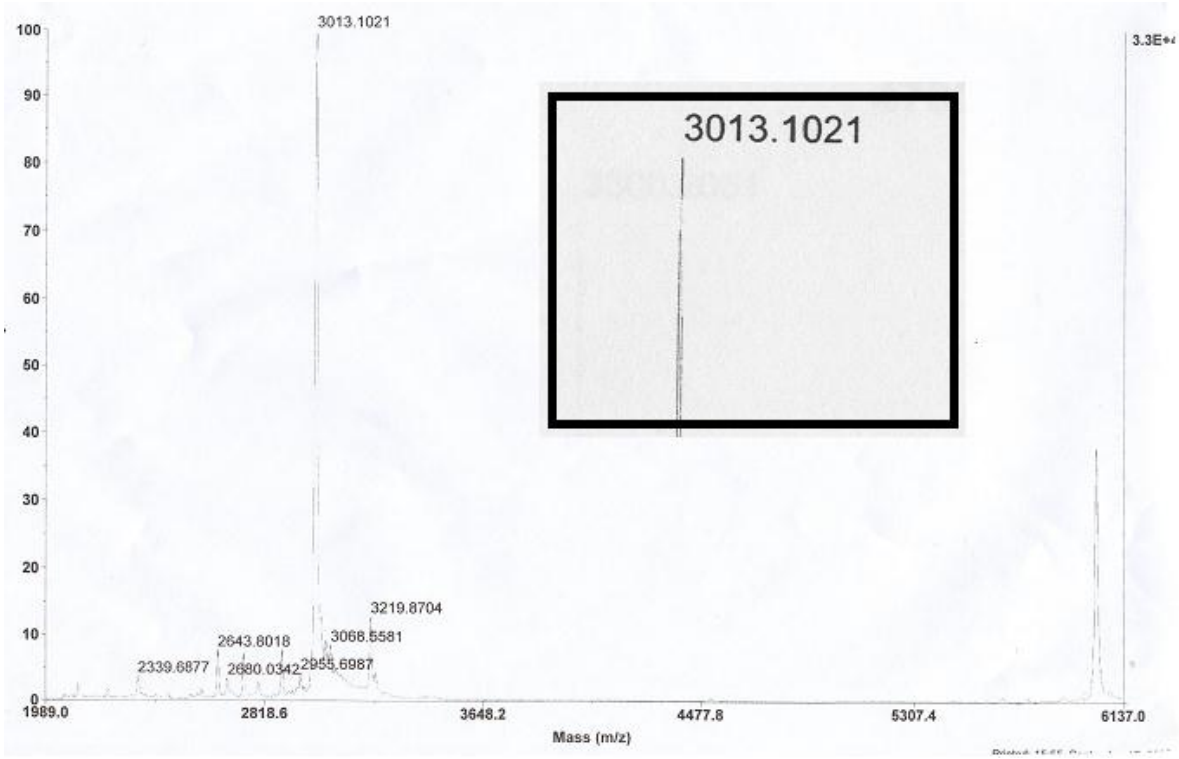

NH_2-GASGPFPQPELPYGC HBVS Dimer (RY 323)

Expected Molecular Weight: 3303.74

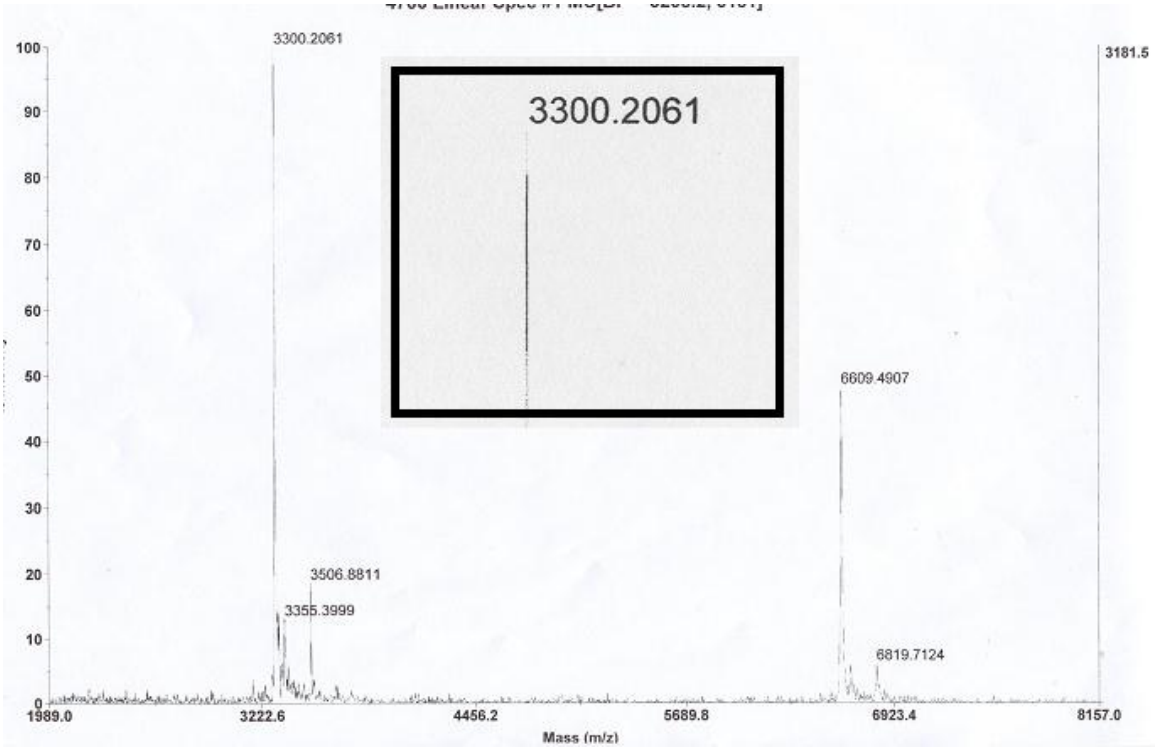

NH_2-CGASGPFPQPELPYG TMEA Trimer (RY 131)

Expected Molecular Weight: 4942.4

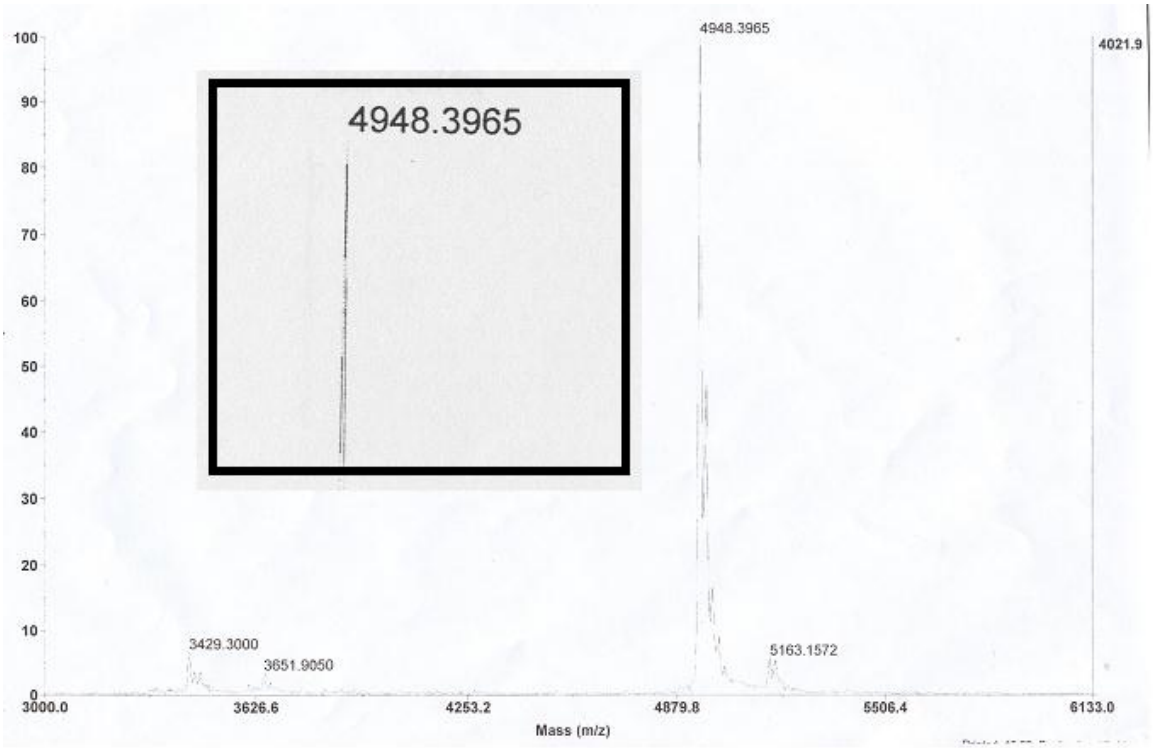

NH_2-GASGPCPQPELPYG TMEA Trimer (RY 231)

Expected Molecular Weight: 4501.19

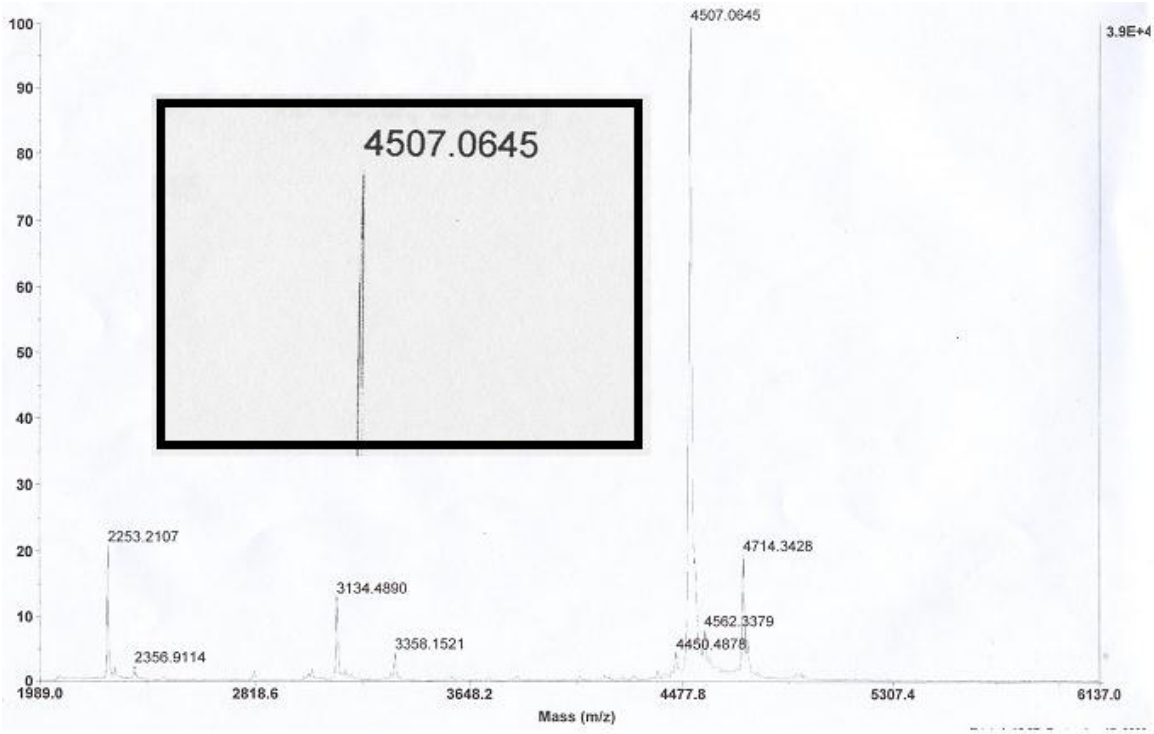

NH_2-GASGPFPQPELPYGC TMEA Trimer (RY 331)

Expected Molecular Weight: 4942.4

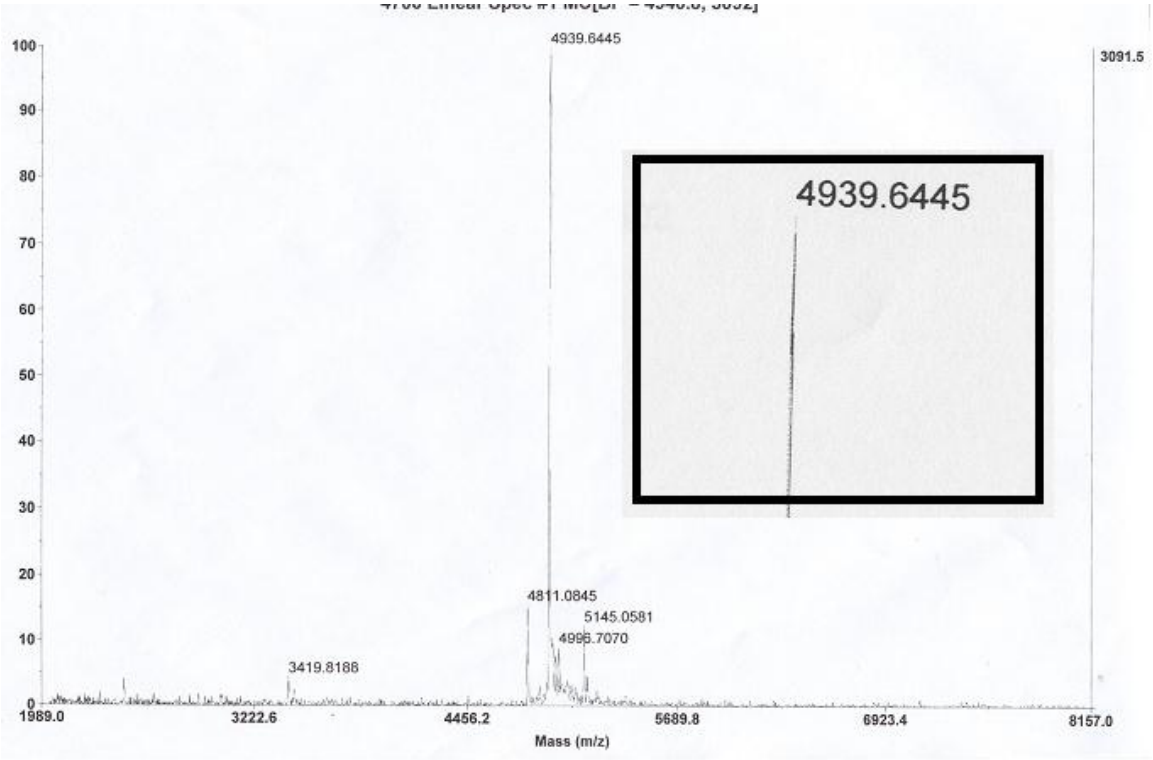

NH_2-CGASGPFPQPELPYG G0 PAMAM Tetramer (RY 141)

Expected Molecular Weight: 8179.4

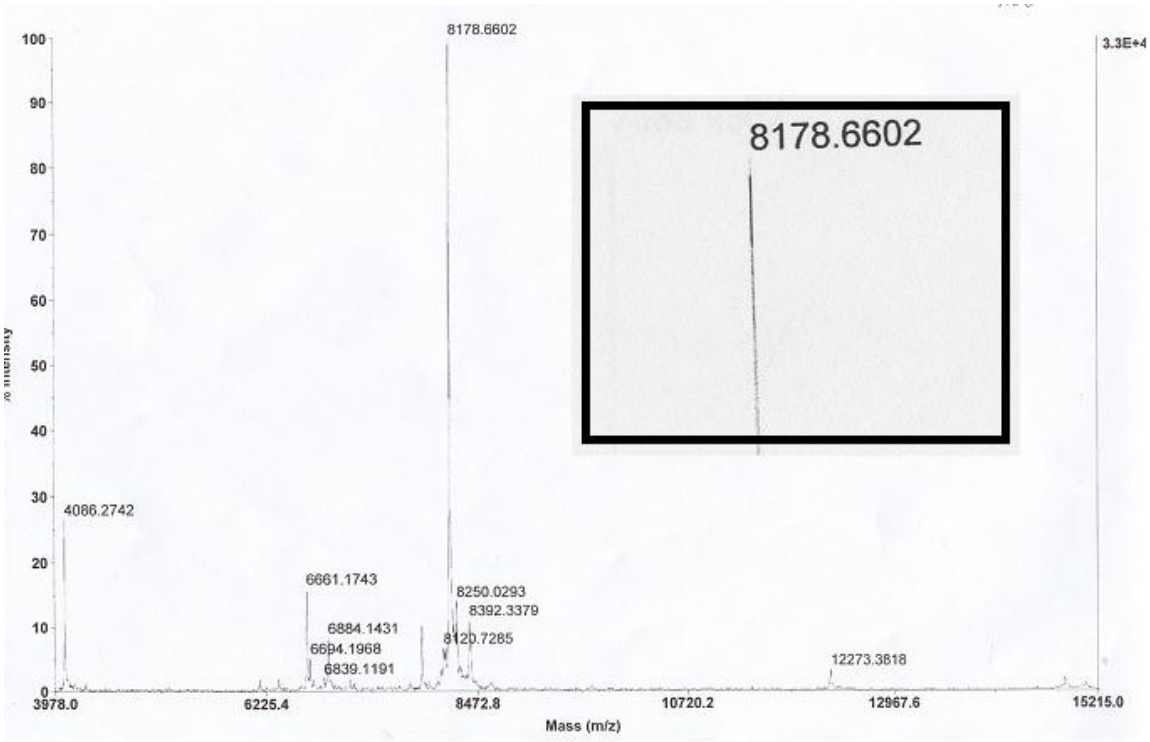

NH_2-GASGPCPQPELPYG G0 PAMAM Tetramer (RY 241)

Expected Molecular Weight: 7591.12

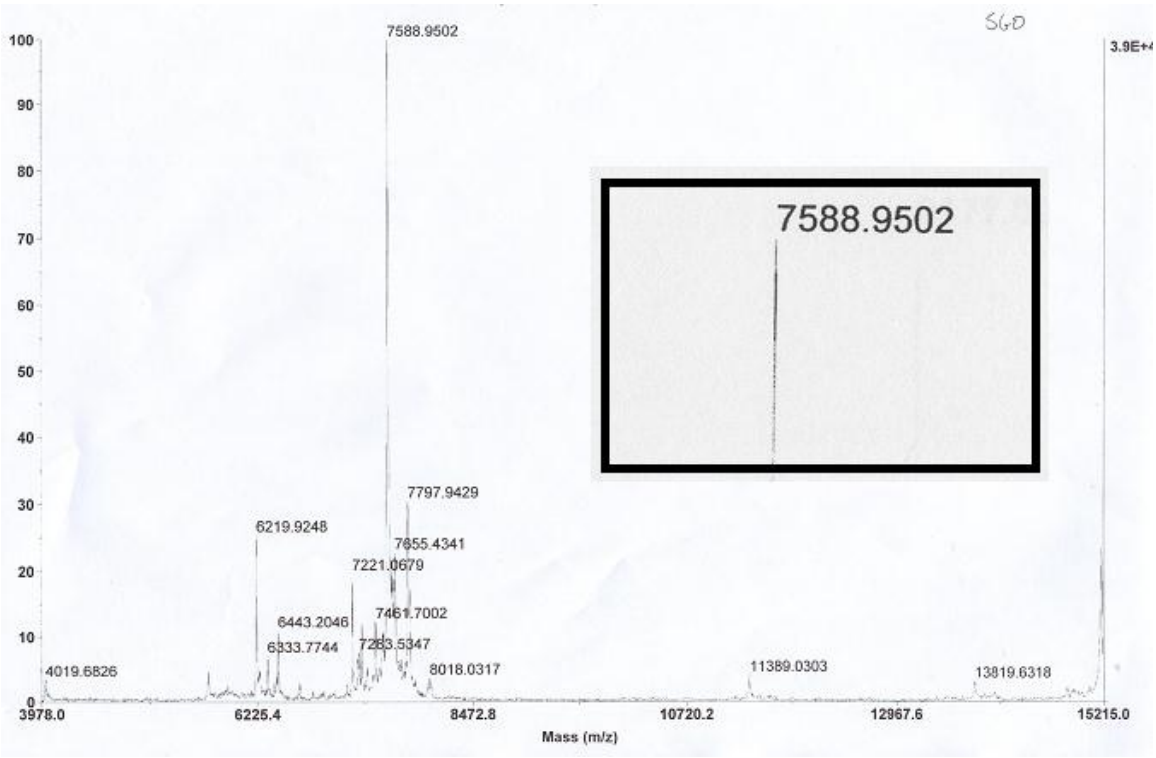

NH_2-GASGPFPQPELPYGC G0 PAMAM Tetramer (RY 341)

Expected Molecular Weight: 8179.4

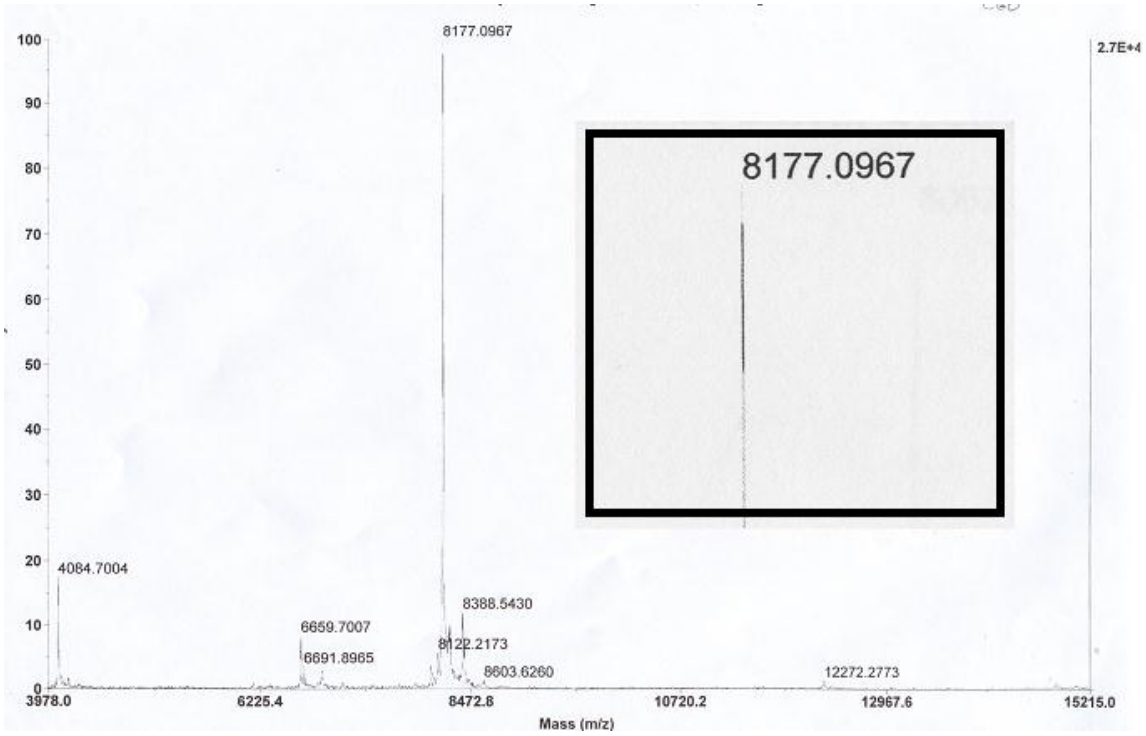

NH_2-GASGPFPQPELPYG MAPs Tetramer (RY 441)

Expected Molecular Weight: 6064.19

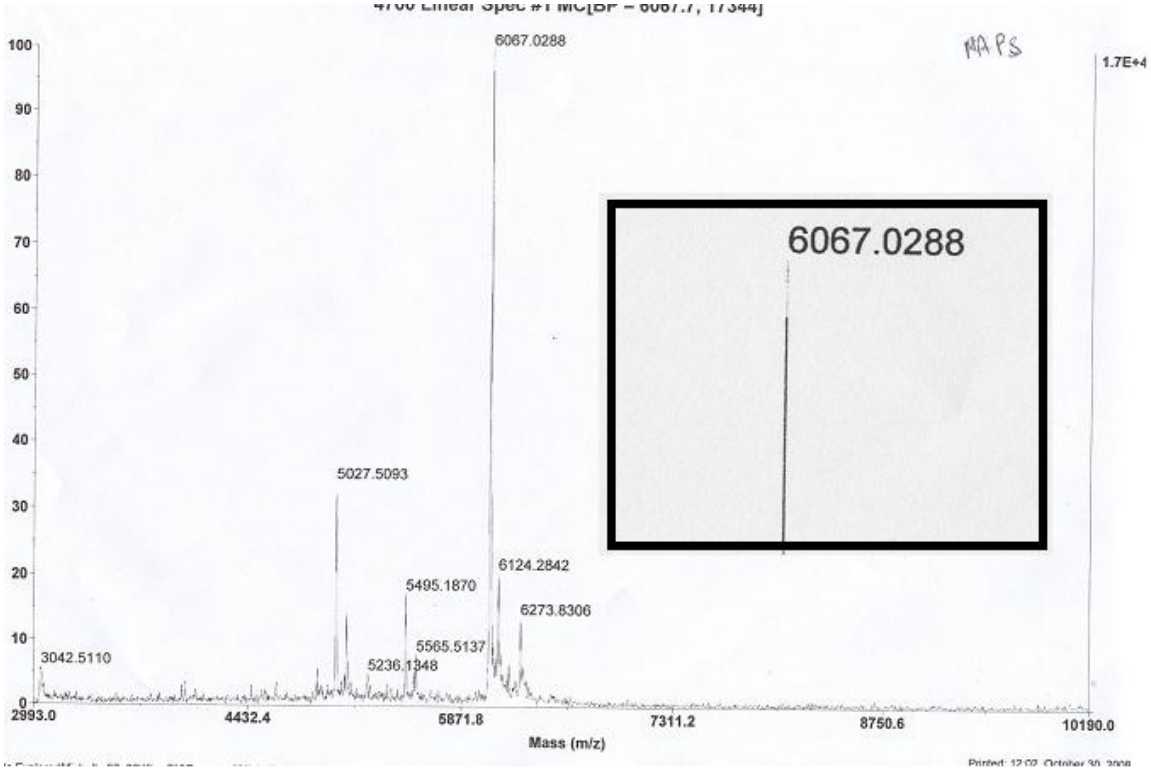

NH_2-CGASGPFPQPELPYG G1 PAMAM Octamer (RY 181)

Expected Molecular Weight: 19574.48

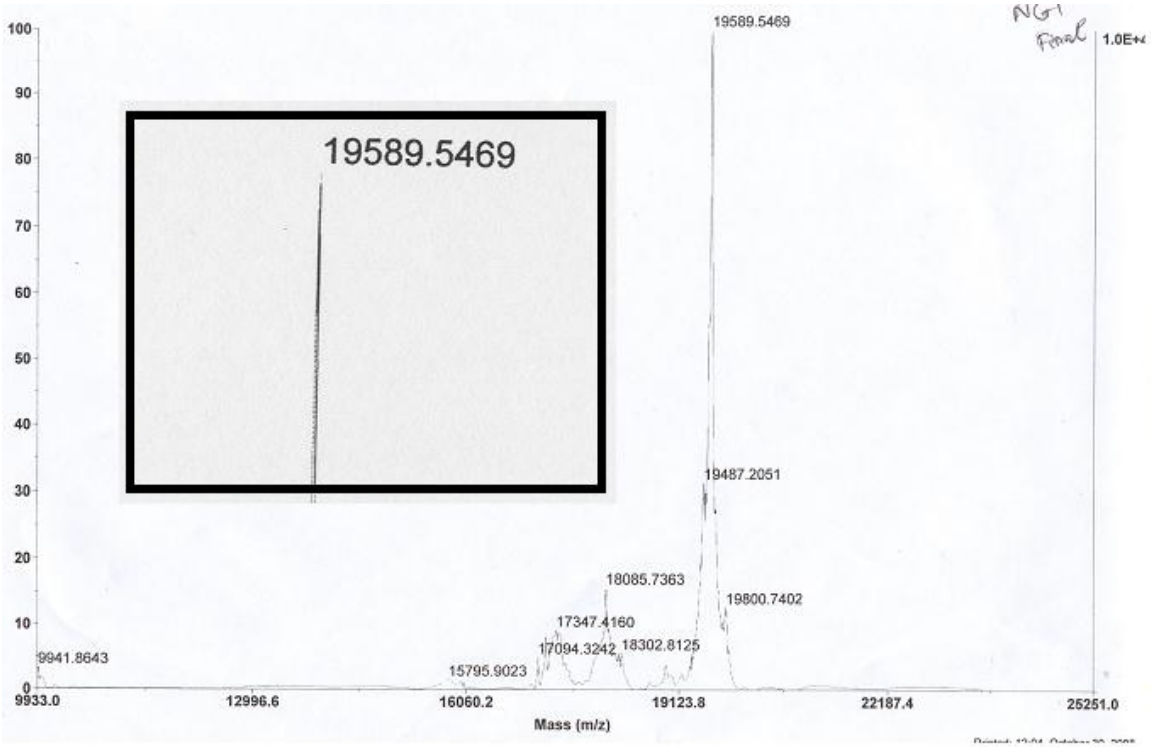

NH_2-GASGPCPQPELPYG G1 PAMAM Octamer (RY 281)

Expected Molecular Weight: 18397.9

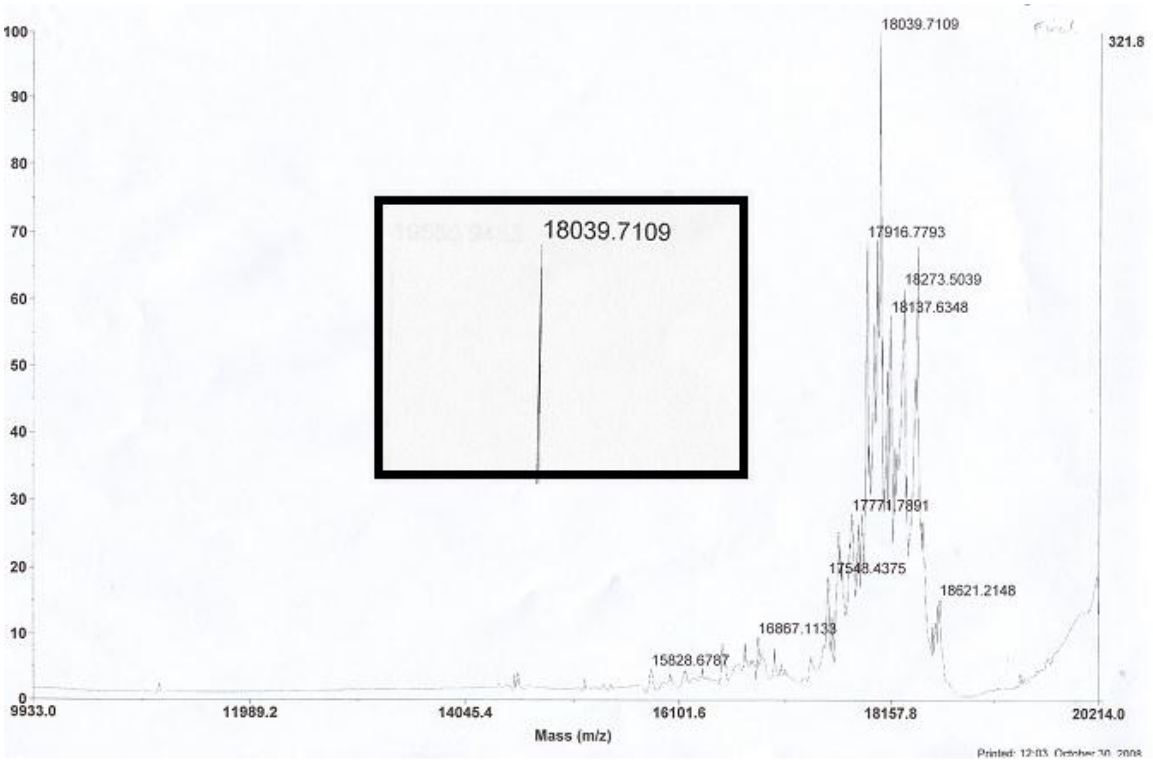

NH_2-GASGPFPQPELPYGC G1 PAMAM Octamer (RY 381)

Expected Molecular Weight: 19574.48

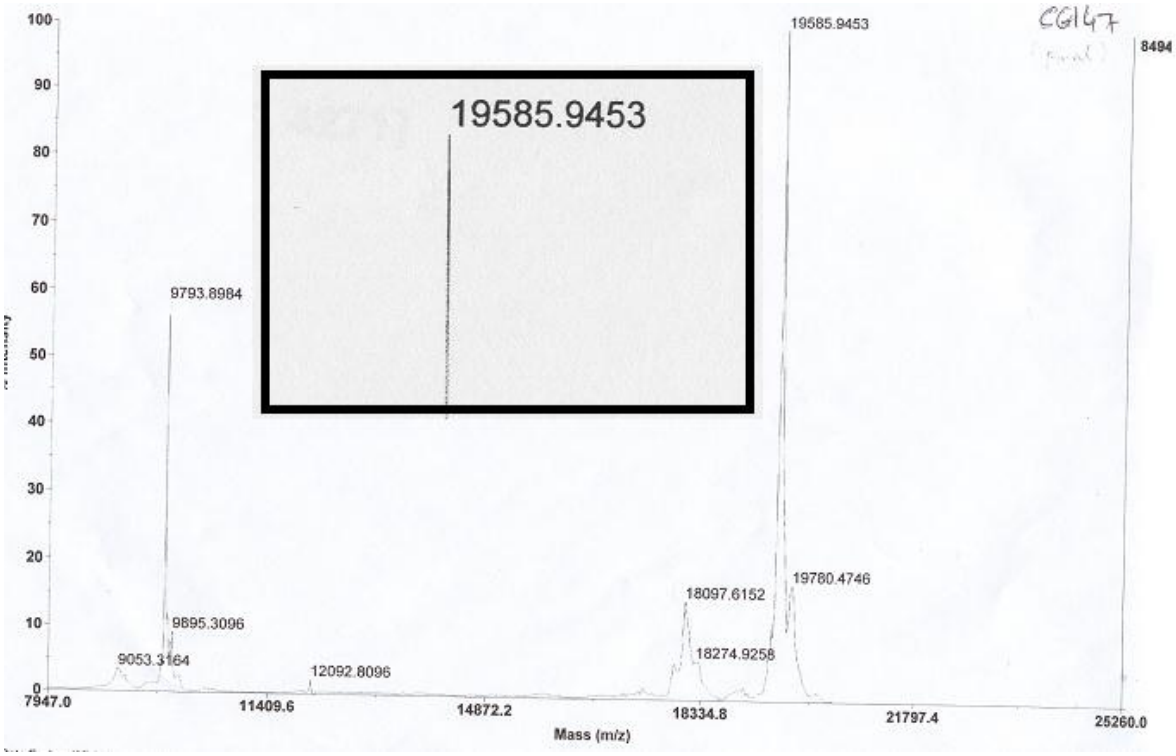

APPENDIX C: Linker Lengths and PAMAM Core Span

(Pierce) Commercially Available Linkers (Length and Functionality)

Dimer (Disulfide linkage)

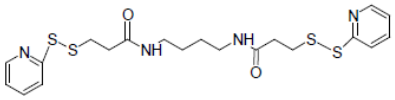

1,4-di-[3'-(2'-pyridyldithio)propionamido]butane (DPDPB) linker (19.9 Angstrom)

Dimer/Trimer (thioether linkage)

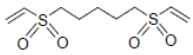

1,6-hexane-bis-vinylsulfone (HBVS) linker (14.7 Angstrom)

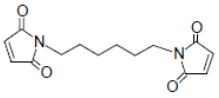

Bis(maleimido)hexane (BMH) linker (13.0 Angstrom)

Heterofunctional Linkers/Dendritic Molecules (amide and thioether linkages)

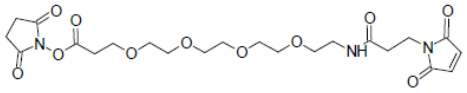

Succinimidyl-[(N-maleimidoproprionamido)-tetraethyleneglycol]ester (NHS-PEO4-Maleimide) linker (24.6 Angstrom)

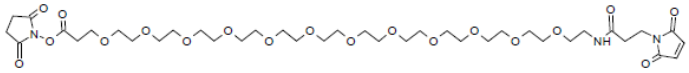

Succinimidyl-[(N-maleimidoproprionamido)-dodecaethyleneglycol]ester (NHS-PEO12-Maleimide) linker (53.4 Angstrom)

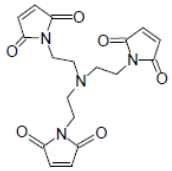

Tris-[2-maleimidoethyl]amine (TMEA) linker (10.3 Angstrom)

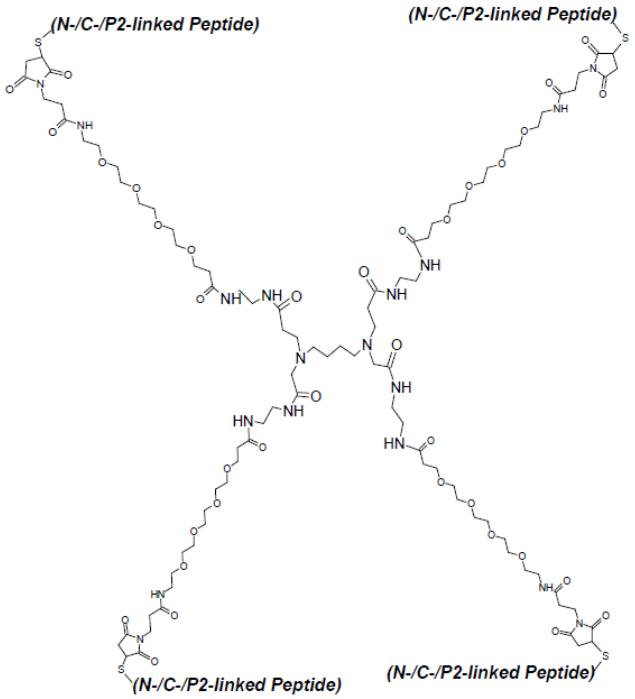

G0 PAMAM Tetramer (~63.2 angstroms)

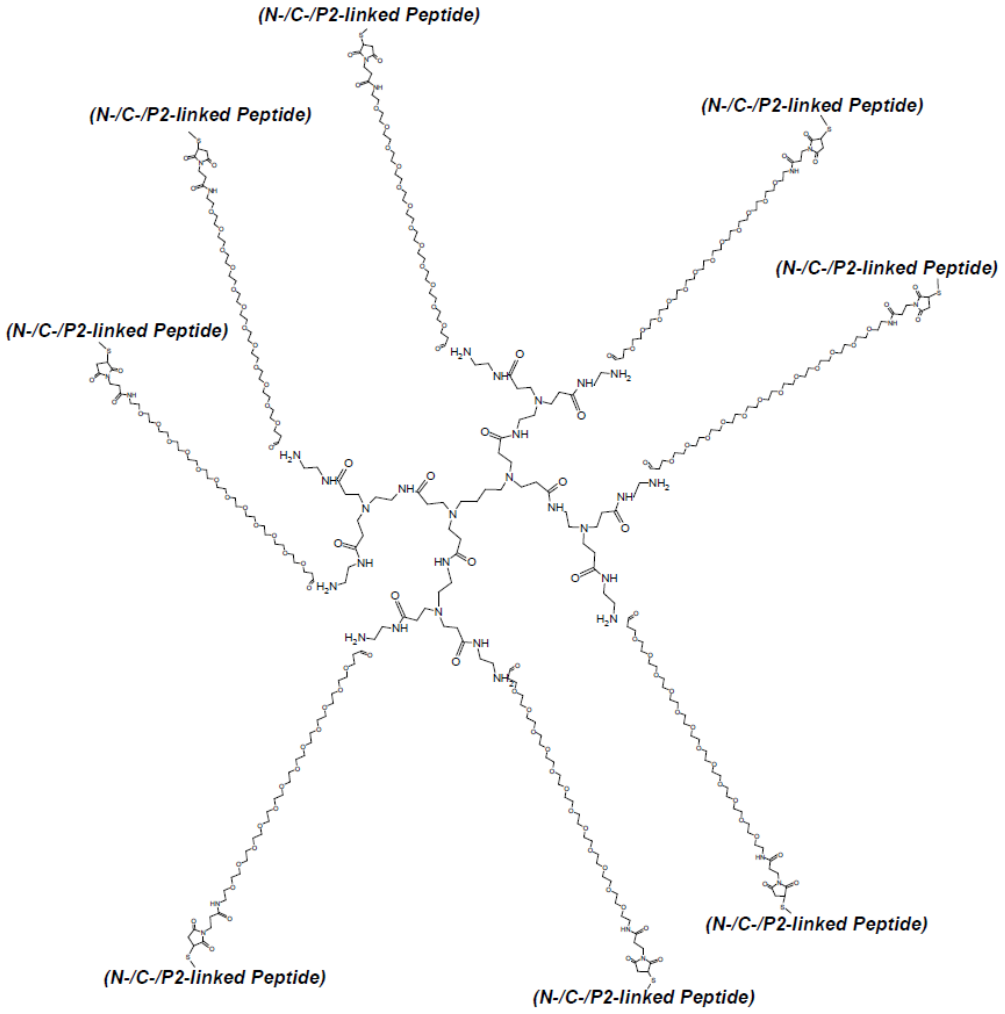

G1 PAMAM Octamer (125.8 angstroms)